REPORT DOCUMENTATION PAGE

Form Approved
OMB No. 0704-0188

1. REPORT DATE *(DD-MM-YYYY)*	**2. REPORT TYPE**	**3. DATES COVERED** *(From - To)*
20-05-2020	Technical Report	June, 2019 - May, 2020

4. TITLE AND SUBTITLE

Impact of Nafion© PEM Fuel Cell Membrane Thickness on In-Situ and Room Temperature Internal Structure Durability at Operating Temperatures Above 100°C Characterized using XRD

5a. CONTRACT NUMBER

5b. GRANT NUMBER

5c. PROGRAM ELEMENT NUMBER

6. AUTHOR(S)

Theodore E. Burye

5d. PROJECT NUMBER

5e. TASK NUMBER

5f. WORK UNIT NUMBER

7. PERFORMING ORGANIZATION NAME(S) AND ADDRESS(ES)

US Army CCDC Ground Vehicle Systems Center (GVSC)
Ground Vehicle Power and Mobility (GVPM)
6501 E. 11 Mile Road
Warren, MI 48397

8. PERFORMING ORGANIZATION REPORT NUMBER

OPSEC 4179

9. SPONSORING / MONITORING AGENCY NAME(S) AND ADDRESS(ES)

US Army CCDC Ground Vehicle Systems Center (GVSC)
Ground Vehicle Power and Mobility (GVPM)
6501 E. 11 Mile Road
Warren, MI 48397

10. SPONSOR/MONITOR'S ACRONYM(S)

11. SPONSOR/MONITOR'S REPORT NUMBER(S)

12. DISTRIBUTION / AVAILABILITY STATEMENT

DISTRIBUTION A. Approved for public release; distribution unlimited. OPSEC# 4179.

13. SUPPLEMENTARY NOTES

14. ABSTRACT

15. SUBJECT TERMS

16. SECURITY CLASSIFICATION OF:			**17. LIMITATION OF ABSTRACT**	**18. NUMBER OF PAGES**	**19a. NAME OF RESPONSIBLE PERSON**
a. REPORT	**b. ABSTRACT**	**c. THIS PAGE**	Same As Report (SAR)	101	Theodore Burye
UNCLAS	UNCLAS	UNCLAS			**19b. TELEPHONE NUMBER** *(include area code)* 586-282-3047

Impact of Nafion© PEM Fuel Cell Membrane Thickness on In-Situ and Room Temperature Internal Structure Durability at Operating Temperatures Above 100°C Characterized using XRD

Prepared by:

Dr. Theodore Burye
Chemical Engineer
theodore.e.burye2.civ@mail.mil
Fuel Cell Technologies
Ground Vehicle Power and Mobility (GVPM)
Combat Capabilities Development Command (CCDC) Ground Vehicle System Center (GVSC)

Acknowledgements

X-ray Diffraction (XRD) data was acquired from the Ground Vehicle Systems Centers (GVSC's) Metallurgy laboratory. Demetrios Tzelepis, from the Characterization & Failure Analysis group, assisted with operation of the XRD equipment. Ian Toppler, from the Characterization & Failure Analysis group, assisted with data collection and operation of the XRD equipment.

Table of Contents

List of Figures

1. Abbreviations List

CCDC: Combat Capabilities Development Command
CBO: Cross Beam Optics
GVSC: Ground Vehicle Systems Center
IC: Internal Combustion
ICSD: Inorganic Crystal Structure Database
MEA: Membrane Electrode Assembly
PB: Parallel Beam
PEM: Proton Exchange Membrane
RH: Relative Humidity
WH: Williamson-Hall
XRD: X-Ray Diffraction

2. Introduction

As the U.S. Army develops the next generation of combat vehicles, the electrical power required to operate these vehicles is projected to increase substantially. These vehicles will be asked to perform additional mission roles, such as silent watch and export power, and incorporate power intensive equipment such as next-generation sensors and jamming devices. High power density systems are required to provide this additional power while still fitting into the current vehicle space claim. The Army recognizes fuel cells as a potential solution as they have high power densities and are more efficient than comparable internal combustion (IC) engines [1, 2, 3].

Many different types of fuels cells exist, but the Proton Exchange Membrane Fuel Cell (PEMFC) is widely used by commercial markets as it is considered the most mature. PEMFCs are more mature due to extensive research and development commercially, being produced extensively and being used in stationary power generation applications by a number of companies [3, 4, 5, 6] over the years. The fact PEMFCs have extensive development and are more commercially available increases their attractiveness to the U.S. Army for vehicle integration since there less risks are present.

In addition to stack performance losses caused by thermal-cycle degradation/seal degradation [7, 8, 9, 10] and electrocatalyst degradation [11, 12, 13, 14], there also exists the potential for thermal degradation of the polymer membrane [15, 16] which transports protons from the anode to the cathode electrodes. Changes to proton transport during operation, or across the entire life of the stack, may negatively impact power output of the stack and should be avoided or minimized. PEMFC manufacturers often state not to exceed 65°C when operating the stack. This temperature restriction may be in place to reduce catalyst coarsening or agglomeration [11, 13] at elevated temperatures, but may also exist to limit thermal degradation to the polymer membrane in the Membrane Electrode Assembly (MEA).

Since thermal degradation can occur within the membrane at elevated temperature, it is important to understand that when PEMFCs are integrated into combat vehicles, heat rejection is substantially more difficult than in commercial vehicles. The heat rejection is more difficult due to ballistic grills reducing air flow. Ultimately this decreased heat rejection could potentially increase stack operating temperatures to as high as 140°C, which is well above the 65°C recommended operating temperature.

One commonly used membrane material for construction in PEMFCs and other fuel cell types is Nafion© [17, 18, 19, 20] which is the brand name for a sulfonated tretrafluoroethylene based fluoropolymer-copolymer. Nafion© can be formulated in different thicknesses [21, 22, 23] when incorporated into the stack. This study used three different formulations, which had similar starting material properties, but varied in their material thickness. The three materials were Nafion© 115, Nafion© 117 and Nafion© 1110, which had thicknesses of 127µm, 183µm and 254µm, respectively.

The objective of this study was to characterize the effect of stack operating temperatures above 60°C (such as 120°C and 140°C) on the In-situ Nafion© material structural properties using different Nafion© material thicknesses and contrast those results against results obtained at 60°C, to understand if thermal degradation could be mitigated simply by using different material thicknesses. In-situ X-Ray Diffraction (XRD) analysis of each material was performed to determine the durability of the internal structure of each material as a function of temperature, time and repeated temperature cycles. This analysis will

provide valuable insight into internal changes that occur and indicate whether Nafion© has potential to be used in PEMFCs when incorporated into combat vehicles.

3. Experimental Operating Conditions

3.1. Introduction

The following section describes the sample preparation and characterization techniques used for each applied operating temperature and Nafion© material thickness.

3.2. Sample Preparation

30 cm x 30 cm sheets of Nafion© 115, Nafion© 117 and Nafion© 1110 were purchased from the Fuel Cell Store (https://www.fuelcellstore.com). 1.27 cm x 1.27 cm samples were cut from each material sheet before being characterized. As stated earlier the Nafion© 115 had a thickness of 127µm, while the Nafion© 117 had a thickness of 183µm and Nafion© 1110 had a thickness of 254µm. These three materials will be referred to as 115, 117 and 1110 for the remainder of this paper.

3.3. Characterization Techniques

3.3.1. X-Ray Diffraction (XRD)

XRD was performed using a SmartLab X-ray Diffraction (XRD) system (Rigaku Americas Corporation; The Woodlands, TX, USA) with a multi-temperature attachment to adjust the in-situ XRD operating temperature, with samples being heated between 25°C and 240°C. Samples were heated at a 10°C/min ramp rate and held at each temperature for either 10 minutes, 2 hours, 8 hours or 24 hours.

The tube voltage and current were 40kV and 44mA. The incident optics used a parallel beam (PB) Cross Beam Optics (CBO) selection slit, a Soller slit 0.5° incident parallel slit, a 1.000° incident slit and a 5.0mm length limiting slit. The receiving optics used a 1.000mm receiving slit #1, a PSA 0.5° receiving optical device, a Soller slit 0.5° receiving parallel slit and a 20.000mm receiving slit #2. Finally, data was also collected using a step scan mode, 2-Theta range of 5-60°, a step width of 0.0500°, a scan speed of 6.000 sec, a copper target and no filter attachment.

4. Baseline Measurements for Nafion© 115, 117 and 1110 at Room Temperature

4.1. Introduction

The following section will establish the baseline in-situ XRD data for the 115, 117 and 1110 samples. This baseline information will be used for comparison against all future XRD scans at different heating temperatures, heating times and number of heating cycles. Establishing the following baseline information is also useful to help determine whether XRD peak positions changed and whether the relative intensity ratios between peaks, within a single sample, changed after heating. Changes to the peak positions or relative peak intensity ratios all can point to structural changes that influence material properties.

All samples characterized using the XRD were "dry". These dry samples were not completely dehydrated of all water but were allowed to equilibrate to the relative humidity (RH) of the lab, which was held between 20% and 25% RH. Nafion© membranes used in PEM fuel cells contain a higher water content than 20-25% RH during operation and this difference in sample water content could raise questions of the validity of the results presented in this paper. The difference in water content is not viewed to change the results presented in this paper for the following reasons.

Increased water content within the polymer has been shown to influence the melt temperature, crystallization temperature [24] and other properties linked to the behavior of the polymer internal structural. Typically, literature [24, 25] studies have shown increasing the water content in the polymer results in these transition event temperatures decreasing. Literature DSC studies [24, 25, 26, 27, 28] studying Nafion© and other polymer materials have identified a large endothermic transition event which occurred between ~80°C and ~190°C. Processing conditions and material type can all influence the temperature range of this peak but multiple studies have proposed a similar explanation for this peak. These studies have proposed this transition event is caused by an order-disorder transition within the polymer matrix clusters. Hydrating the polymer sample is hypothesized to promote the order-disorder at lower temperatures because the water has a plasticizing effect, thus increasing the mobility of clusters within the polymer. If this order-disorder transition temperature were to be lowered enough, due to the sample being hydrated, it could impact the findings in this paper by increasing the degradation beyond what was reported.

Raw DSC scan data was collected from all three materials after being heated at 120°C and 140°C for 0 (baseline), 2, 8 and 24 hours. Dry and saturated samples were characterized using DSC after being heated at 120°C and 140°C, shown in Figure 90 and Figure 91, respectively. DSC data was collected for the following reasons. First, it was important to determine if a similar transition event could be duplicated and, if it could duplicated, then at what temperature did the transition occur for the dry samples. Second, it was important to determine how large an impact saturating each sample had on the transition temperature. The following results were observed from these DSC studies.

Dry samples all produced a dominant endothermic peak which is, based on the literature studies referenced, the transition temperature where each polymer sample started to become more disordered. This transition temperature occurred between 191°C and 231°C and was dependent upon the processing

conditions (such as heating temperature and heating duration) and sample thickness. In contrast baseline samples had this transition temperature occur very close to 220°C. Despite this broad transition temperature range the lowest temperature was 191°C and was not close to either processing temperature (120°C or 140°C). Saturated samples were tested next and all those samples also produced a dominant endothermic peak similar to the literature studies and dry Nafion© samples. Saturating the samples did appear to lower the transition temperature between 163°C and 220°C. The baseline sample transition temperature was decreased to 171°C to 188°C. Samples heated at 140°C or thicker sample materials (such as the 1110) demonstrated the largest change in transition temperature reduction. Overall the transition temperature, when samples were saturated, was not reduced below the upper processing temperature of 140°C.

These findings indicate changes observed in the internal structure characterized by XRD would not be significantly different since this transition event is always outside the processing conditions used in this study.

4.2. Nafion© 115, 117 and 1110 X-Ray Diffraction (XRD) Baseline Measurements

XRD scans were performed for the different material samples to determine whether the internal structure, if any existed, was dependent upon the material thickness. Three samples for each material thickness were used.

Figure 1 shows baseline XRD scans for 115 (blue data), 117 (green data) and 1110 (orange data) samples. These baseline scans show two broad peaks located at 16.7° and 39.3° and two narrow, sharp peaks located at 39.7° and 46.1°. The two broad peaks are from the Nafion© material and will be referred to Peak I and Peak II, respectively, for the rest of the paper. The two narrow, sharp peaks are from the platinum sample holder used in the XRD multi-temperature stage and their Miller indices are (111) and (200), respectively. The Miller indices were identified using the Inorganic Crystal Structure Database (ICSD) [29].

The peak intensities for all three datasets were normalized against the 1110 sample so samples could be compared more easily. All future samples will have their baseline scans normalized to the peak intensity of this initial 1110 sample. Scans were normalized to minimize changes in peak intensity caused by differences in the sample baseline intensities. Changes observed in peaks intensity should result from the different experimental parameters (material thickness, heating temperature, heating duration, number of heating cycles) used, which were varied one at a time. An initial inspection of the three scans shows that sample peaks did not shift between the different material thicknesses and the relative peak intensities also appear to not have changed as the sample thickness changed.

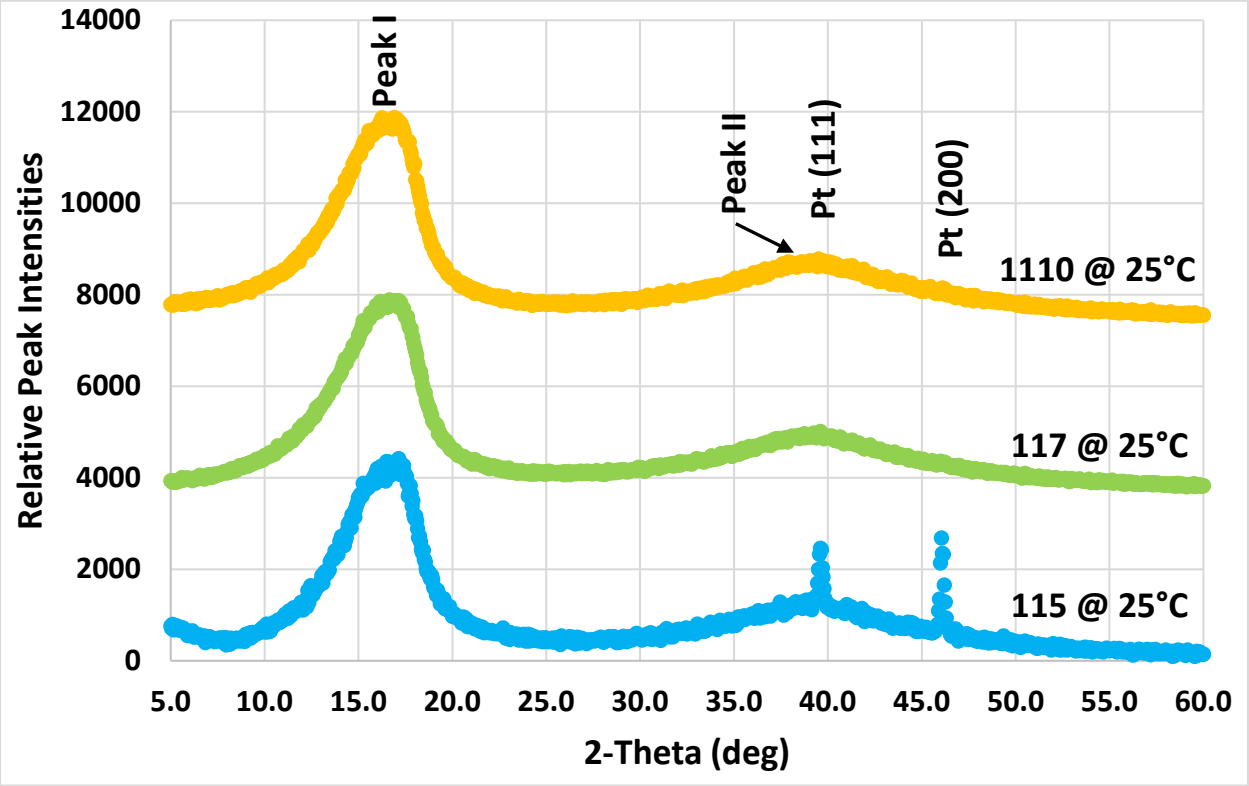

Figure 1: Baseline XRD Scans for 115, 117 and 1110 Samples taken at 25°C.

Figure 2 shows the calculated relative peak intensity ratio values for the 115, 117 and 1110 samples using the peak intensity values from Figure 1. The peak ratio values were calculated being dividing the peak intensity of Peak I by the peak intensity of Peak II. Peak intensities were determined by subtracting the relative peak intensity at the bottom of each peak from the peak intensity at the top. Comparing peak intensity ratio values for each sample is one method of determining if the structural properties of the sample has changed. Since these three sample materials should be structurally the same these peak ratios should also be the same.

Comparison of the calculated ratio values shows that, within the calculated standard deviation, the samples are the same, which is not surprising. The average peak ratio for all three materials was 4.43. The small difference in peak ratios can be attributed to human error induced from reading the raw data from the XRD scans, as the scans have some noise.

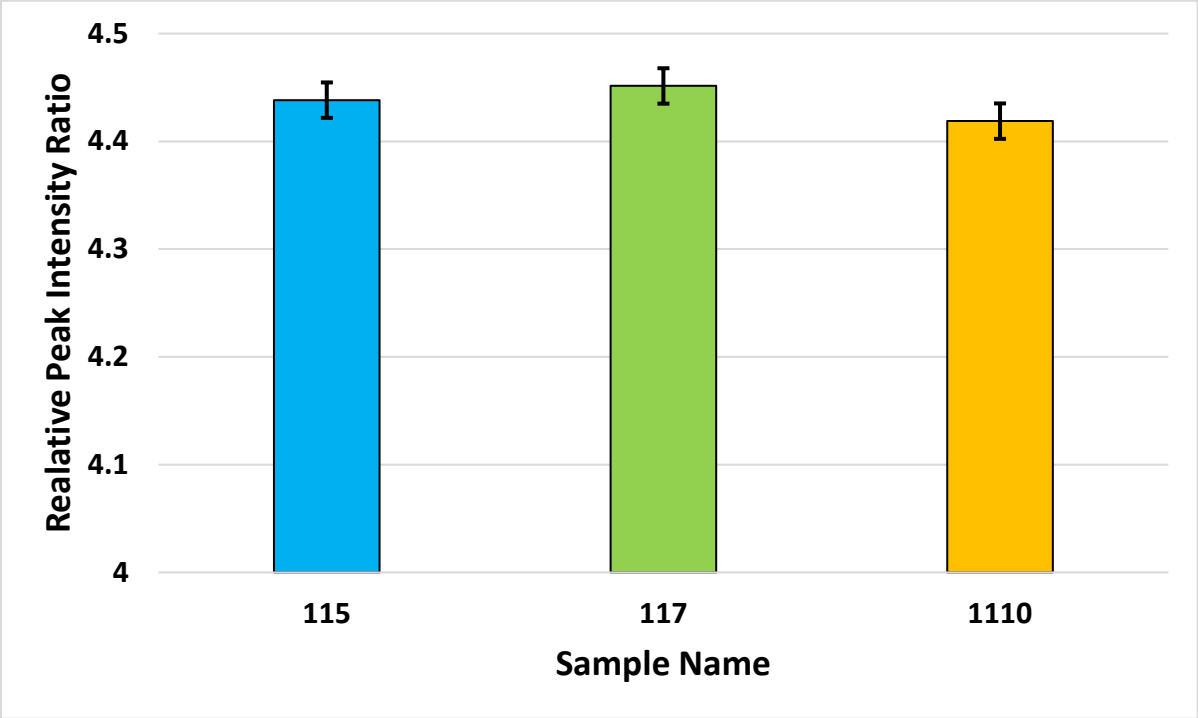

Figure 2: Calculated Relative Peak Ratio Values for 115, 117 and 1110 Samples taken at 25°C.

4.3. Baseline Measurement Summary

In summary, baseline In-Situ XRD measurements were taken at 25°C for the 115, 117 and 1110 sample materials to determine whether the material thickness impacted the XRD scans. The raw XRD scans and the calculated data from those scans show all three materials were the same within their determined standard deviation, which was expected.

The next section will start to investigate the effect of temperature on the different material thicknesses with respect to how their structural properties change. In-Situ temperature measurements will be taken from 25°C to 240°C.

5. Impact of Temperature on 115, 117 and 1110 Material Structure Compared to Baseline XRD Measurements

5.1. Introduction

After establishing that the baseline raw XRD scans and parameters were identical for all three materials and independent of material thickness, at least when characterized 25°C, the effect of operating temperature on the different material thicknesses will be investigated. All three materials will have their Peak I and II 2-Theta positions, Peak I and II intensities and peak ratios compared against the baseline data after being heated. Specific changes to actual material properties would be very difficult to determine simply based on the following XRD results presented in this paper. Additional characterization tests, such as Electrochemical Impedance Spectroscopy (EIS) (to determine proton conductivity) or tensile measurements (to determine mechanical strength), would be needed to identify specific material properties. The following results presented in this paper are still beneficial as the following information can help indicate operating temperatures that start to cause internal structural changes, which can be correlated to actual property changes in later studies and help explain trends in material property variations.

5.2. In-Situ Nafion© 115, 117 and 1110 XRD Measurements Compared to Baseline Measurements

The following 115, 117 and 1110 samples were heated from 25°C to 240°C using a 10°C ramp rate, followed by a 10 min hold at each temperature to allow the sample to equilibrate before taking each XRD measurement. Each membrane thickness had one sample characterized across the entire temperature range, with a total of three samples used in this section. The specific temperatures used for each sample were: 25°C, 30°C, 60°C, 80°C, 100°C, 120°C, 140°C, 160°C, 180°C, 200°C, 220°C and 240°C. The majority of the temperatures had a 20°C temperature separation to allow for an even temperature profile distribution. Temperatures between 25°C and 60°C were not as regularly spaced since Nafion© is not expected to structurally change significantly at these lower temperatures. Finally, all samples had their raw XRD peak intensity data normalized with the 1110 baseline data described in Section 4.

Figure 3, Figure 4 and Figure 5 shows the In-Situ XRD scans for the 115, 117 and 1110 samples, respectively, heated at the operating temperatures listed above. An initial inspection of the raw XRD data of the three sample materials shows a few interesting trends. First, all three materials showed a decrease in peak intensity followed by an increase for Peak I, occurring between 100°C and 160°C. Second, following the increased peak intensity all three materials lower their Peak I intensity drastically. Finally, Peak I shifted to lower 2-Theta values as the temperature was increased. This shift in peak 2-Theta positon, while gradual at first, became more pronounced after 140°C for the 115 material. While this may be simply a coincidence, this shift started to become more significant after Peak I noticeably started to decrease its intensity, where these two changes may be related. These observations will be analyzed in greater detail and possible explanations will be discussed.

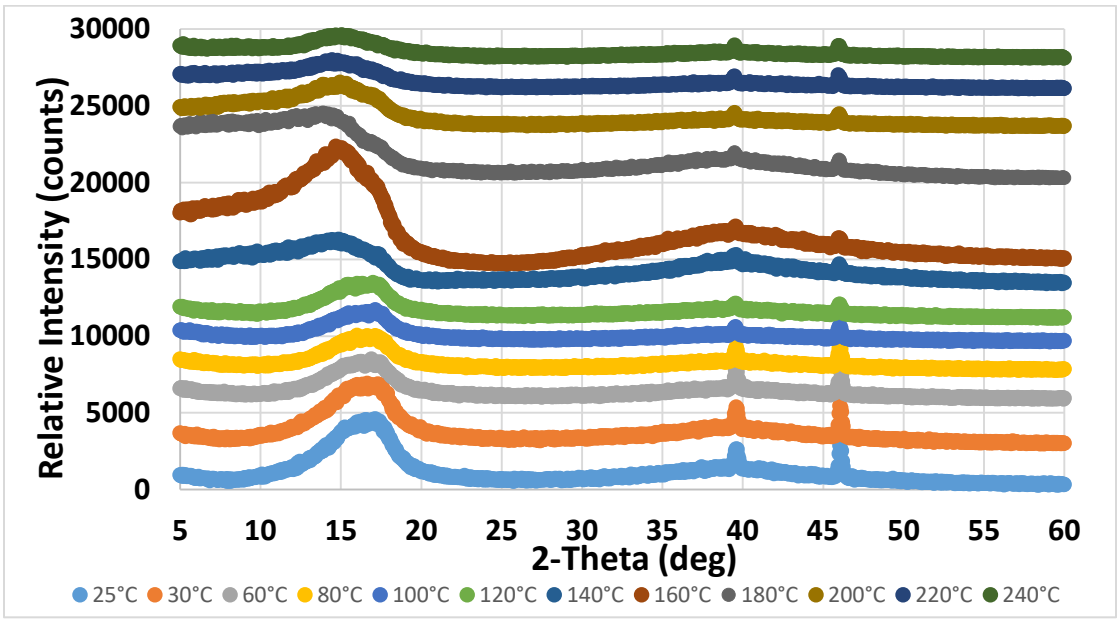

Figure 3: In-Situ Raw XRD Scans for 115 Samples Heated from 25°C to 240°C using a 10 Minute Hold before each Measurement.

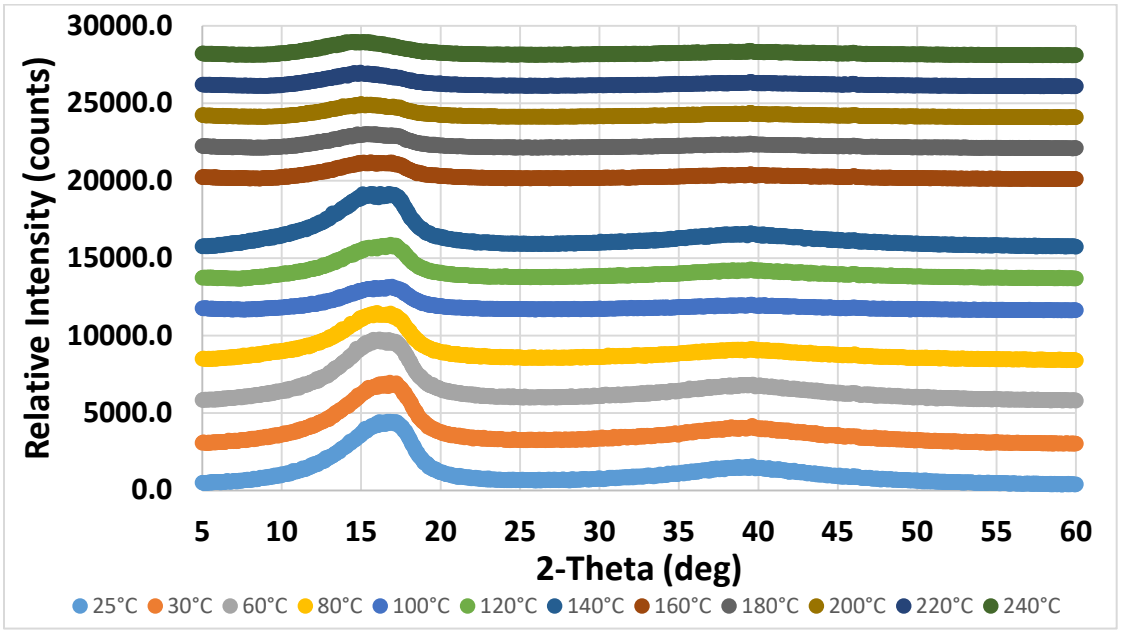

Figure 4: In-Situ Raw XRD Scans for 117 Samples Heated from 25°C to 240°C using a 10 Minute Hold before each Measurement.

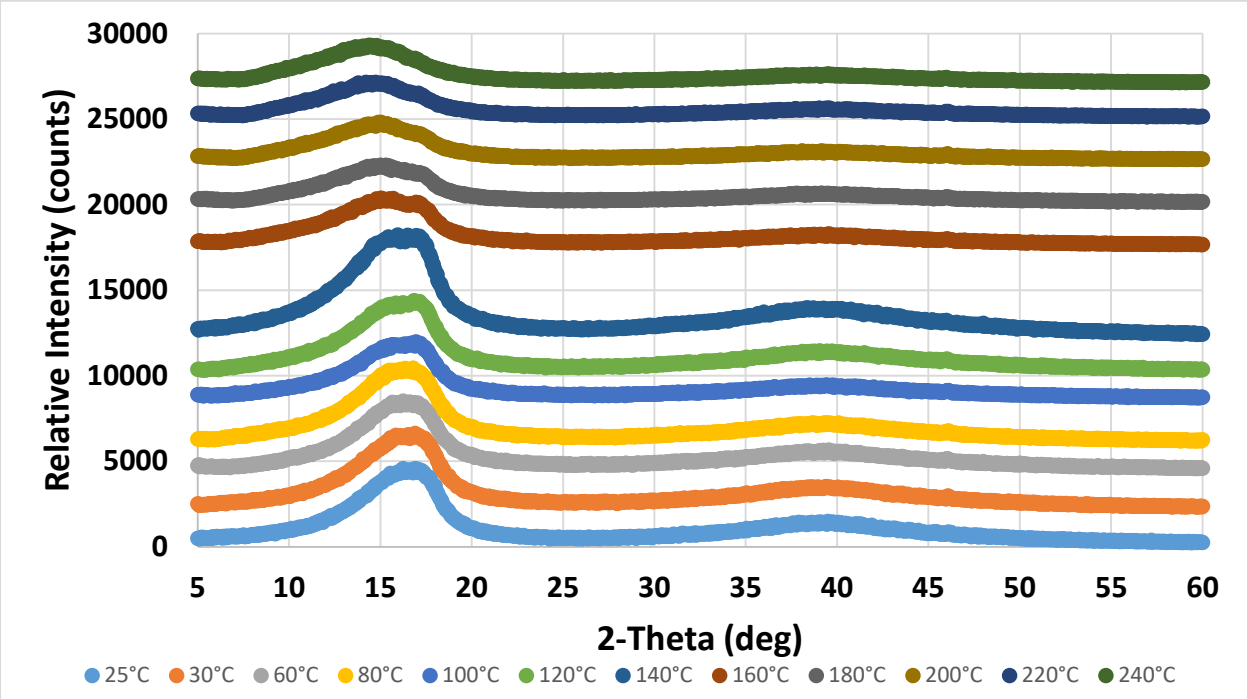

Figure 5: In-Situ Raw XRD Scans for 1110 Samples Heated from 25°C to 240°C using a 10 Minute Hold before each Measurement.

Next, the raw XRD data was then analyzed more closely by calculating the structural parameters which could provide a more accurate picture of how each material responded than could be accomplished through visual observations. Calculated parameters included: 1. Material peak 2-Theta positions, 2. Relative peak intensity percentages compared to their baseline and 3. Peak intensity ratios (ratios between Peak 1/Peak II). These five parameters were calculated for each of the following sections. Each material also had their calculated parameters plotted as function of temperature, shown below. In addition to normalizing the baseline (25°C) data against the 1110 baseline material in Section 4 the calculated peak intensity values were also normalized as a relative percent increase or decrease compared to their respective starting, normalized, baseline scans. Normalizing each calculated peak intensity as a percent increase/decrease allowed for peak intensity differences from material thickness to be eliminated and each material could be compared on same scale.

Figure 6 and Figure 7 showed the calculated 115 (green data), 117 (orange data) and 1110 (red data) 2-Theta peak positions for Peak I and Peak II, respectively. The first point to mention is that, despite being heated to 240°C, Peak II never altered its 2-Theta position for any operating temperature or any of the different sample thicknesses (all data points overlapped on this plot). As mentioned above, Peak I did change with respect to both operating temperature and sample thickness. When the position of Peak I was calculated all three materials showed a gradual decrease in position from 16.7° to ~16.1° 2-Theta when heated from 25°C to 140°C. While this may appear to be a small change it still amounts to a 3.59% reduction in peak position. Further heating from 160°C to 240°C caused the three materials to deviate from each other. The thicker 117 and 1110 materials continued to gradually decrease their peak positon

at a similar rate until the peak position was ~14.9 at 240°C, which was a 10.8% decrease from their starting position. The 115, however, drastically decreased its 2-Theta position at 160°C and then increased slightly, ultimately reaching a similar position as the 117 and 1110 materials at 240°C.

Potential explanations for why samples would change their peak 2-Theta position can be found in literature for materials which have a mostly crystalline structure (i.e. a very low amorphous phase component to their structure). Some common reasons behind a 2-Theta peak shifts are: 1. Alterations to internal material strain/stress from lattice parameter expansion/contraction [30, 31, 32], 2. Increased or decreased particle/grain sizes within the material [30, 31, 32], 3. Composition changes [33, 34, 35, 36] or 4. Material phase changes [37, 38, 39, 40]. Since polymer materials typically have both an amorphous and crystalline component [41, 42, 43] the reasons listed above need to be evaluated to determine if similar results can be inferred from a 2-Theta peak shift for a polymer material.

First, literature [44] has shown polymer samples can alter their stress/strain states which can be calculated using the Williamson-Hall method (WH) [45] (which is based on the Scherrer equation [46]). There are a few caveats that need to be considered when using the WH method. The first point to consider is only the crystalline portion of the polymer sample can be used to calculate stress/strain information. A second point is the material needs to have at least two crystalline peaks (to form a straight line), but three or more peaks are more desirable to considerably reduce error in the calculations. The last point to consider when using the WH method is that the crystalline component of the sample need to be smaller than 100-200 nm in any one dimension, otherwise large errors are introduced. While Nafion© meets all these requirements, with its crystalline clusters/bundles typically 50-100 nm in size [47, 48], it can be difficult to accurately determine the strain in the material [49]. In addition, Nafion© contains only two crystalline peaks and would add additional error to the measurements. While internal stress changes may be causing Peak I to shift it is not possible to make an accurate determination at this time.

Second, literature has shown both polymer cluster aggregate sizes [47, 48] and crystalline nanoparticle grain size imbedded inside the polymer [14] can be determined using the WH method with the same caveats as before. The samples used in this study do not contain crystalline nanoparticles, so particle or grain size determination is not possible. The polymer cluster size can be determined instead, but the same limitations would apply here as with calculating strain. Polymer cluster size may be changing but it is not possible to make an accurate determination of the polymer cluster size and correlate those changes to Peak I 2-Theta position.

Finally, polymer materials have been shown to alter their composition and exhibit changes in material phases [50, 51] when an external energy source disrupted the polymer structure. The literature studies clearly showed the peak positions, peak intensities and peak intensity ratios, within the polymer sample being characterized, were changed and thus composition and material phases were altered. While the literature sources used a radiation source to alter their polymer samples the application of an external heat source would be expected to degrade polymer samples too. In addition, literature [52, 53] has shown 2-Theta peak broadening has been linked to an increase in the disorder of the polymer structure reinforcing that material composition can be altered. While this is not a metric which can have a physical

number attached it does provide the most plausible explanation for observed changes in peak 2-Theta position.

Figure 8 and Figure 9 show the calculated 115 (green data), 117 (orange data) and 1110 (red data) normalized peak intensities for Peak I and Peak II, respectively. While the calculated intensity values shifted there are a few trends which can help separate how the different material thicknesses behaved as a function of heating temperature. The first observation was, from temperatures between 25°C and 120°C, the thicker the membrane material the smaller the reduction in relative peak intensity for both peaks. The 1110 peak intensities remained, on average, only 6.4% to 7.1% below its starting peak intensity. The 117 was the second closest and was on average 23.2% to 26.4% lower than its initial value. The 115 was the worst and on average was nearly a third of its starting intensity at 36.3% to 36.5%. Second, between 140°C and 160°C, all three materials increased their relative peak intensities. This increase is the observed peak increase in peak height mentioned earlier, which may be related to the cross-linked chains becoming more crystalline or adjusting to a more preferred orientation. This increase in Nafion© crystallinity has been observed in literature [54] after annealing the polymer at 140°C for 7 days. The increased crystallinity observed in this paper may initial stages of a similar anneal process. The increase in peak intensity was similar for both the 117 and 1110 at 46.4% and 59.5%, respectively. The 115 had a significantly larger increase in peak height with an increase of 167.7%.

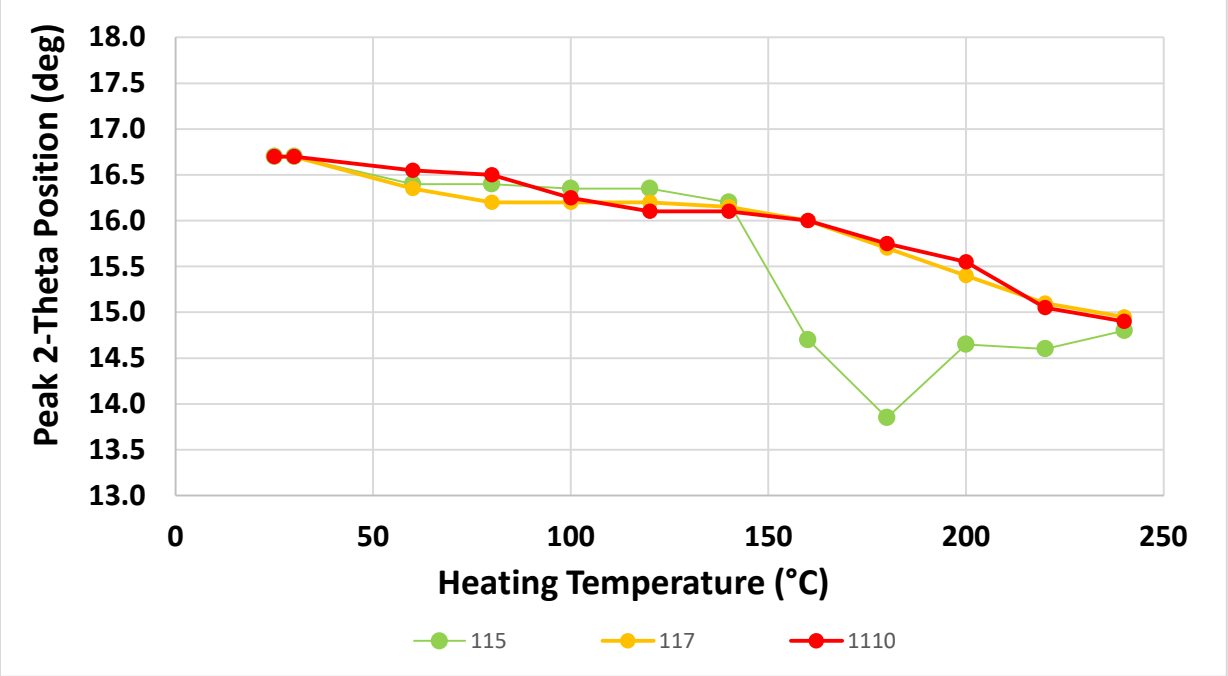

Figure 6: Calculated 115, 117 and 1110 2-Theta Peak Position for Peak I

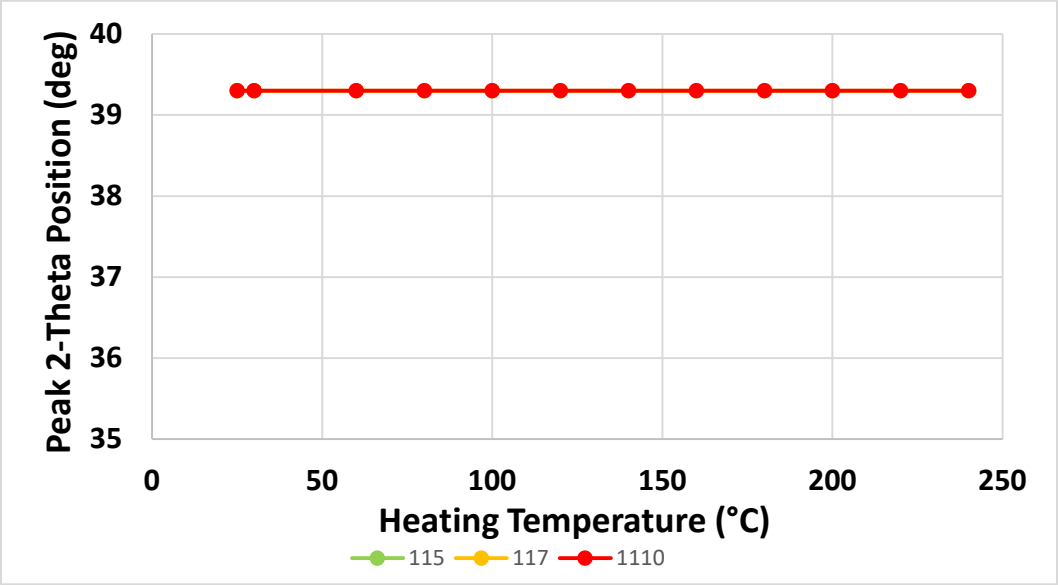

Figure 7: Calculated 115, 117 and 1110 2-Theta Peak Position for Peak II

Third, after the crystallization event all three materials reduce their relative peak intensities to around the same magnitude, which was ~50% to 17% of their respective initial peak height. It was difficult to visually identify that Peak II was changing intensity too, but after comparing the results it appears to proportionally change in a similar magnitude as Peak I. The results shown in Figure 9 (Peak II) are the same throughout the remainder of this study. Peak II did not show any changes in its 2-Theta position for any membrane thickness, In Situ or post-heating, despite samples being subjected to elevated temperatures for different amounts of time and cycling patterns. All future Peak II 2-Theta position results will be moved to the supplementary information section at the end of this paper for reference.

Three common mechanisms exist which potentially can explain the increased peak intensities observed, which are: 1. Increase sample crystallinity [55, 56], 2. Increased grain size or cluster size and 3. Changes to the sample preferred grain orientation [57, 58, 59]. First, increased sample crystallinity typically results in multiple peak intensities increasing by a similar percentage. Careful inspection of the calculated relative peak intensities does show a common change in peak intensity between both peaks at each temperature, but many times the magnitude of change is not the same for both peaks. Since both peaks change intensities in similar directions it is possible that the sample crystallinity is only one component and a second is working in tandem. Second, as pointed out earlier cluster sizes within the polymer are possible to determine but an accurate determination of their actual sizes is difficult. The process of depolymerization, defined as the "process of converting a polymer into a monomer or a mixture of monomers" [60], can decrease the size of these clusters by the conversion of the polymer into multiple monomers. This reduction in cluster size could broaden the peaks and reduce their overall intensity. Finally, materials with a preferred grain orientation will have a peak or peaks with a substantially larger intensity due to the grains aligning in that orientation. While the polymer samples in this study do not contain grains they contain the clusters of cross-linked carbon chains. Literature has shown polymers can have a preferred fiber alignment/orientation [61, 62, 63] and could deform and change their preferred

orientation [64]. Based on these previous studies it appears possible heating the different sample thicknesses could be decreasing or increasing their preferred orientation and thus altering the Peak I and II intensities. From this review of literature and the analysis of calculated parameters the changes observed in sample peak intensity appear to be the result of all three mechanisms in different quantitative amounts. Isolating how much impact each process had on peak intensities is outside the scope of this paper.

Figure 10 shows how the calculated peak intensity ratio between Peak I and Peak II compare. Comparing changes in peak ratios does have the potential to be misleading and needs to be compared alongside the other information presented. Ratios can hide important information, such as changing peak intensities, if the magnitude of those changes are similar, such as the case with these materials. Despite this drawback it should not be ignored and can be a valuable tool to quickly isolate when structural properties are changing and the magnitude of those changes. As mentioned previously, determining peak intensity ratios is a valuable method to help isolate when sample peak intensity changes are dominated by a preferred orientation over changes in sample crystallinity.

Peak intensity ratios were calculated by dividing the intensity of Peak I by the intensity of Peak II for each temperature. Despite the changes to peak intensities shown above ratio values stayed relatively constant for 115 up to 120°C, while the 117 and 1110 did not start to deviate until after 140°C. These calculated peak ratios also help identify when each material starts to change its preferred orientation. The 115 starts to be change orientation at temperatures above 120°C, while 117 and 1110 start to change at temperatures above 140°C. As with the other calculated parameters the 115 showed much larger variations in its values which could be very detrimental to fuel cell operation in combat vehicles.

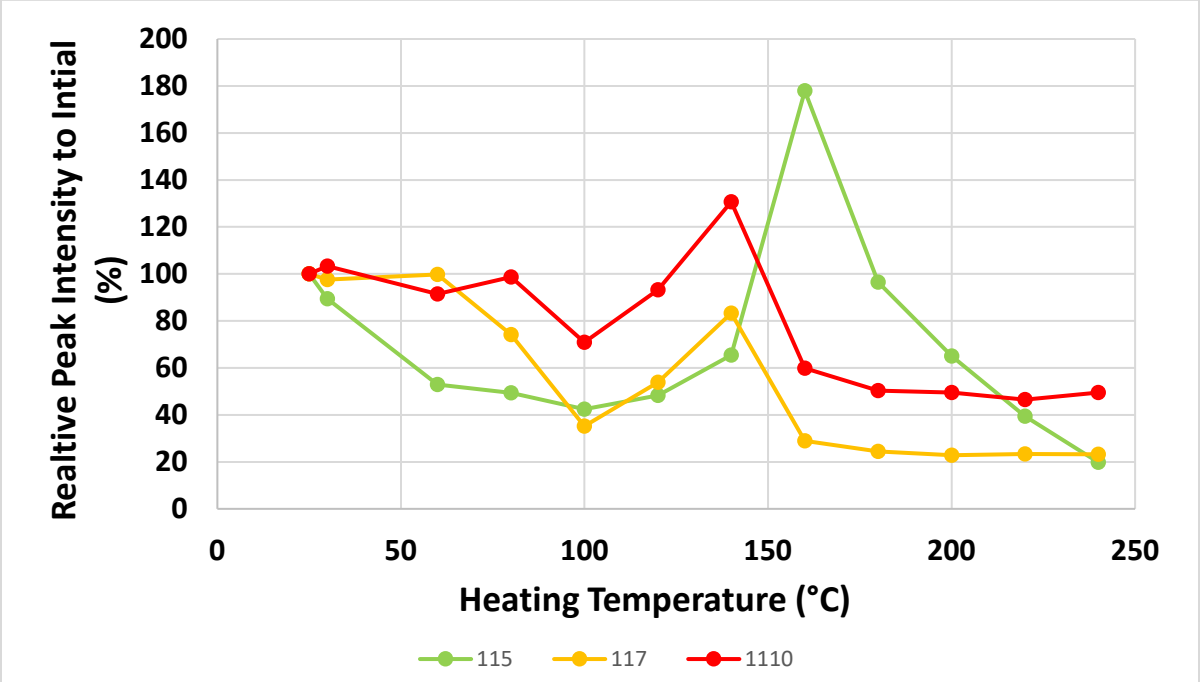

Figure 8: Calculated 115, 117 and 1110 Relative Peak Intensity for Peak I

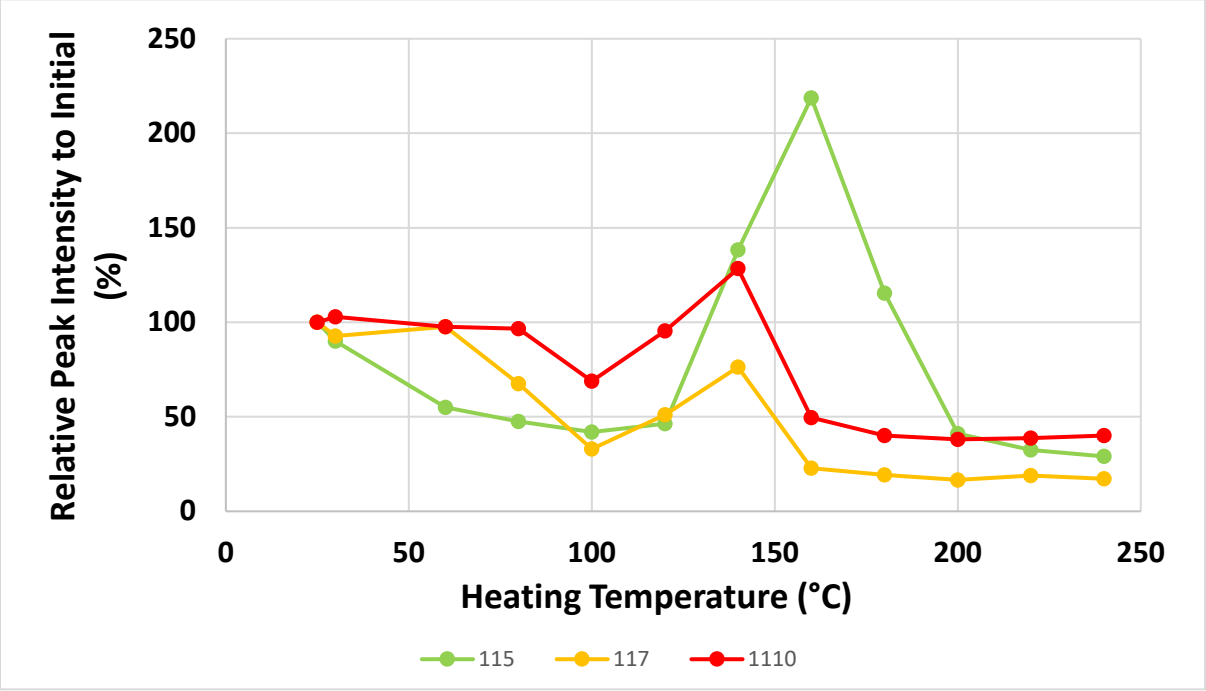

Figure 9: Calculated 115, 117 and 1110 Relative Peak Intensity for Peak II

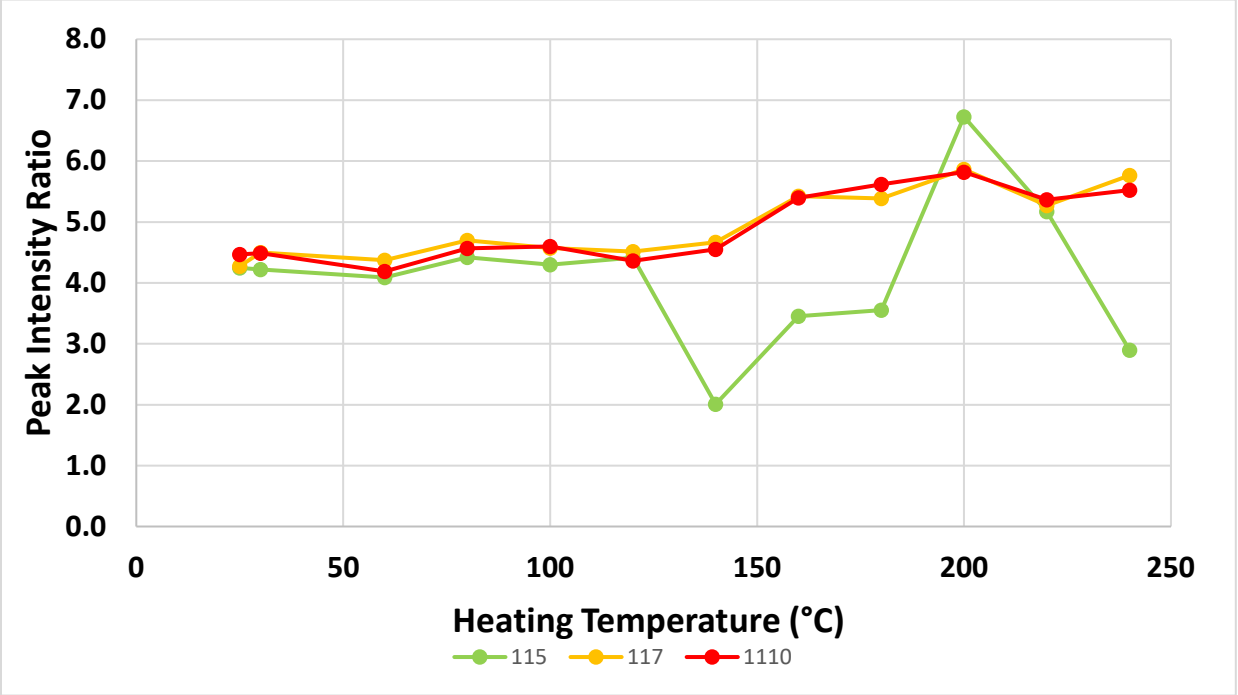

Figure 10: Calculated 115, 117 and 1110 Peak Ratio Intensities between Peak I and Peak II

These initial results provide some useful information into how the material thickness impacts structural changes when being heated at different operating temperatures. While all three materials do not appear immune to being structurally altered it does appear that, in general, the thicker materials such as the 117 and 1110 showed changes that occur more gradually and less severe while the 115 showed changes which were more dramatic and catastrophic. It is also important to note that the scope of this paper is not to determine the mechanism behind observed structural changes, such XRD peak location shifting or peak intensity adjustments. Further analysis of that information will be left for a future study.

5.3. In-Situ Nafion© 115, 117 and 1110 XRD Measurements Summary

In summary, the following trends were observed for the 115, 117 and 1110 materials heated from 25°C to 240°C.

1. All three materials showed structural changes but the 115 showed the most dramatic and severe changes. Changes to 117 and 1110 materials were much more gradual as the temperature increased.
2. All three materials increased their Peak I intensities when heated between 140°C and 160°C. The 117 and 1110 had it occur at 140°C, while the 115 had it occur at 160°C. This increased peak intensity could be related to the cross-linked polymer chains arranging to a more preferred orientation.
3. The starting 2-Theta position of Peak I shifted to lower 2-Theta values for all three materials as the temperature increased. This peak shift was gradual for the 117 and 1110 materials but the 115 showed a dramatic change in position after 120°C.
4. Peak II did not appear to change it 2-Theta position for any of the three materials or for any operating temperature.

6. Impact of Temperature on 115, 117 and 1110 Materials Structural Ability to Return to Baseline XRD Measurements

6.1. Introduction

Section 5 demonstrated the effect of temperature for different Nafion© material thicknesses, but the ability of each material to return to its baseline conditions also needs to be investigated. If the material properties remain permanently changed after being returned to room temperature then performance issues can become compounded over time after multiple heating and cooling cycles.

6.2. Post-Heating Nafion© 115, 117 and 1110 XRD Measurements Compared to Baseline Measurements

To test how well samples returned to their original structural configuration they were heated to 60°C, 120°C, 140°C or 240°C using a 10°C/min ramp rate using a starting temperature of 25°C. Samples were then held at that each temperature for 10 minutes to allow it to equilibrate. After each sample was equilibrated, XRD measurements were taken and each sample was cooled back down to a final temperature of 25°C using a 10°C/min ramp rate, and a final XRD measurement was taken. In-Situ XRD measurements were also recorded for each sample after reaching their maximum heating temperature. This was done so each sample was heated the same amount of time as samples tested in Section 5. The XRD measurement recorded for each sample after cooling to 25°C was conducted so structural changes could be determined by comparing these results to the original baseline scans.

Figure 11, Figure 12 and Figure 13 show the 115, 117 and 1110 In-Situ raw XRD scans, respectively, taken at 25°C after being cooled. Plots have each scan labeled with their respective heating temperature. Scan data was normalized in the same manner as previously described in Section 4. Each scan is visually compared against their baseline scan using peak position and peak intensity as was done in Section 5. The 1110 material appeared have the most structural stability as it had the least difficulty returning to its baseline. However, even with that increased stability the 1110 still lacked the capability of returning fully to its baseline at temperatures above 60°C. At temperatures above 60°C all three materials showed moderate to severe differences between their baseline scans and scans taken after being cooled to 25°C. One difference that manifested above 60°C for all three materials was a significant increase in the Peak I and II intensities, compared to their baseline scans. As mentioned in Section 5 the increased peak intensities could be related to a changes in sample crystallinity, cluster size or preferred polymer cross-link orientation. Each material was slightly different but both peaks reached their maximum intensities between 120°C and 140°C. A second observed difference was that samples increased their Peak I 2-Theta position and produced a small sharp peak on the right-hand side of Peak I. Further analysis would be required to confirm the specific cause, but changes to the peak shape (such as peak splitting) can indicate phase change within the material [37, 38, 39], which was previously shown to be possible in polymer materials in Section 5.

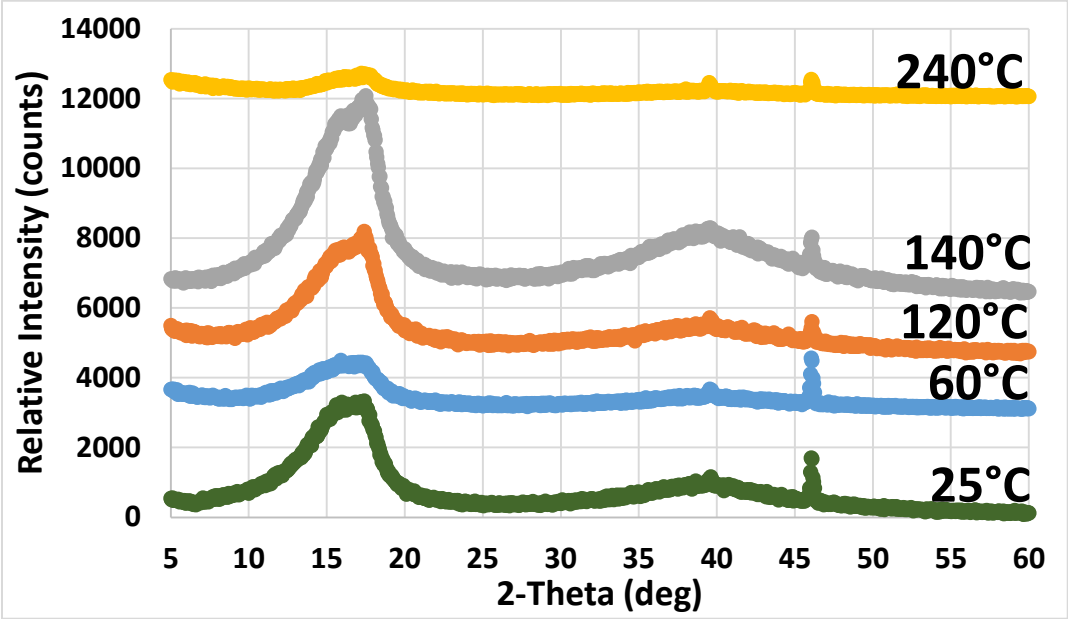

Figure 11: Post-Heating Raw XRD Scans for 115 taken after being Heated to 25°C, 60°C, 120°C, 140°C and 240°C.

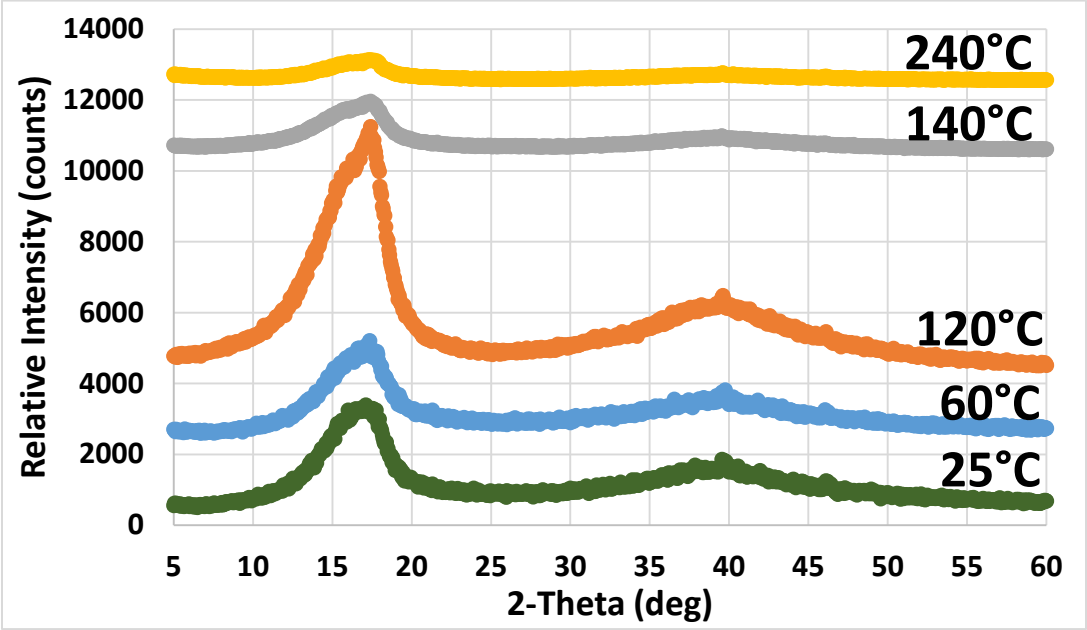

Figure 12: Post-Heating Raw XRD Scans for 117 taken after being Heated to 25°C, 60°C, 120°C, 140°C and 240°C.

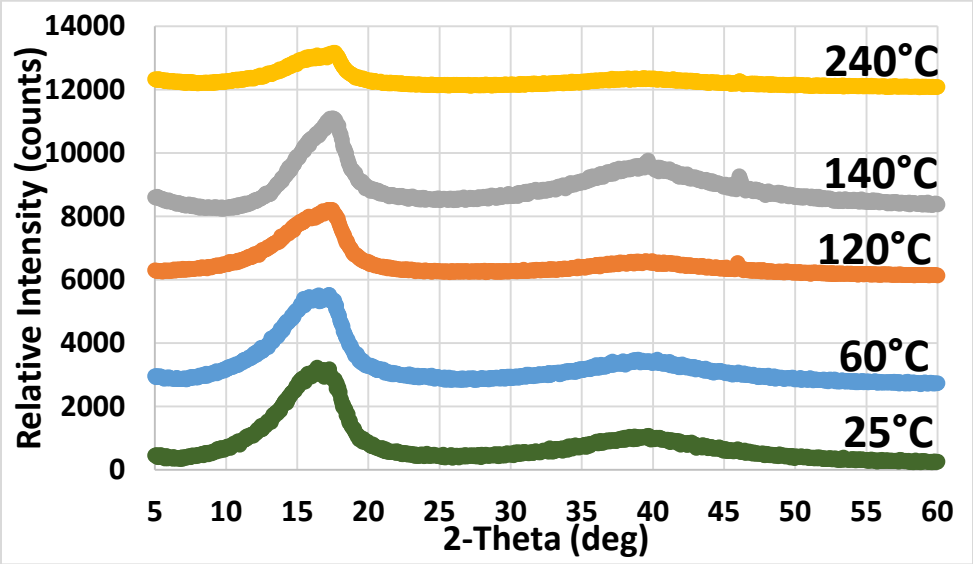

Figure 13: Post-Heating Raw XRD Scans for 1110 taken after being Heated to 25°C, 60°C, 120°C, 140°C and 240°C.

Figure 14 shows the calculated 115, 117 and 1110 peak position for Peak I. The Peak II calculated 2-Theta position was found to not change as was included in the Supplemental Information section at the end of this paper for reference. Calculated 115 results are shown as green data, 117 results are shown as orange data and 1110 results are shown as red data. The initial baseline value for each parameter is shown as a dashed line. The calculated values for each peak show some interesting trends in how each material behaves when returned to 25°C. First, the Peak I 2-Theta position did show some variation even when heated at 60°C. Heating sample at 60°C, which is similar to the typical operating temperatures by PEM fuel cell stacks, showed the ability to altered both the 115 and 117 samples enough so they were not able to return to their original baseline positions. Both materials increased their respective 2-Theta values by approximately 4.2%, which is fairly significant. The 1110 was the only material able to return to its baseline 2-Theta position, but when heated above 100°C the 1110 material did not return to its baseline. Temperatures above 100°C continued to increase Peak I's position to a maximum of ~17.6° after being heated up to 240°C. As with the results in Section 5, there could be a number of different explanations behind these changes, but those are outside the scope of this paper.

Figure 15 and Figure 16 show the peak intensities of Peak I and Peak II after being heated, respectively. As previously observed the 1110 material remained relatively close to its baseline peak intensities, at least when compared to the 115 and 117 materials. The 115 showed the largest increase in peak intensity and, on average, increased between 105.7% and 114.5% above the original intensity. The 117 increased the next largest amount between 16.2% and 39.2%. Finally, the 1110 actually showed an average decrease between 0.2% and 15.7%, which still stays the closest to its original values. In the end, all three materials, when heated to 240°C, only retained 17-37% or their original peak intensity when returned to 25°C. These results also show an increased structural disorder which resulted in a permanent change within the each

sample material, similar to what was observed and discussed in Section 5. The same analysis conducted in Section 5 on the significance of peak intensity changes can be applied here as well.

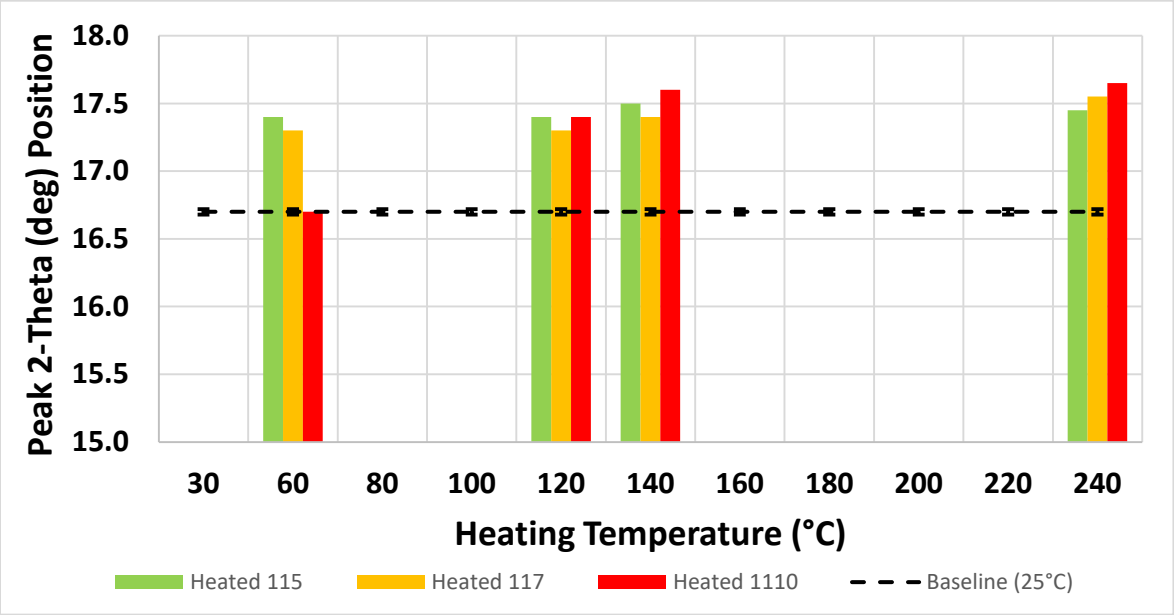

Figure 14: Calculated 115, 117 and 1110 2-Theta Peak Position for Peak I Compared to Baseline Measurements

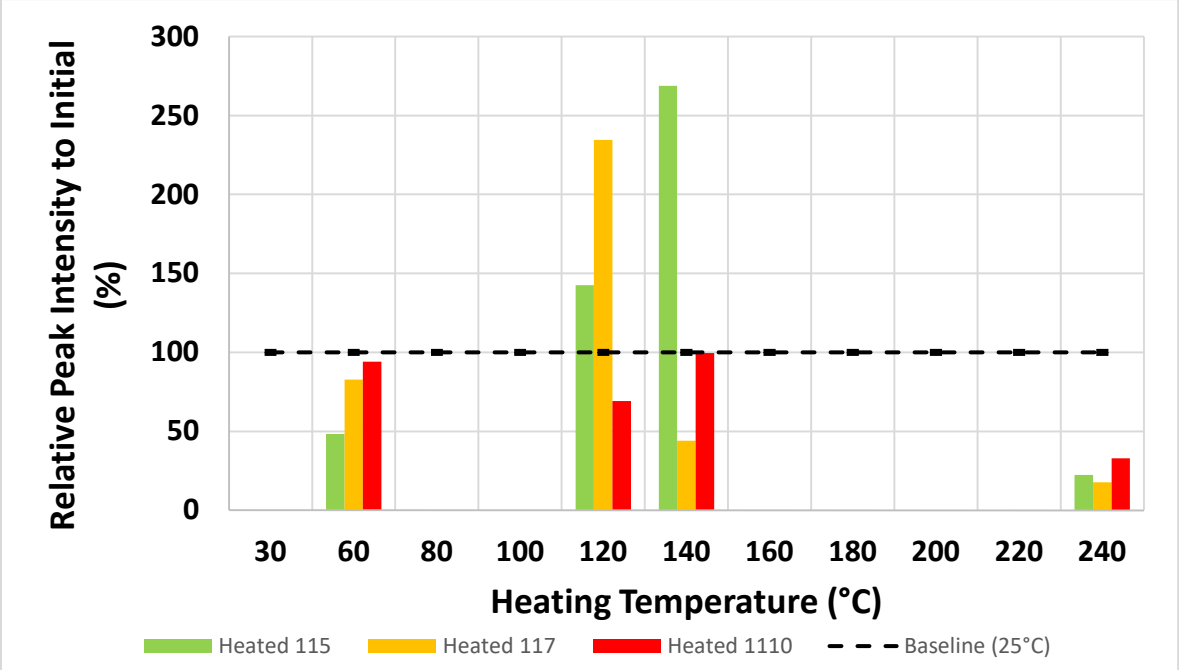

Figure 15: Calculated 115, 117 and 1110 Relative Peak Intensity for Peak I

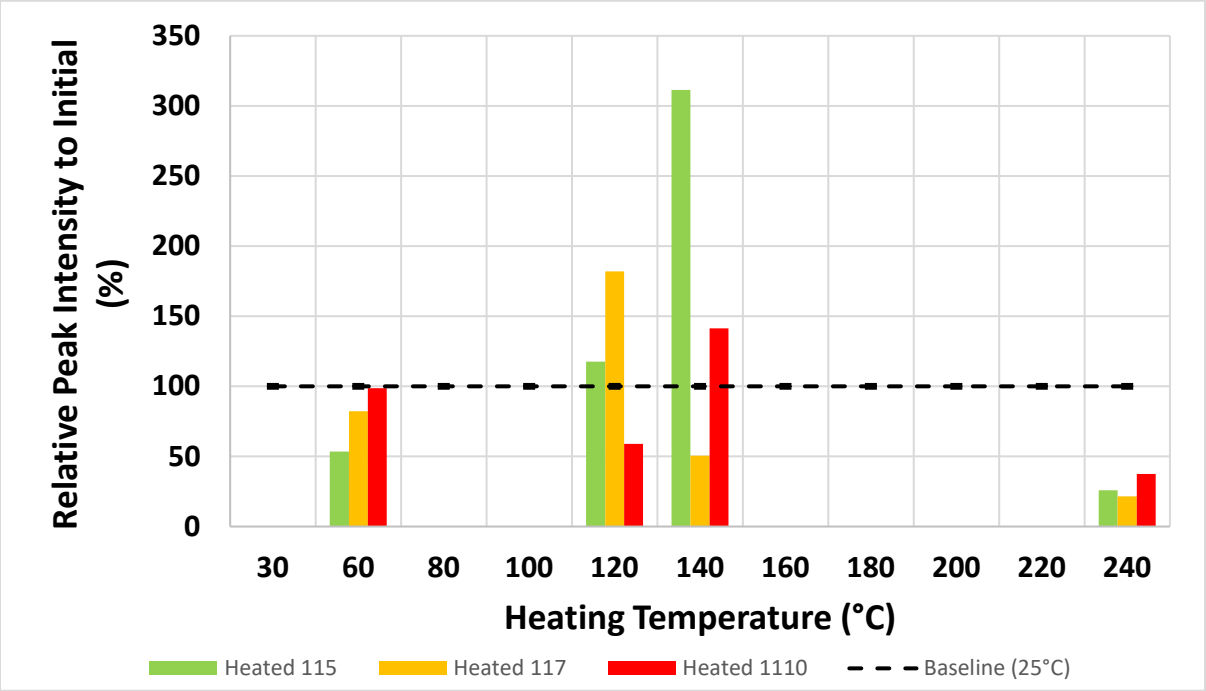

Figure 16: Calculated 115, 117 and 1110 Relative Peak Intensity for Peak II

Figure 17 shows the peak intensity ratio values for 115, 117 and 1110 at 25°C after being heated. A significant portion of these results deviated from the original baseline measurements. The only two measurements where the samples were the same as their baseline values were the 117 and 1110 heated to 60°C. Overall these results show a number of critical pieces of information that need to be mentioned. First, even though manufacturers typically suggest stacks be operated between 60°C-65°C, heating at 60°C was sufficient to permanently change the 115 material statistically outside the error bars. Further analysis would need to be conducted to determine the impact these structural changes had on actual material properties. A second point is all samples heated above 100°C did not return to their baseline when cooled. This final point is important since the material properties will most likely not be the same for subsequent stack operations, since changes to either the cross-linked polymer cluster orientation and/or size could easily change the material proton conduction. This in turn will make the stack performance not as consistent.

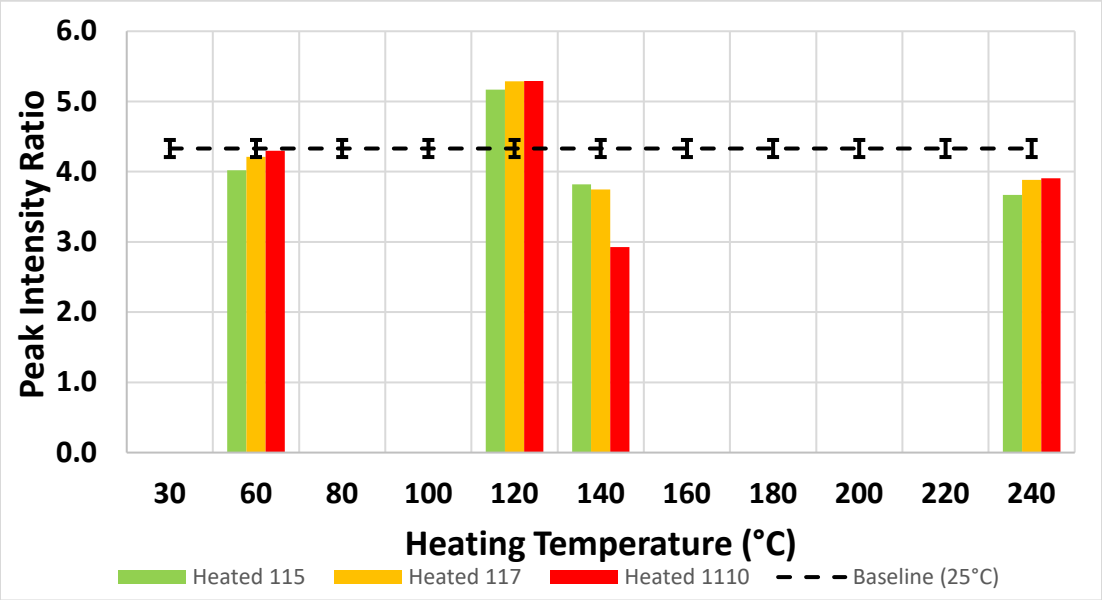

Figure 17: Calculated 115, 117 and 1110 Peak Intensity Ratios

6.3. Post-Heating Nafion© 115, 117 and 1110 XRD Measurements Summary

In summary, the following trends were observed for the 115, 117 and 1110 materials when returned to 25°C after being heated to 60°C, 120°C, 140°C and 240°C.

1. The 115 material was the most unstable. All its calculated parameters statistically deviated from its original baseline at all operating temperatures, except for the Peak II 2-Theta position, which did remain consistent for all temperatures.
2. The 117 material was the second most unstable material. All its calculated material parameters, except for the Peak II 2-Theta position and peak intensity ratio, statistically deviated from their original baseline values.
3. The 1110 material was the most stable. All its calculated material parameters were able to return to their baseline configuration after being heated to 60°C. Operating temperatures above 60°C resulted in permanent structural changes, which prevented the 1110 membrane from returning to its original baseline.
4. While all materials tested were unable to return to their original baseline after being heated above 100°C the material thickness was still an important factor. As sample thicknesses increased, calculated structural parameters deviated less from their respective its baseline. This is important since the actual material properties (such as proton conductivity, mechanical strength, etc) may be within an acceptable limit for the application using each membrane material. Evaluations of actual material properties still need to be correlated to these structural changes observed to determine their severity.

7. Impact of Heating Duration and Temperature on 115, 117 and 1110 In-Situ and Post-Heating Materials Structure Compared to Baseline XRD Measurements

7.1. Introduction

The characterization work performed in Sections 5 and 6 focused on the instantaneous impact temperature had on the membrane internal structural degradation during operation and after being returned to near room temperature. These previous characterization studies are important as they provided a preliminary look at how membrane thickness and temperature impacted the internal structure, but conclusions made from these analyses are not adequate for real-world applications. Two issues which need to be corrected with these previous tests are: 1. The heating duration of each test was too short compared to the duration expected in actual applications. Fuel cell stacks are expected to be operated for hours to days at a time, instead of a 10 minute hold and 2. Fuel cell stacks are operated near a constant temperature and heating at lower temperatures may influence the results of tests at elevated temperatures (such as testing the same sample at 120°C and then 160°C later).

The following characterization experiments assumed the fuel cell stack is operated either at a constant 60°C, 120°C or 140°C for 2, 8 or 24 hours. Heating samples at 240°C was not performed for these tests since all previous results have showed peak intensities diminished significantly aftet 200°C. The heating durations used are assumed to be adequate as stacks are hypothesized to be operated continuously from a few hours up to one day when used in combat vehicles. The 115, 117 and 1110 materials will be separately heated to those temperatures and then held for the specified amounts of time. As mentioned in Section 6 the Peak II calculated 2-Theta position was shown in the Supplementary Information section at the end of this paper for reference, since no changes were observed. Measurements taken while being heated will be compared to the XRD data taken in Section 6 (10 minute hold) while being heated, which has not been shown in this paper yet. Measurements taken after being cooled to 25°C will be compared to the previously reported data from Section 6 and baseline measurements. All samples had their baseline scans normalized as previously described in Section 4. Subsequently, all scans taken In-Situ and post-heating will also be normalized too. Since all the baseline scans used for the following samples look identical (due to being normalized) they will not be physically shown to improve plot readability. Please refer to the baseline scan information in Section 4 for reference. These baseline measurements will, however, be taken into account later in this section to analyze how the In-Situ and post-heating scans compare against their respective baseline scans.

7.2. Long-Term In-Situ and Post-Heating Nafion© 115, 117 and 1110 Raw XRD Scan Comparison

7.2.1. Raw XRD Scan Comparison In-Situ and Post-Heating at 60°C Operating Temperature

The following results investigate the effects of membrane thickness when heated to 60°C and held at that temperature for 2, 8 and 24 hours prior to taking raw XRD scans. Scans were also taken after each sample was cooled to 25°C to investigate how easily each sample could return to its baseline. As mentioned in Section 7.1 all the following In-Situ and post-heating scans will be characterized in much greater detail against their baseline measurements at the end of Section 7. The following results at 60°C simply compare structural changes that occurred as a function time In-Situ and post-heating.

Figure 18 shows the raw XRD scan data after heating the 115 membrane to 60°C and holding at that temperature for the different lengths of time. The raw data, at first glance, appears to relatively stable and both Peak I and II do not change shape or intensity significantly. This is an expected outcome since Nafion© is commonly used in PEM fuel cells operating at 60°C for prolonged periods of time.

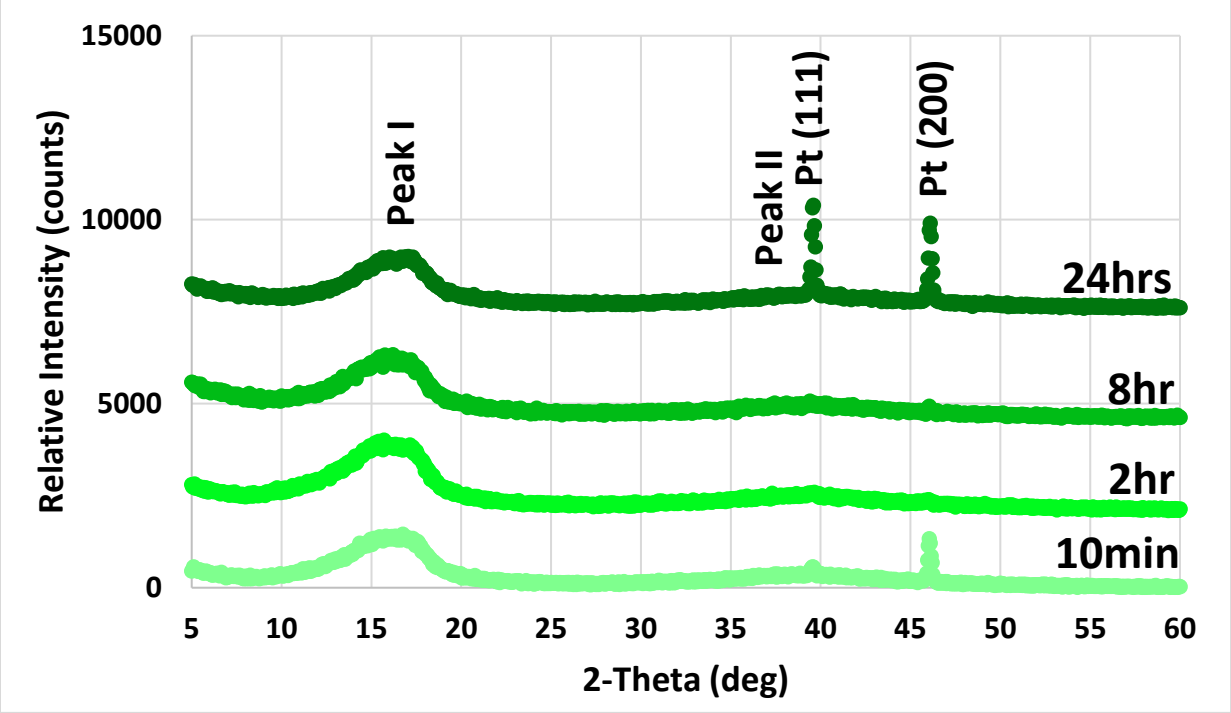

Figure 18: In-Situ Raw XRD Scans for 115 Taken after Heated to 60°C and held for 10 min, 2hrs, 8hrs and 24hrs.

Figure 19 shows the raw XRD scans, taken at 25°C, after heating the 115 membrane to 60°C. In a similar fashion to the 115 In-Situ results these post-heating scans appear to show the 115 did not change peak shape or intensity significantly, as a function of heating time, when returned to near room temperature.

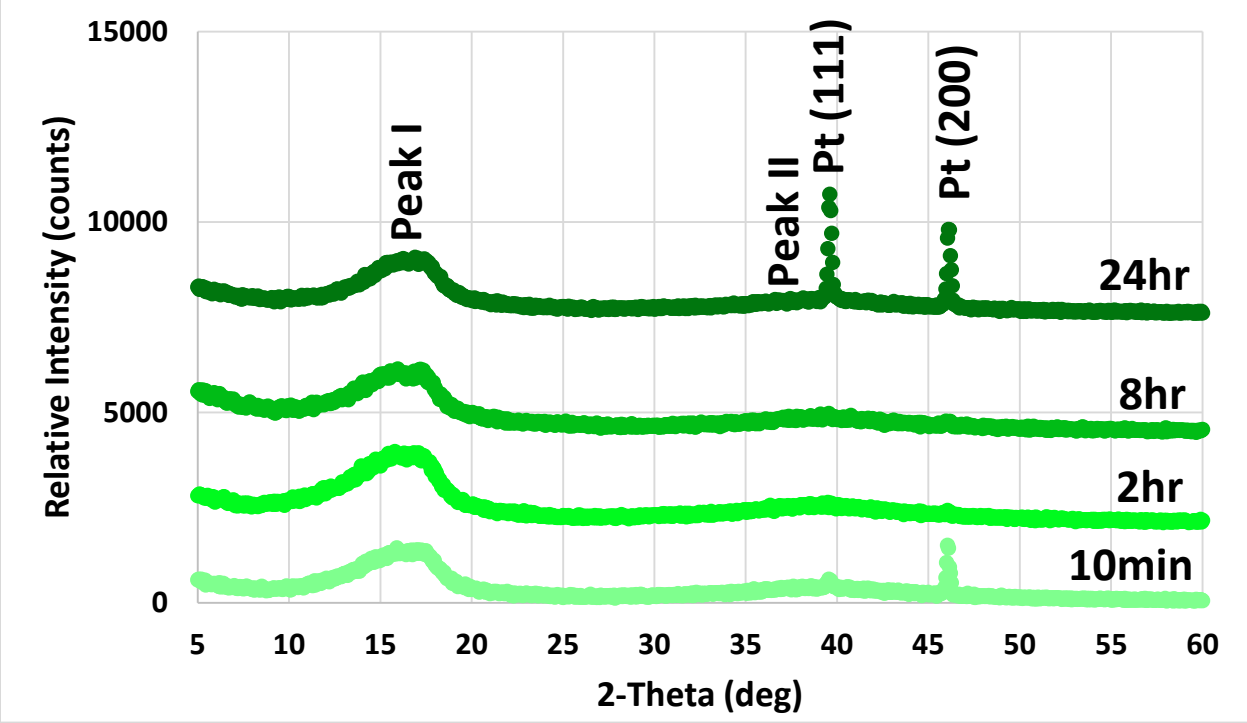

Figure 19: Post-Heating Raw XRD Scans for 115 Taken at 25°C after Heated to 60°C and held for 10 min, 2hr, 8hr, and 24hr.

Figure 20 shows the raw XRD scans after heating the 117 membrane to 60°C and holding at that temperature for the different lengths of time. The peak intensities for the 117 scans does not change significantly, but Peak I does appear to shift its position slightly to lower 2-Theta values as the heating duration was increased to 24 hours.

Figure 21 shows the raw XRD scans, taken at 25°C, after heating the 117 membrane to 60°C. These post-heating results show noticeable changes to both the peak intensity and position as a function of time. Both the 2 and 8 hour samples showed reduced peak intensities, which indicate the polymer is depolymerizing. After 24 hours peak intensities drastically increased, which signals the membrane then started to crystalize.

Figure 22 shows the raw XRD scans after heating the 1110 membrane to 60°C and holding at that temperature for the different lengths of time. In a similar fashion to the In-Situ 115 and 117 results these scans show the 1110 membrane did not change significantly as a function of time. If Peak I did change in position it was minimal and was not noticeable from visual observation of this plot.

Figure 23 shows the raw XRD scans, taken at 25°C, after heating the 1110 membrane to 60°C. Unlike the post-heating 117 membrane, the 1110 does not show any noticeable change in peak intensity, however a small side peak can be seen on Peak I after being heated for 24 hours. This was not something observed in any of the 115 or 117 post-heating scans and, as mentioned previously, could indicate subtle changes to the material phase or composition. Changes in the 1110 material composition or phase may be less pronounced due to the membrane being thicker.

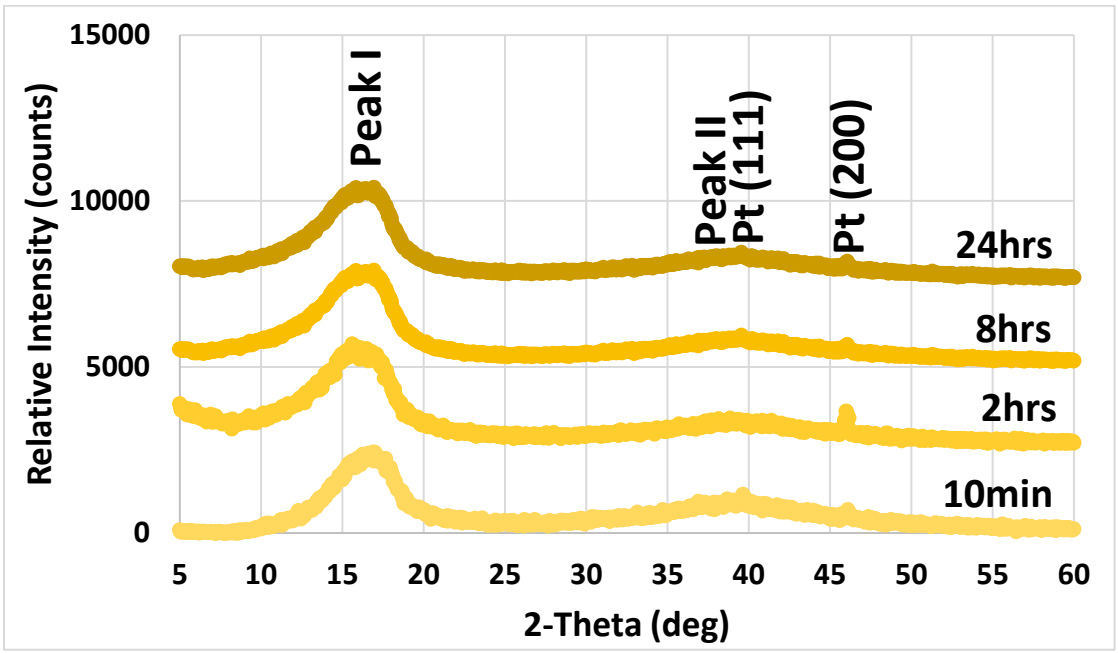

Figure 20: In-Situ Raw XRD Scans for 117 Taken after Heated to 60°C and held for 10 min, 2hrs, 8hrs and 24hrs.

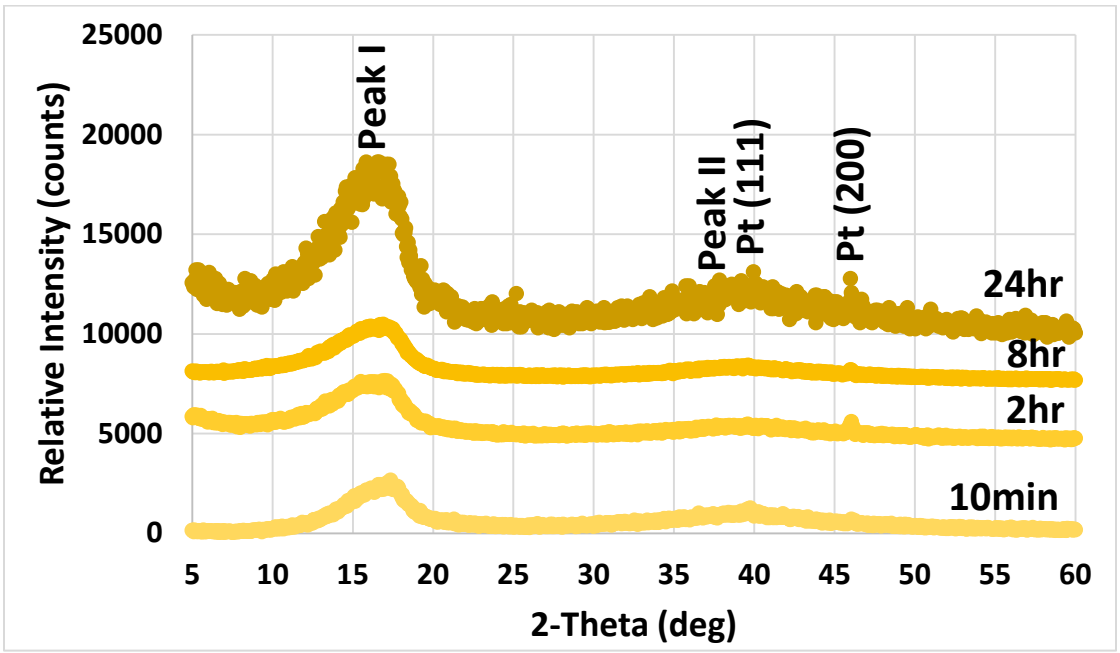

Figure 21: Post-Heating Raw XRD Scans for 117 Taken at 25°C after Heated to 60°C and held for 10 min, 2hr, 8hr, and 24hr.

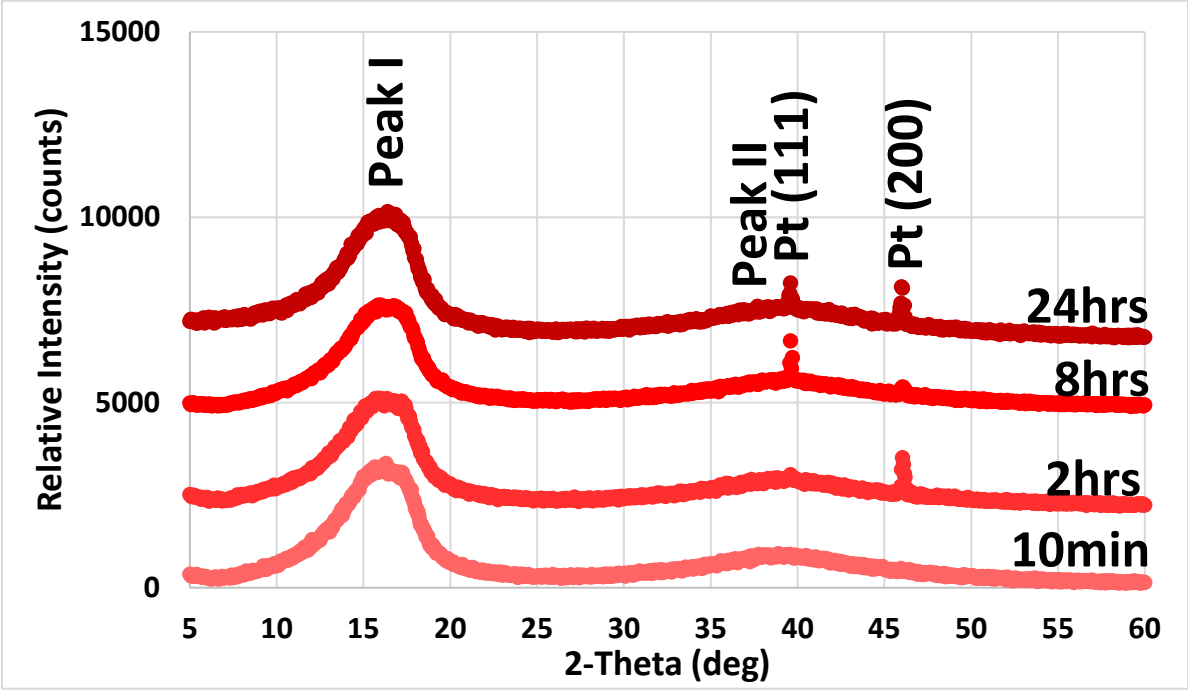

Figure 22: In-Situ Raw XRD Scans for 1110 Taken after Heated to 60°C and held for 10 min, 2hrs, 8hrs and 24hrs.

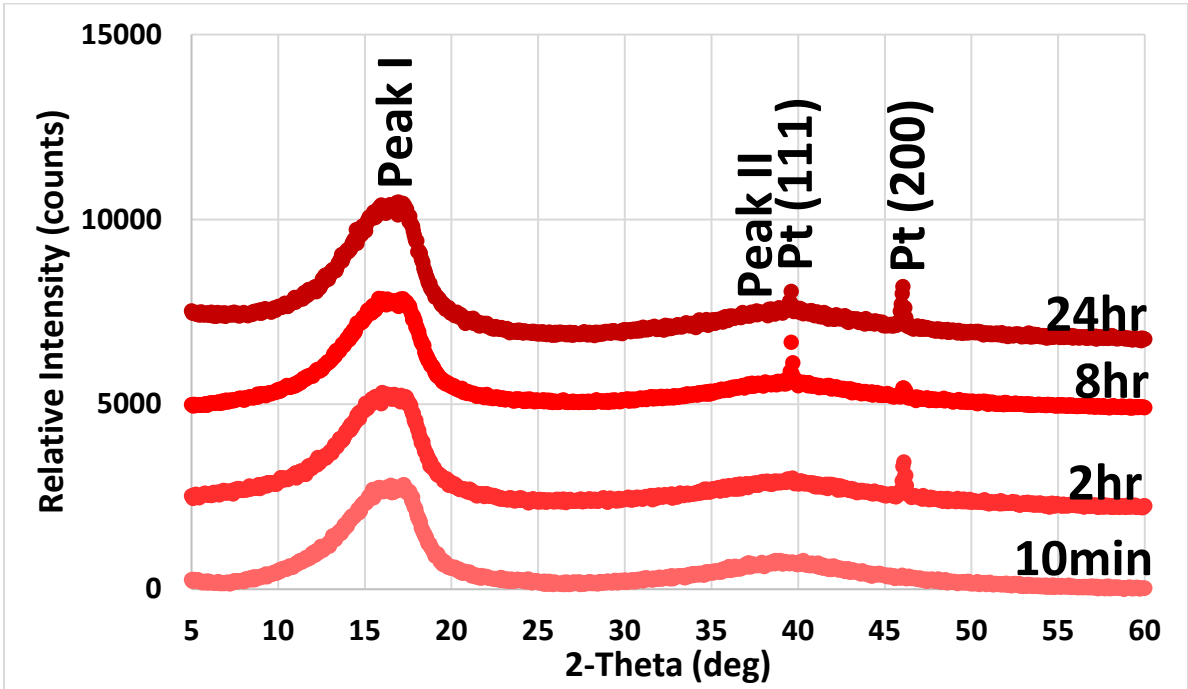

Figure 23: Post-Heating Raw XRD Scans for 1110 Taken at 25°C after Heated to 60°C and held for 10 min, 2hr, 8hr, and 24hr.

7.2.2. Raw XRD Scan Comparison In-Situ and Post-Heating at 120°C Operating Temperature

Figure 24 showed the raw XRD scans after heating the 115 membrane to 120°C and holding at that temperature for 2, 8 and 24 hours. The results, for the most part, stayed relatively similar to each other. There does appear to be a small increases and decreases in the Peak I and II intensities, which were influenced by the heating duration. For example, samples heated for 2 hours showed an increase in peak intensity, compared to samples heated for 10 minutes, while samples heated for 8 and 24 hours showed a decrease.

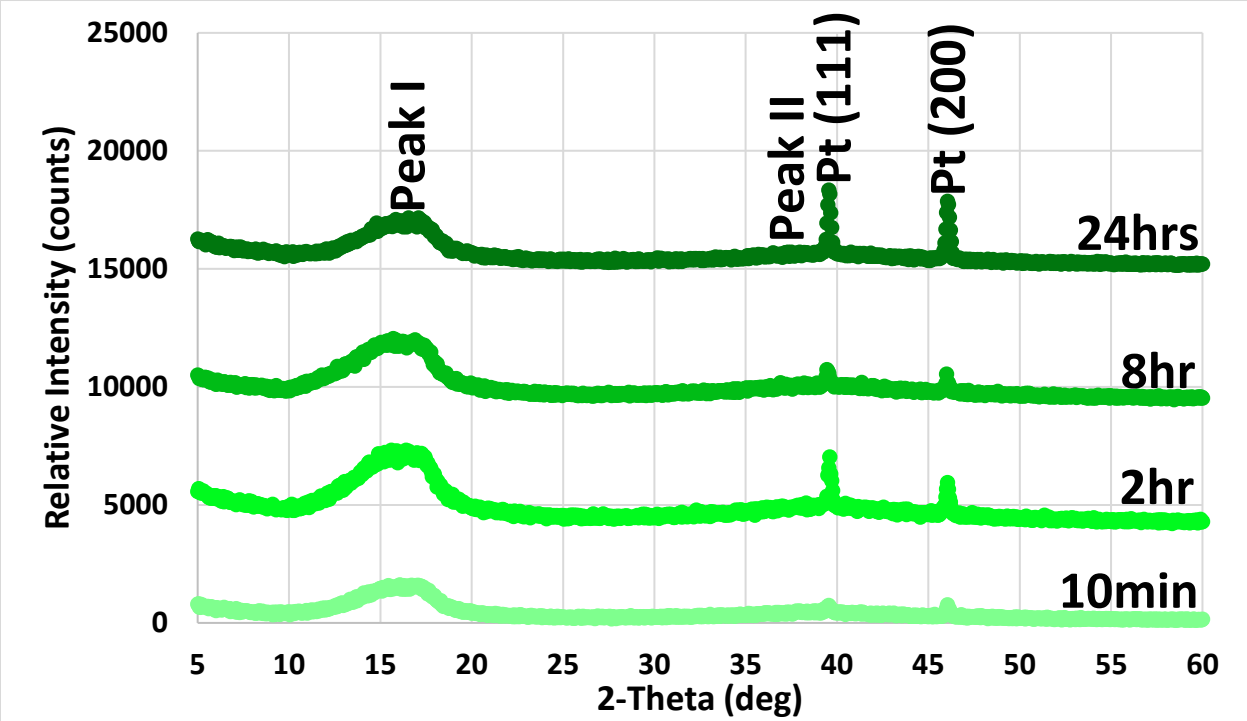

Figure 24: In-Situ Raw XRD Scans for 115 Taken after Heated to 120°C and held for 10 min, 2hrs, 8hrs and 24hrs.

Figure 25 showed the raw XRD scans, taken at 25°C, after heating the 115 membrane to 120°C. Unlike the 60°C post-heating result heating at 120°C significantly increased peak intensity of the 115 samples after being cooled to 25°C. The percentage that peaks increased that intensities were more substantial after being heated for 2 hours, but then did not change noticeably afterwards. Peak II did appear to be reduced in comparison to Peak I after 24 hours of heating, which may suggest a restructuring of the preferred orientation occurred. Similar to the 60°C 1110 post-heating results a side peak appeared on the right side of Peak I, but is much more noticeable possibly due to the increased operating temperature used. As mentioned previously the addition of a side peak can indicate the sample is forming additional phases or the sample symmetry is changing. Since the polymer does not have a pre-defined crystal structure the addition of peaks may point towards changes in the polymer chain backbone structure.

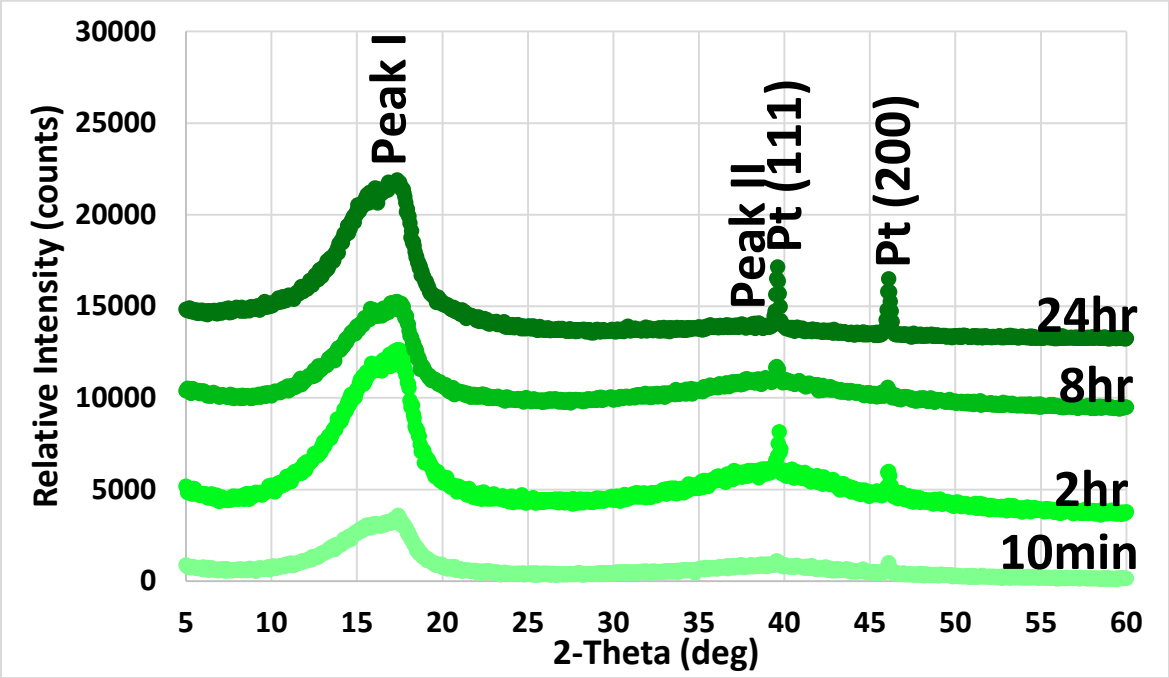

Figure 25: Post-Heating Raw XRD Scans for 115 Taken at 25°C after Heated to 120°C and held for 10 min, 2hr, 8hr, and 24hr.

Figure 26 showed the raw XRD scans after heating the 117 membrane to 120°C and holding at that temperature for 2, 8 and 24 hours. The 117 membrane structural durability was compromised significantly more after being heated to 120°C, then what was observed for 60°C. A loss in structural durability occurred through changes to peak intensity, shape and position. First, Peak I lowered its 2-Theta position slightly, as the heating duration was increased. Next, the Peak I and II intensities were increased after being heated for the initial 10 minute hold experiment at 120°C, but then was reduced in intensity drastically for the remainder of the heating durations. Finally, a side peak formed on Peak I again and remained visible for all heating duration XRD scans.

Figure 27 shows the raw XRD scans, taken at 25°C, after heating the 117 membrane to 120°C. Many of the same structural changes previously described were observed here. Overall the impact of these structural alterations resulted in the 117 polymer not being capable of returning to its baseline scan conditions. Peak intensities for both Peak I and II increased and decreased as a function of time, however no clear trends could be discerned. The same side peak formed on Peak I but is more noticeable. Finally, the only process which was not observed was Peak I shifting it 2-Theta position.

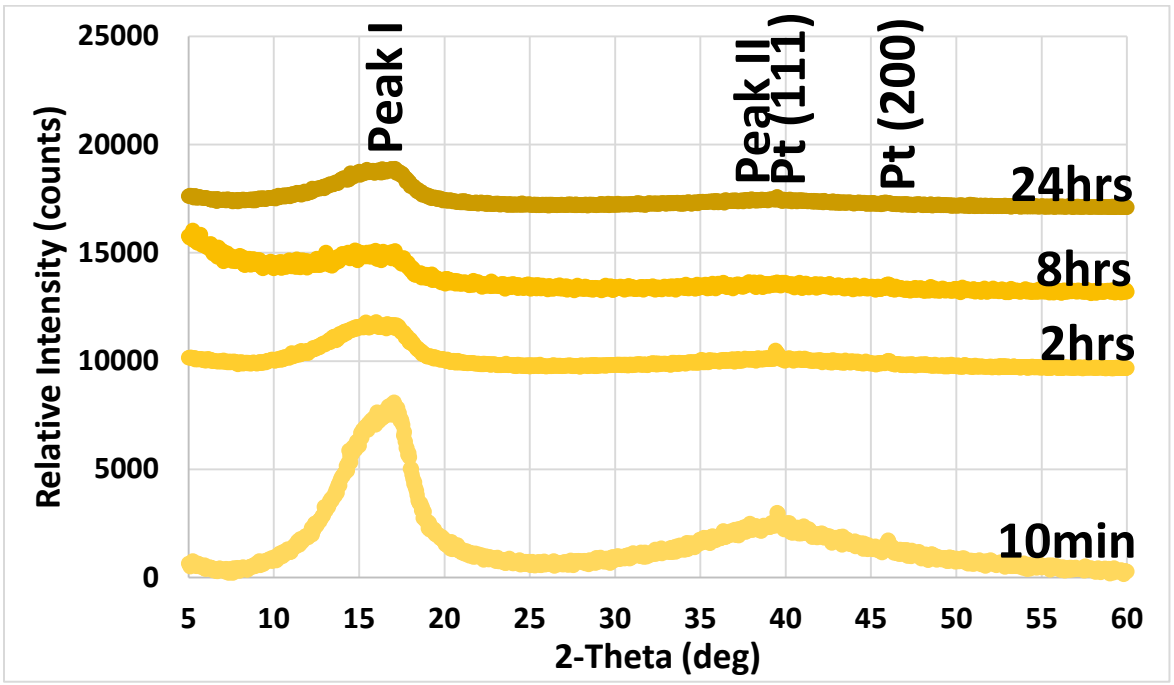

Figure 26: In-Situ Raw XRD Scans for 117 Taken after Heated to 120°C and held for 10 min, 2hrs, 8hrs and 24hrs.

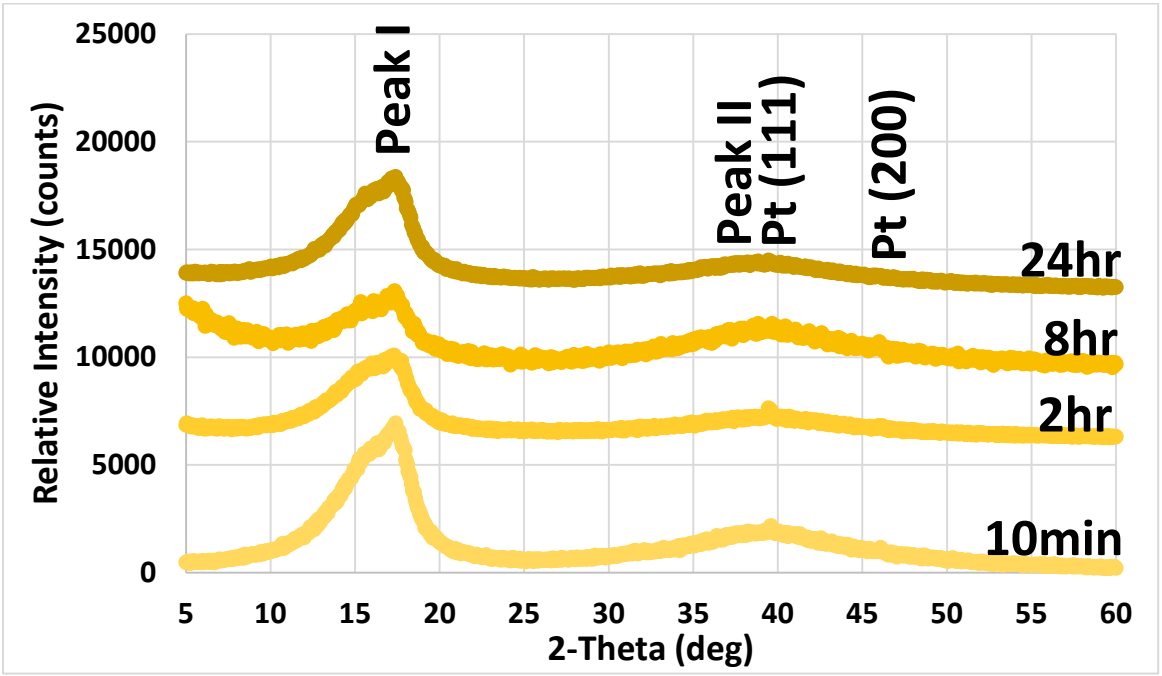

Figure 27: Post-Heating Raw XRD Scans for 117 Taken at 25°C after Heated to 120°C and held for 10 min, 2hr, 8hr, and 24hr.

Figure 28 showed the raw XRD scans after heating the 1110 membrane to 120°C and holding at that temperature for the different lengths of time. The 1110 membrane material appeared to not fluctuate its Peak I or II intensities as significantly as the 115 or 117 materials, but still did show alterations. Peak I showed the small side peak had shifted its 2-Theta position, but these are not as severe as was observed with 115 and 117 and simply may be the result of the 1110 membrane having increased thickness.

Figure 29 showed the raw XRD scans, taken at 25°C, after heating the 1110 membrane to 120°C. As had been observed with the 115 and 117 membrane materials the post-heated 1110 results also showed significant changes to peak intensity, position and shape. As previously mentioned with the 117 membrane these changes were significantly and prevented any 1110 sample from returning to its baseline. Observed irregularities included: 1. Peak I and II increasing and decreasing their peak intensities as a function of time, 2. Peak I changing its 2-Theta position, and 3. A side peak forming on Peak I. As with the 117 120°C results these observations also did not follow a trend as a function of time.

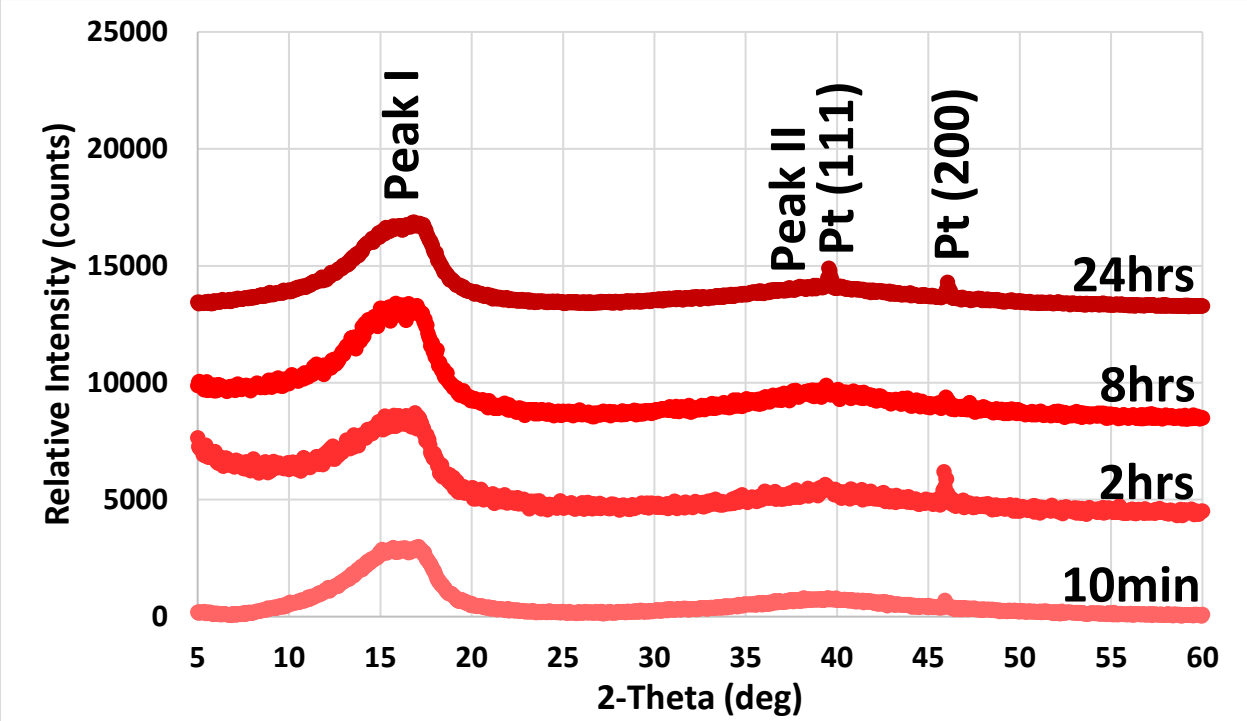

Figure 28: In-Situ Raw XRD Scans for 1110 Taken after Heated to 120°C and held for 10 min, 2hrs, 8hrs and 24hrs.

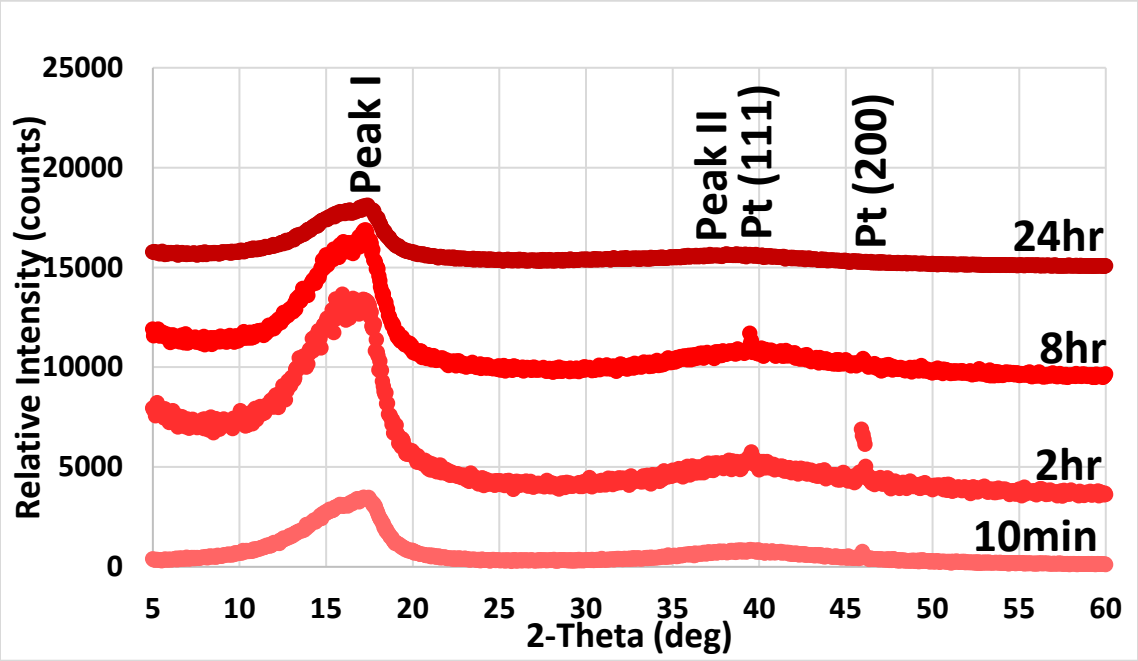

Figure 29: Post-Heating Raw XRD Scans for 1110 Taken at 25°C after Heated to 120°C and held for 10 min, 2hr, 8hr, and 24hr.

7.2.3. Raw XRD Scan Comparison In-Situ and Post-Heating at 140°C Operating Temperature

Figure 30 showed the raw XRD scans after heating the 115 membrane to 140°C and holding at that temperature for 2, 8 and 24 hours. While the previous two In-Situ 115 raw XRD plots did not show drastic changes that could be observed visually these raw XRD results start to depict noticeable changes. The most noticeable observable structural changes were the Peak I intensity started to increase as the heating duration increased as well as a side peak forming on Peak I.

Figure 31 showed the raw XRD scans, taken at 25°C, after heating the 115 membrane to 140°C. These results are some of the most dramatic yet with large swings in peak intensity, position and shape. The shape of Peak I, after 24 hours of heating, appeared very differently from what had been observed in previous sections. The shape of Peak I, previously, was broad with a rounded top but the 24 hour scan showed Peak I as tall with a pointy top. The top of the peak also occurred where the side peak appeared earlier.

Figure 32 showed the raw XRD scans after heating the 117 membrane to 140°C and holding at that temperature for 2, 8 and 24 hours. The 117 membrane did not show significant changes while being heated as a function of time. This lack of noticeable change in the 117 structure happens in stark contrast to the In-Situ changes observed when heating to 120°C. This is hypothesized to happen due to the polymer for the following reason. When looking back at Section 5 the Peak I and II intensities for 117 showed a large increase in peak intensity when heated at 140°C. Being at the top of this crystallization peak may provide some increased structural stability as a function of time.

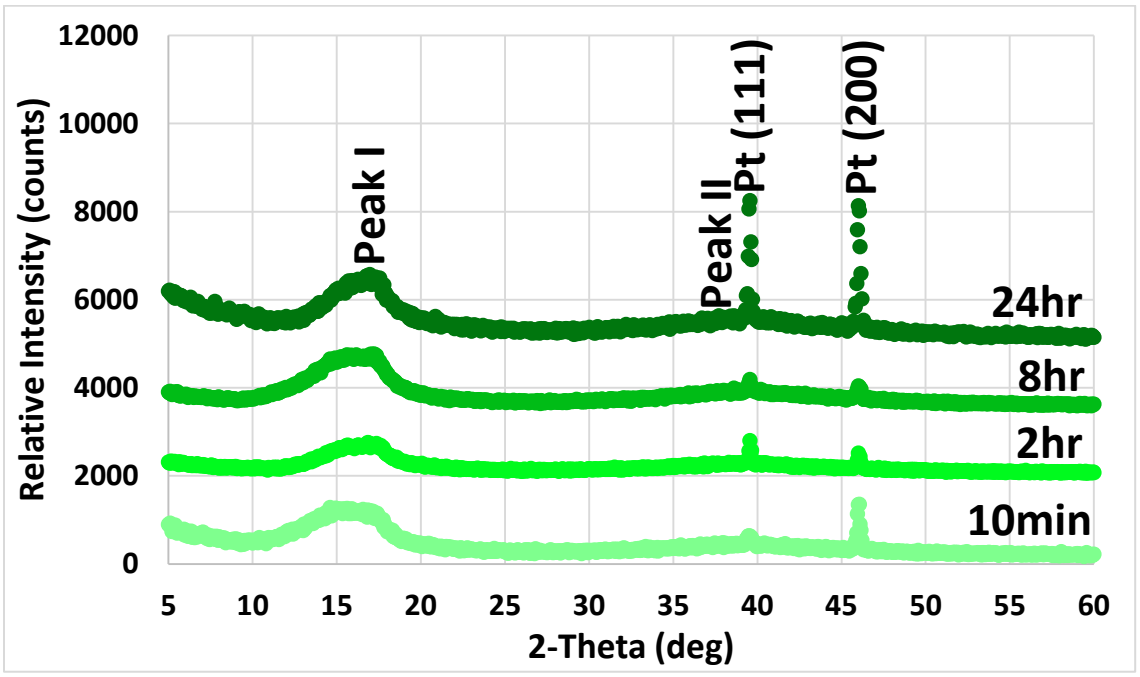

Figure 30: In-Situ Raw XRD Scans for 115 Taken after Heated to 140°C and held for 10 min, 2hrs, 8hrs and 24hrs.

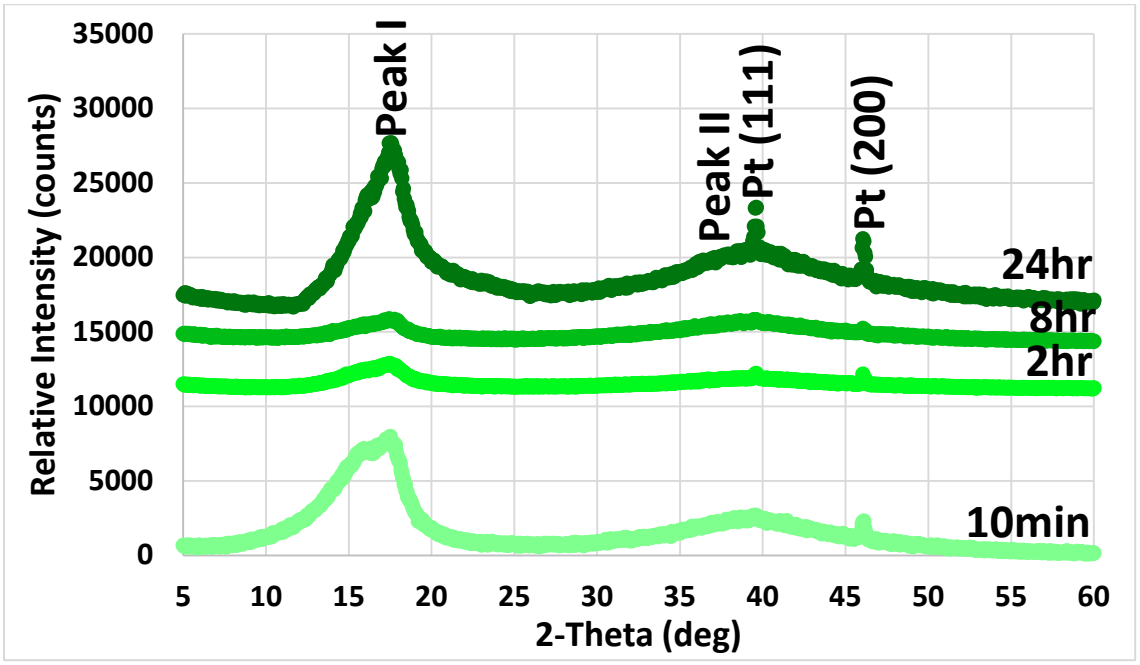

Figure 31: Post-Heating Raw XRD Scans for 115 Taken at 25°C after Heated to 140°C and held for 10 min, 2hr, 8hr, and 24hr.

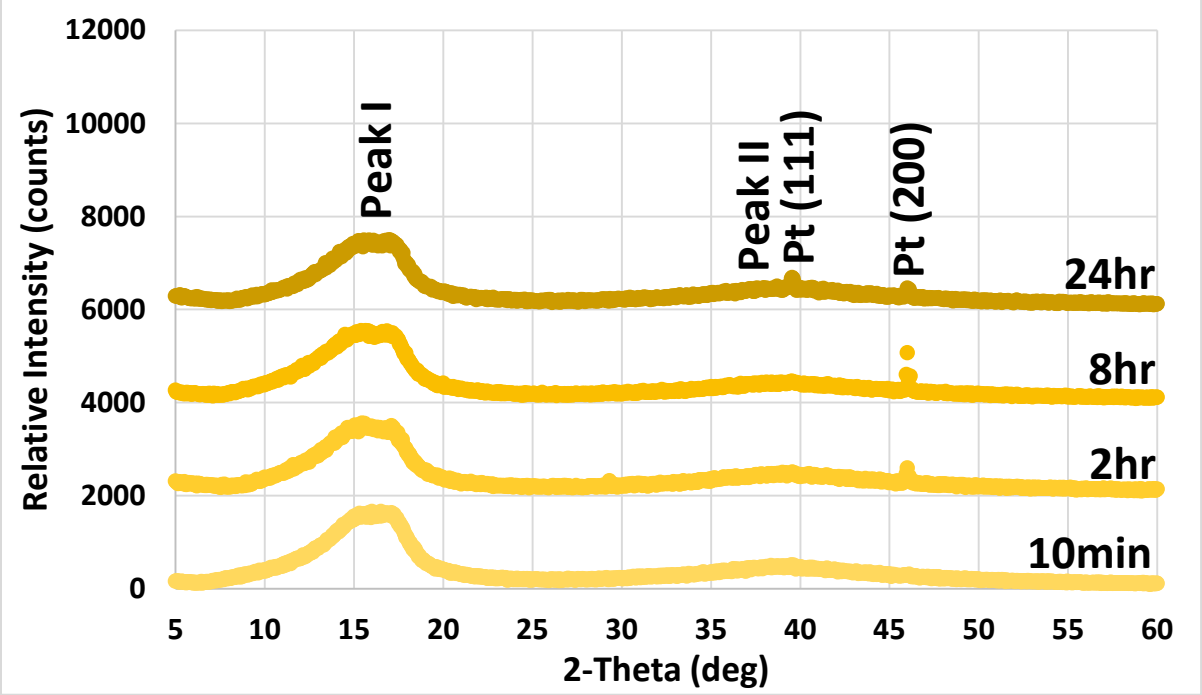

Figure 32: In-Situ Raw XRD Scans for 117 Taken after Heated to 140°C and held for 10 min, 2hrs, 8hrs and 24hrs.

Figure 33 showed the raw XRD scans, taken at 25°C, after heating the 117 membrane to 140°C. The observed results show similar trends as other post-heating scans. Peak I and II changed the intensities as a function of heating duration, Peak I altered its 2-Theta position and the side peak made an appearance too. The increased peak intensity observed in Section 5, which was mentioned for the 140°C In-Situ results, may have influenced the membrane post-heating results seen here. One possible hypothesis is an increase in peak intensity during operation could either be caused by increased crystallinity or a change in the preferred orientation. These In-Situ changes initially may disrupt the polymer resulting in a different preferred orientation when cooled. This is supported by the 2 hour scan showing a significant reduction in Peak I intensity but Peak II appeared to increase it intensity, thus indicating the Peak II position is potentially preferred. Continued exposure to the increased In-Situ peak intensity after 8 and 24 hours showed the sample changed its preferred orientation to Peak I. This change could be the result of the stress state of the sample being reduced, such as during an annealing procedure.

Figure 34 showed the raw XRD scans after heating the 1110 membrane to 140°C and holding at that temperature for 2, 8 and 24 hours. Even though the 1110 membrane was resistant to degradation for the previous two operating temperature it started to noticeably degrade when heated to 140°C. The primary changes observed were peak intensity changes, but these were larger than previously observed at 60°C or 120°C. Despite this, even at 140°C, the 1110 material was the most stable and appeared to have the least number of changes as a function of time.

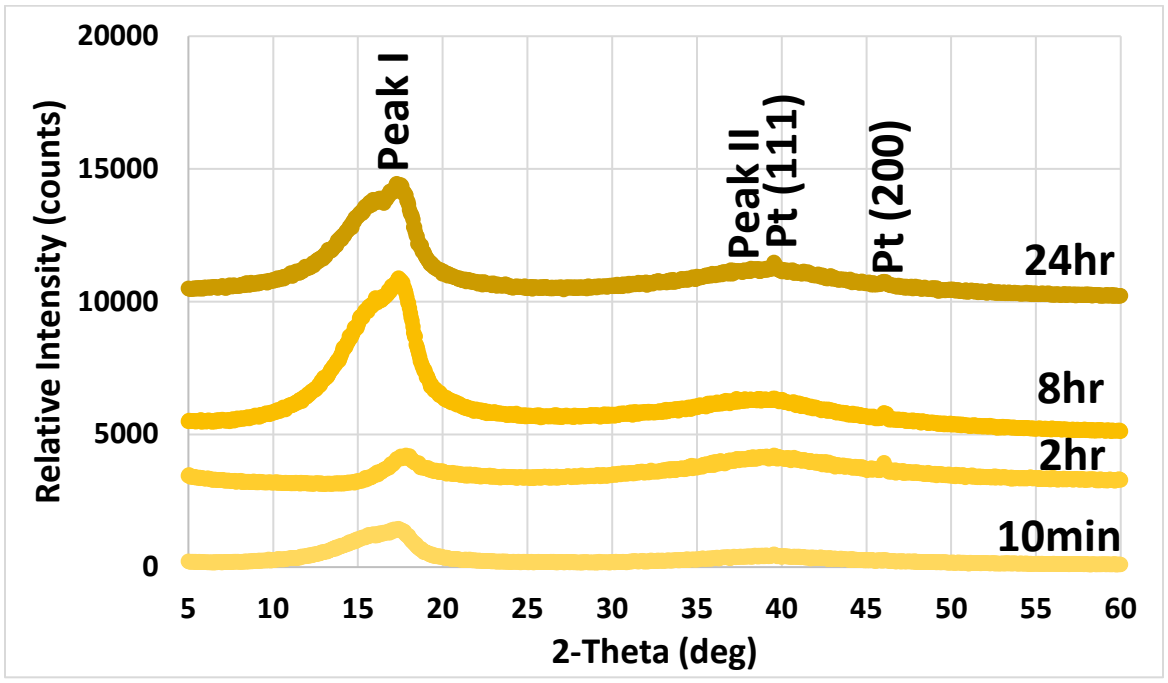

Figure 33: Post-Heating Raw XRD Scans for 117 Taken at 25°C after Heated to 140°C and held for 10 min, 2hr, 8hr, and 24hr.

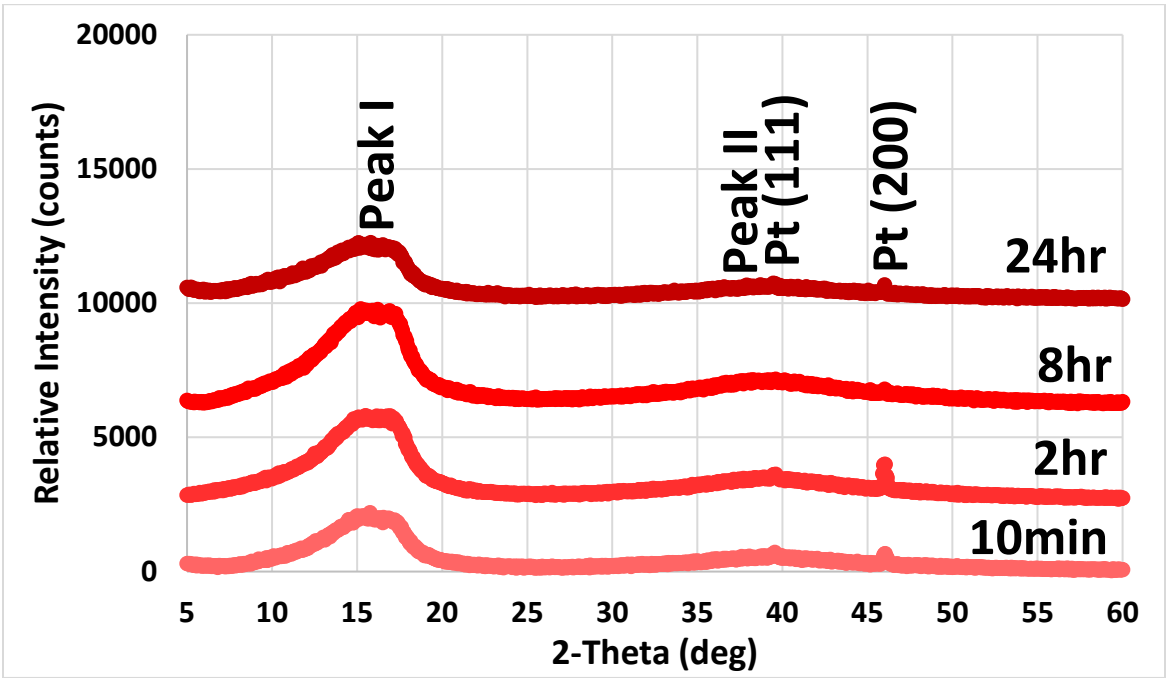

Figure 34: In-Situ Raw XRD Scans for 1110 Taken after Heated to 140°C and held for 10 min, 2hrs, 8hrs and 24hrs.

Figure 35 showed the raw XRD scans, taken at 25°C, after heating the 1110 membrane to 140°C. Peak intensity was observed to increase with time and the additional side peak was also present too. Section 5 also showed a large In-Situ peak intensity increase at 140°C for 1110. As was discussed the increased peak intensity may imprint itself onto the polymer over time. The results shown for the post-heating 1110 material indicate the increased Peak I and II intensities were the result of increased sample crystallinity since both peaks increased similar amounts between experiments. Even with these post-heating results the 1110 membrane appeared the most stable of the three membranes tested.

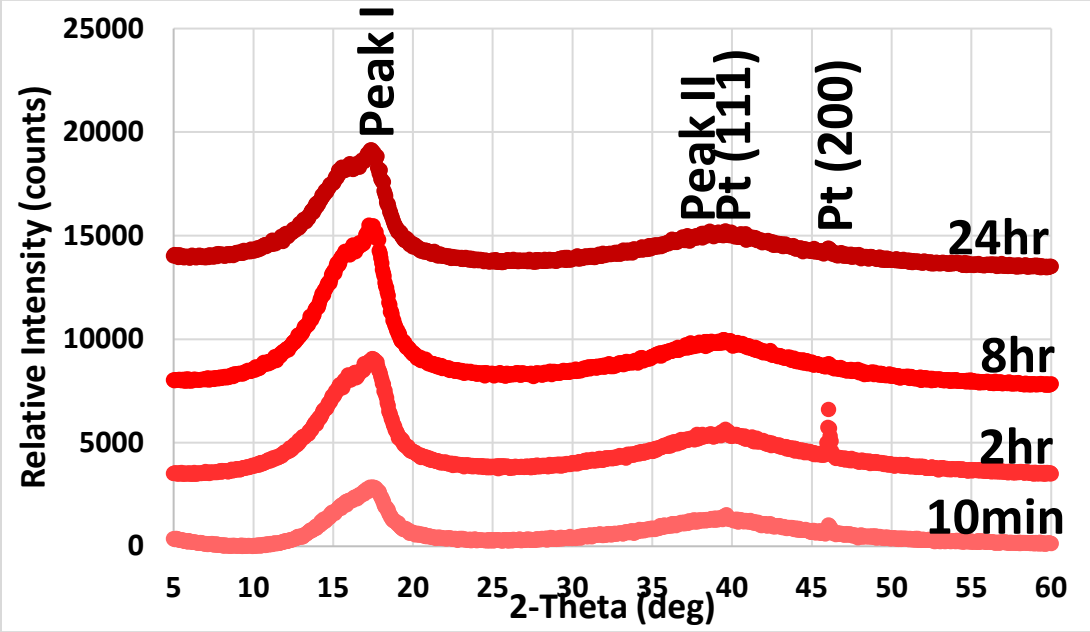

Figure 35: Post-Heating Raw XRD Scans for 1110 Taken at 25°C after Heated to 140°C and held for 10 min, 2hr, 8hr, and 24hr.

7.3. Long-Term In-Situ and Post-Heating In-Depth Analysis of Nafion© 115, 117 and 1110 Raw XRD Scans at 60°C, 120°C and 140°C Operating Temperatures

The following results will take a much more in-depth analysis of the raw data provided in Sections 7.2.2, 7.2.3 and 7.2.4 outlining the changes observed. Analysis of the parameters calculated in this section provide the following information which analysis of the previous sections did not provide. First, Section 6 was focused on understanding changes that occurred to each material post-heating using a 10 minute hold for each temperature. Here, heating duration is also a consideration in addition to temperature and membrane thickness. Second, Section 6 characterized post-heating effects but this sectioned compared both the In-Situ and post-heating results. Following the same established pattern the In-Situ information will be analyzed first followed by the post-heating information. The horizontal dashed line in each plot represents the average baseline value for each parameter being analyzed so deviations from the baseline

can be more easily identified. One final point to mention is that since the time scale on the x-axis uses increments of 1 hour samples heated for 10 minutes appeared at the 0 hour mark on the x-axis.

7.3.1. In-Depth In-Situ and Post-Heating Analysis at 60°C Operating Temperature

Figure 36 showed the 60°C In-Situ Peak I 2-Theta positions for 115, 117 and 1110 after being heated for 10 minutes and 2, 8 and 24 hours. These results confirm the Peak I 2-Theta position did not change drastically for any of the samples tested as a function of time. However, when compared to the baseline a different perspective is shown. The 115 and 117 peak positions were altered the most when compared to their respective baselines with average of deviations of 2.1% and 1.9% respectively. These are substantially larger than the 1110 which had on average only deviated 0.5% from the baseline.

Figure 37 showed the 60°C In-Situ relative Peak I intensity, for 115, 117 and 1110 after being heated for 10 minutes and 2, 8 and 24 hours, as a percentage of its original baseline intensity. The raw data originally indicated that all three membrane materials were relatively stable from just a visual inspection. Closer examination shows that peak intensities do change with time more than first observed. Over the course of 24 hours the 115 varied by 13%, the 117 by 17% and the 1110 by 8.5%. In addition to these temporal peak intensity changes the 115 constantly has a much lower peak intensity than its baseline, and was not able to return to its baseline. These point reinforce the fact the 115 membrane has the lowest structural stability, even when heated to 60°C Both the 117 and 1110 demonstrated more stability and, for the majority of the experiments, were able to return to their original baseline measurements.

Figure 38 showed the 60°C In-Situ relative Peak II intensity, for 115, 117 and 1110 after being heated for 10 minutes and 2, 8 and 24 hours, as a percentage of its original baseline intensity. The relative Peak II intensity values are similar to the relative Peak I intensity values listed above. There are some small differences where the 117 does not appear to deviate quite as much for Peak II, but all other results follow a similar trend as Peak I did.

Figure 39 showed the 60°C In-Situ ratio between Peak I and Peak II for 115, 117 and 1110 after being heated for 10 minutes and 2, 8 and 24 hours. Peak ratios are calculated by dividing the Peak I intensity by the Peak II intensity. Overall, all three materials show some change in their ratio values when heated. The 115 changed the most, while the 117 and 1110 have similar average ratios for all their samples and deviate from the baseline about 0.3-1.2%, which was statistically not significant.

Figure 40 showed the 60°C post-heated Peak I 2-Theta positions for 115, 117 and 1110 taken at 25°C after being heated for 10 minutes and 2, 8 and 24 hours. All three materials showed some deviation from the baseline after returning to 25°C. 115 showed the largest average deviation from the baseline with a ~2.20% average increase over the baseline. The 117 showed the second most change with an average increase of ~1.50% and the 1110, on average, appear to be the most stable and consistent averaging an increase of ~0.75% in its Peak I 2-Theta position.

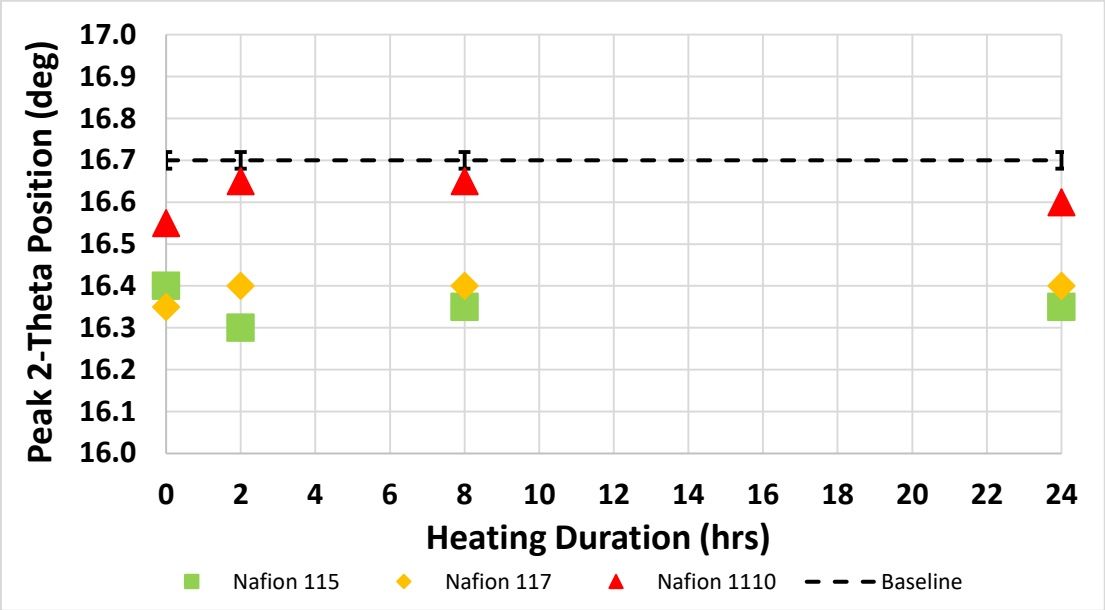

Figure 36: In-Situ Calculated 115, 117 and 1110 2-Theta Peak I Position after Heated to 60°C for 10 min, 2hr, 8hr and 24hr. Results Compared to Peak I Baseline Measurements.

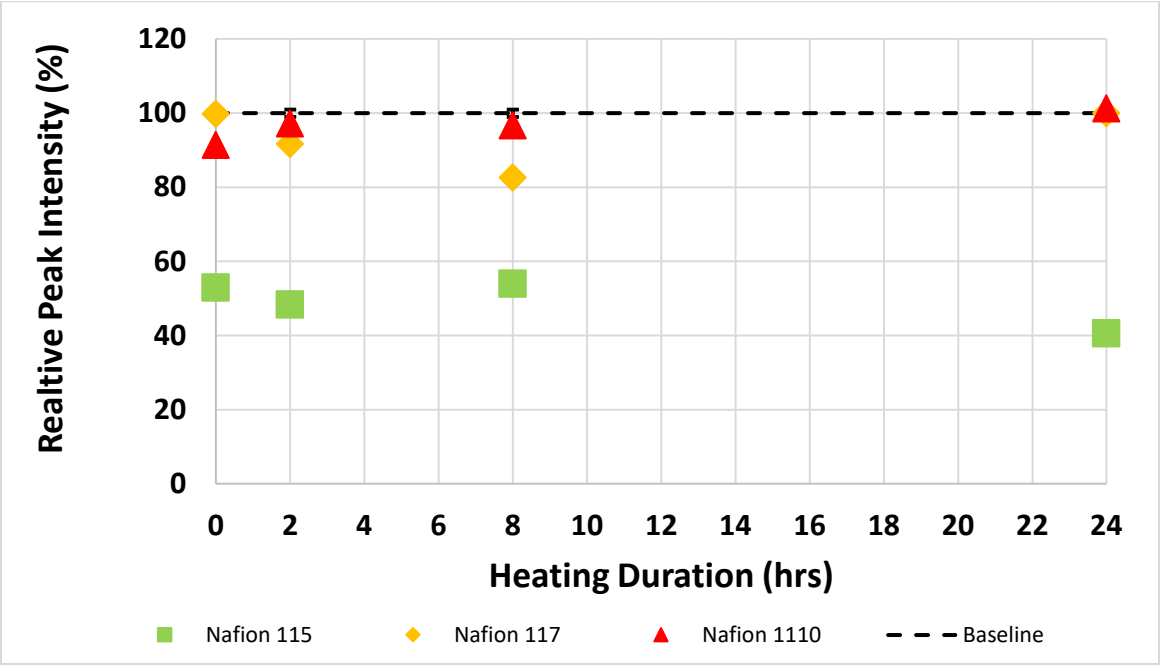

Figure 37: In-Situ Calculated 115, 117 and 1110 Relative Peak I Intensity after Heated to 60°C for 10 min, 2hr, 8hr and 24hr. Results are Compared to Baseline Measurements.

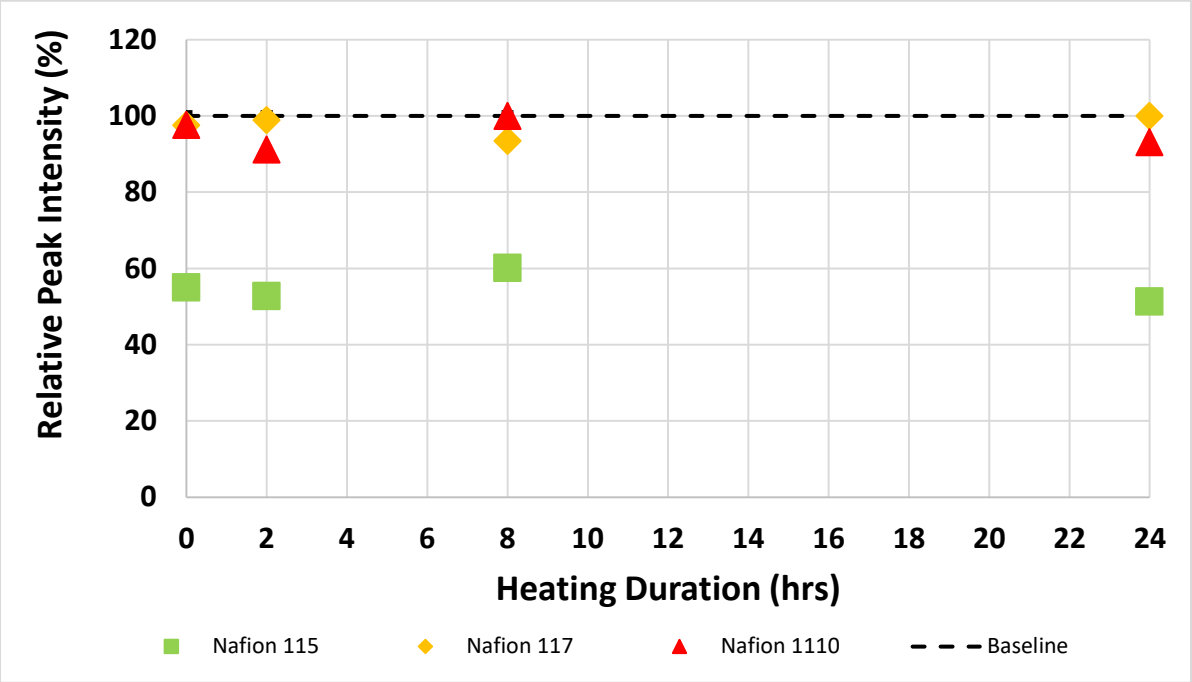

Figure 38: In-Situ Calculated 115, 117 and 1110 Relative Peak II Intensity after Heated to 60°C for 10 min, 2hr, 8hr and 24hr. Results are Compared to Baseline Measurements.

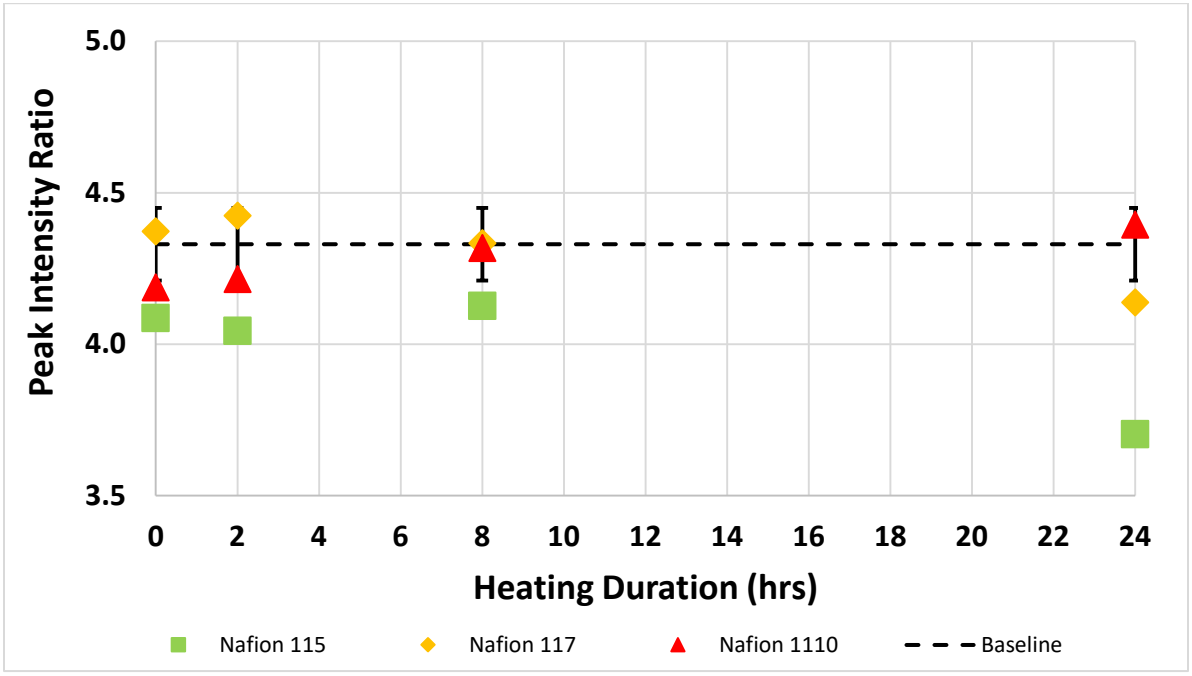

Figure 39: In-Situ Calculated 115, 117 and 1110 Peak Ratio Intensities after Heated to 60°C for 10 min, 2hr, 8hr and 24hr. Results are Compared to Baseline Measurements.

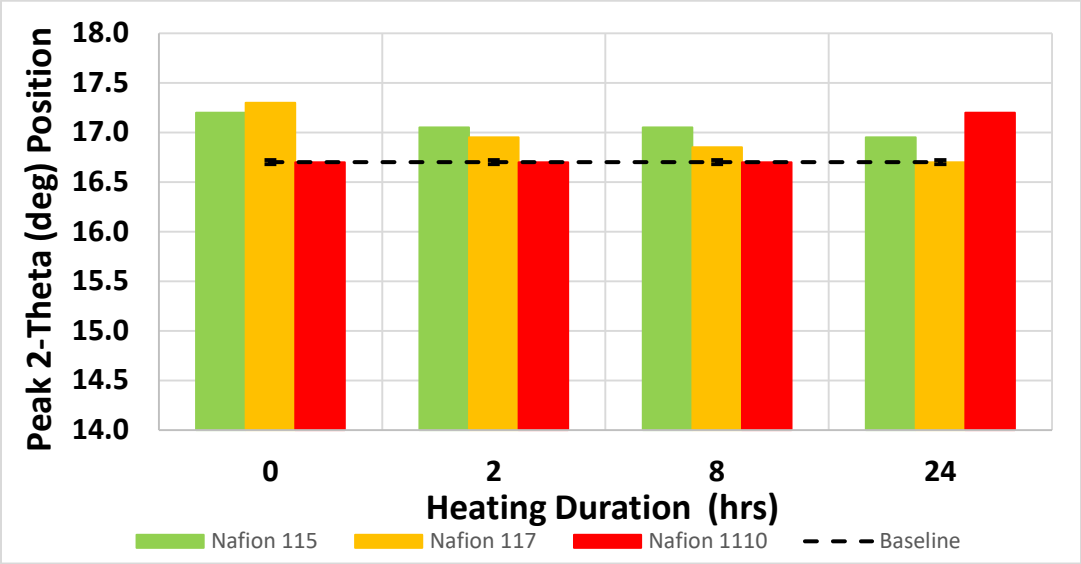

Figure 40: Post-Heating Calculated 115, 117 and 1110 2-Theta Peak I Position Taken at 25°C after Heated at 60°C for 10 min, 2hr, 8hr and 24hr. Results Compared to Peak I Baseline Measurements.

Figure 41 showed the 60°C post-heating relative Peak I intensity for 115, 117 and 1110 after being heated for 10 minutes and 2, 8 and 24 hours, as a percentage of its original baseline intensity. The 115 consistently had lower Peak I intensities than its baseline. Since Peak I intensities are similar to Peak II this suggests the membrane was depolymerized, instead of having its preferred orientation changed. The level of depolymerization also stayed relatively constant with time but did slightly increase over time. The 117 also showed an ~20% decrease in its Peak I intensity which was still closer to the baseline than 115. This decrease in intensity lasted until the sample was heated for 24 hours and then increased it peak intensity by ~140% above the baseline. As the 115 these intensity changes observed with the 117 are also viewed to be cause by depolymerization and crystallization. These results show that despite 117 having a thicker membrane it was not completely immune to degradation. The 1110 membrane was much more stable and returned to its baseline in almost all the tests.

Figure 42 showed the 60°C post-heating relative Peak II intensity, for 115, 117 and 1110 after being heated for 10 minutes and 2, 8 and 24 hours, as a percentage of its original baseline intensity. The trends observed for Peak II match very closely to Peak I described above. The 1110 membrane thickness is still relatively stable compared to the other two and did not deviate significantly from the baseline, while the 117 and 115 showed a much larger variation.

Figure 43 showed the 60°C post-heating ratio between Peak I and Peak II for 115, 117 and 1110 taken at 25°C after being heated for 10 minutes and 2, 8 and 24 hours. Peak ratios are calculated by dividing the Peak I intensity by the Peak II intensity. Overall the peak ratio values for all three materials was stable with heating time but were still offset from the baseline, some more than others. The 115 showed the largest difference from the baseline and was always statistically below the baseline. The 117, for the most part, stayed relatively consistent with the baseline except after being heated for 24 hours and then deviated. The 1110 was the most stable and was always within the error bars of the baseline calculated value.

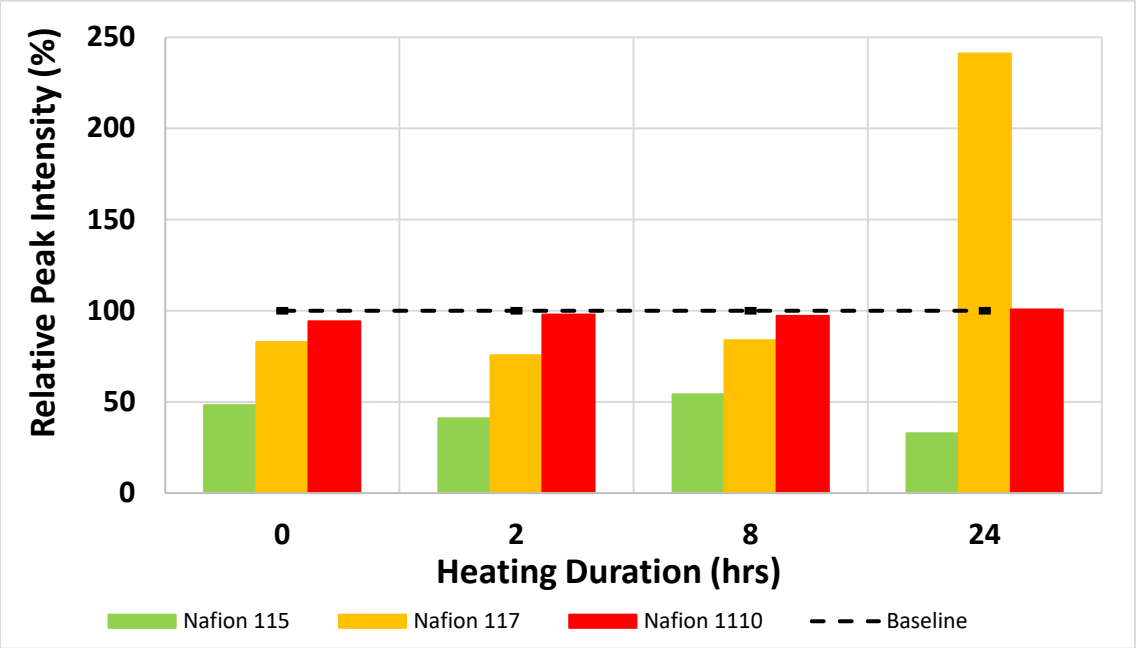

Figure 41: Post-Heating Calculated 115, 117 and 1110 Relative Peak I Intensity after Heated to 60°C for 10 min, 2hr, 8hr and 24hr. Results are Compared to Baseline Measurements.

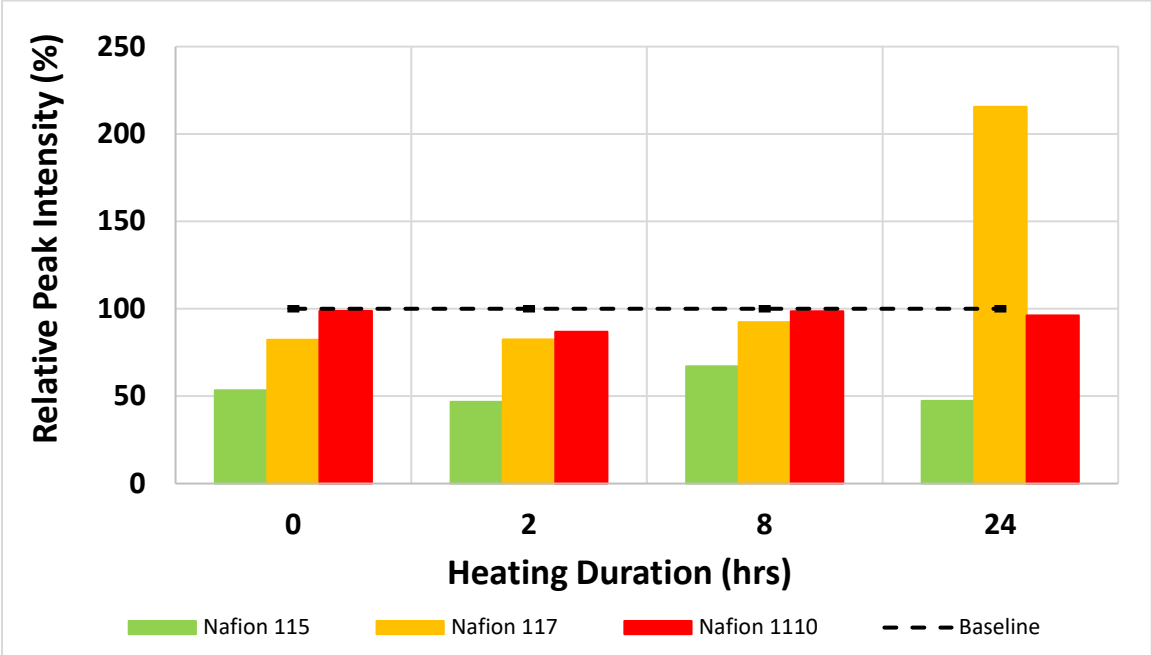

Figure 42: Post-Heating Calculated 115, 117 and 1110 Relative Peak II Intensity after Heated to 60°C for 10 min, 2hr, 8hr and 24hr. Results are Compared to Baseline Measurements.

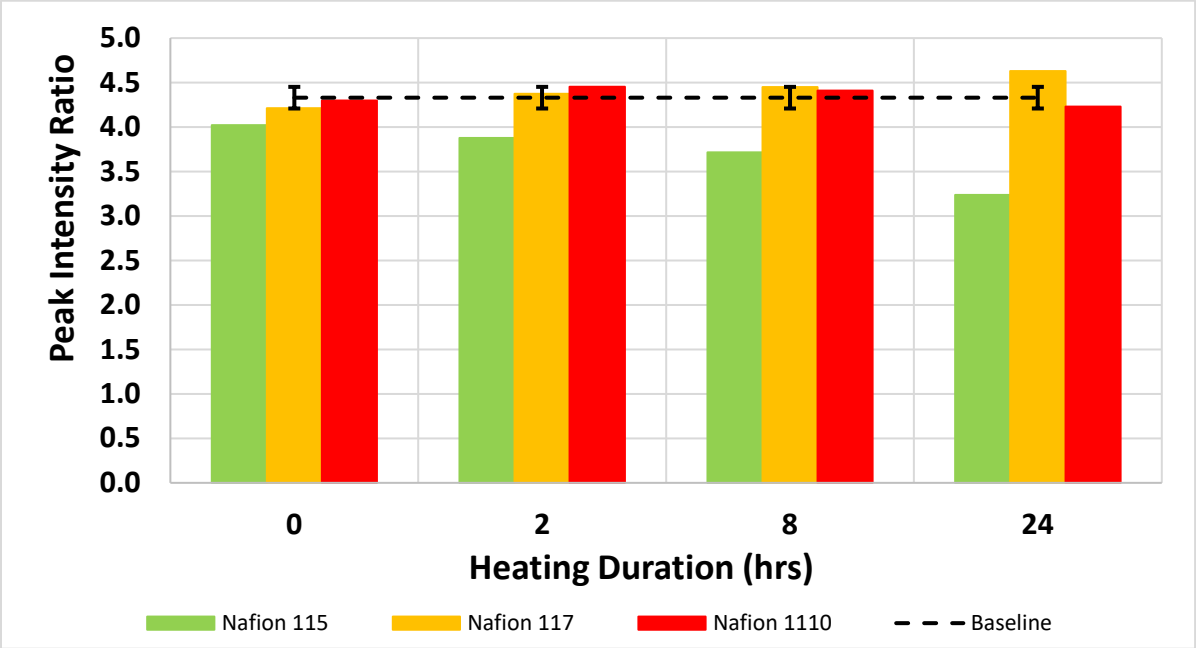

Figure 43: Post-Heating Calculated 115, 117 and 1110 Peak Ratio Intensities after Heated to 60°C for 10 min, 2hr, 8hr and 24hr. Results are Compared to Baseline Measurements.

7.3.2. In-Depth In-Situ and Post-Heating Analysis at 120°C Operating Temperature

Figure 44 showed the 120°C In-Situ Peak I 2-Theta positions for 115, 117 and 1110 after being heated for 10 minutes and 2, 8 and 24 hours. While 60°C In-Situ 1110 material results were relatively close to the baseline these 120°C In-Situ results are all significantly different from the baseline. All three membrane thicknesses, after 24 hours of heating, were reduced between 2% and 3.3% than their baseline value.

Figure 45 showed the 120°C In-Situ relative Peak I intensity, for 115, 117 and 1110 after being heated for 10 minutes and 2, 8 and 24 hours, as a percentage of its original baseline intensity. The relative Peak I intensities for all three material thicknesses are not even close to the baseline for any heating duration. All three materials appear to have trends independent of each other. The 115 consistently maintains a lower intensity then the baseline, the 117 starts higher than the baseline then has its intensity significantly reduced and 1110 starts with a reduced Peak I intensity and gradually increases it above the baseline. None of these results are stable with time or consistent with the baseline.

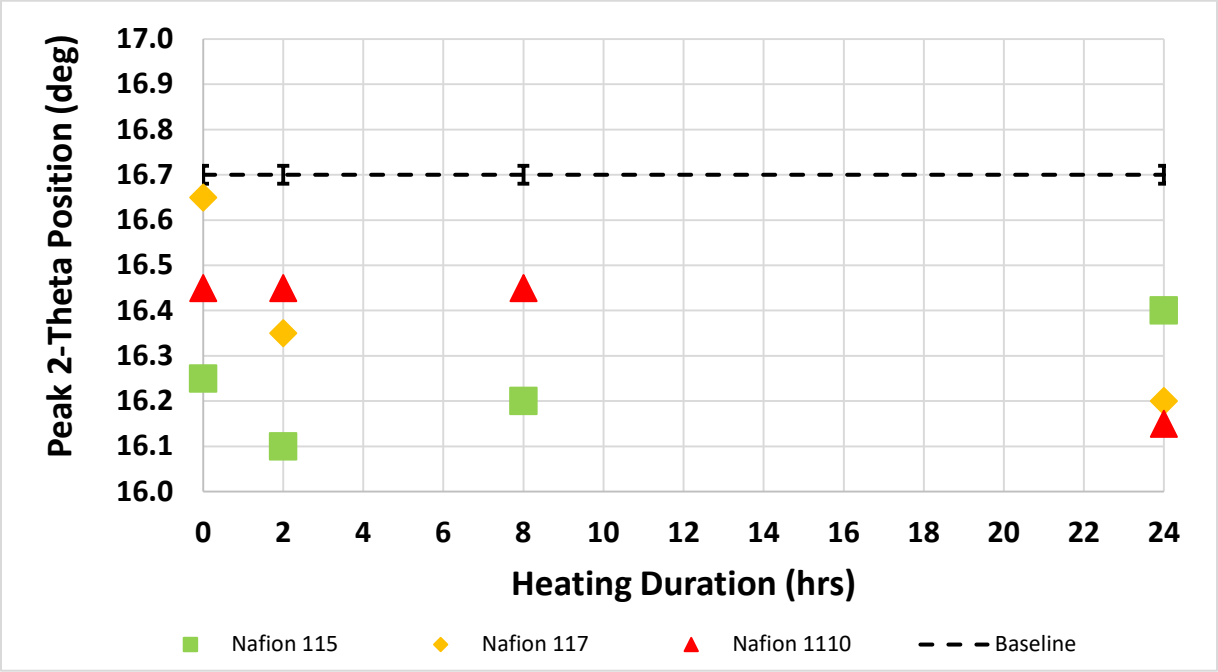

Figure 44: In-Situ Calculated 115, 117 and 1110 2-Theta Peak I Position after Heated to 120°C for 10 min, 2hr, 8hr and 24hr. Results Compared to Peak I Baseline Measurements.

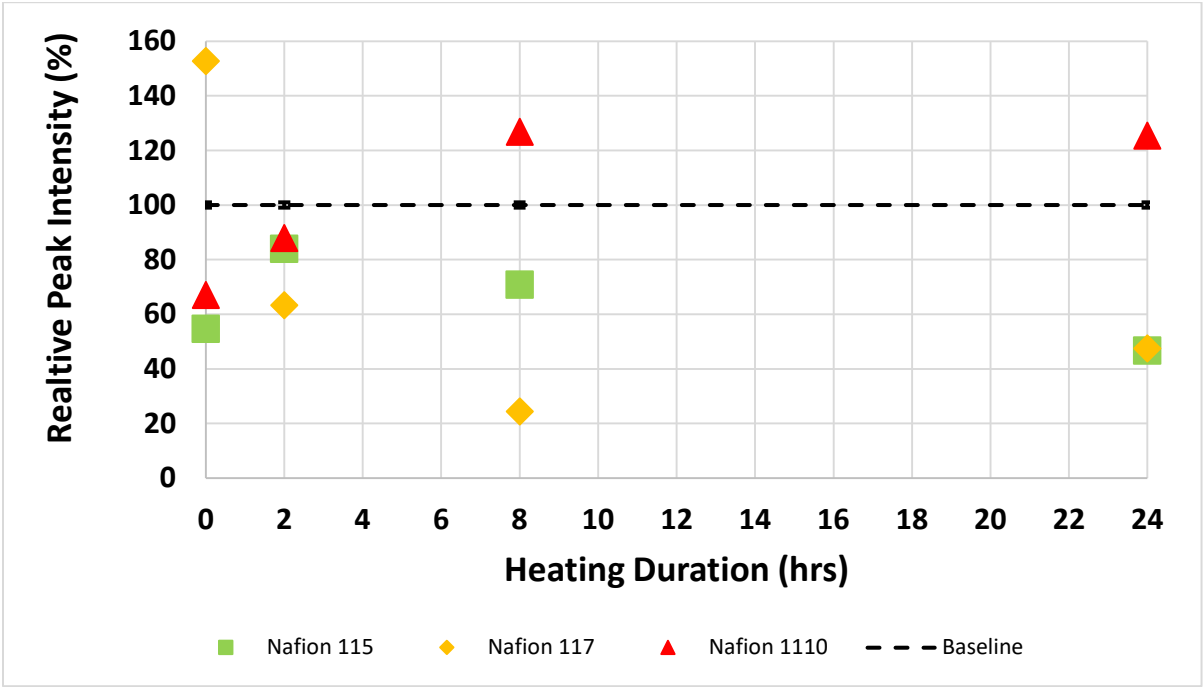

Figure 45: In-Situ Calculated 115, 117 and 1110 Relative Peak I Intensity after Heated to 120°C for 10 min, 2hr, 8hr and 24hr. Results are Compared to Baseline Measurements.

Figure 46 showed the 120°C In-Situ relative Peak II intensity, for 115, 117 and 1110 after being heated for 10 minutes and 2, 8 and 24 hours, as a percentage of its original baseline intensity. The relative Peak II intensity results are consistently different from the baseline in a similar manner to how the relative Peak I intensity results deviated. The largest different was that all three materials had, for the most part, reduced Peak II intensities compared to the baseline, while Peak I showed both increased and decreased intensities. The significance of how Peak I and II alter their peak intensities in response to heating over time will need to be investigated in a future paper.

Figure 47 showed the 120°C In-Situ ratio between Peak I and Peak II for 115, 117 and 1110 after being heated for 10 minutes and 2, 8 and 24 hours. Peak ratios were calculated by dividing the Peak I intensity by the Peak II intensity. The 115 became widely different from the baseline, which is not surprising considering how the 115 material performed in the other calculated In-Situ parameters already shown in this section. Heating both the 117 and 1110 samples resulted their peak ratios having a larger offset from the baseline than observed in Section 7.3.1. Overall the 117 and 1110 were different by 3.6% and 7.0%, respectively from the baseline.

Figure 48 showed the 120°C post-heated Peak I 2-Theta positions for 115, 117 and 1110 taken at 25°C after being heated for 10 minutes and 2, 8 and 24 hours. All three membrane thicknesses had Peak I 2-Theta positions that were significantly larger than the baseline. There does not appear to be much difference as a function of membrane thickness. The only unique point to stick out is that the 1110 material here does not match the baseline, unlike with the 60°C post-heating results, where 1110 was able to return to its baseline for almost all the experiments.

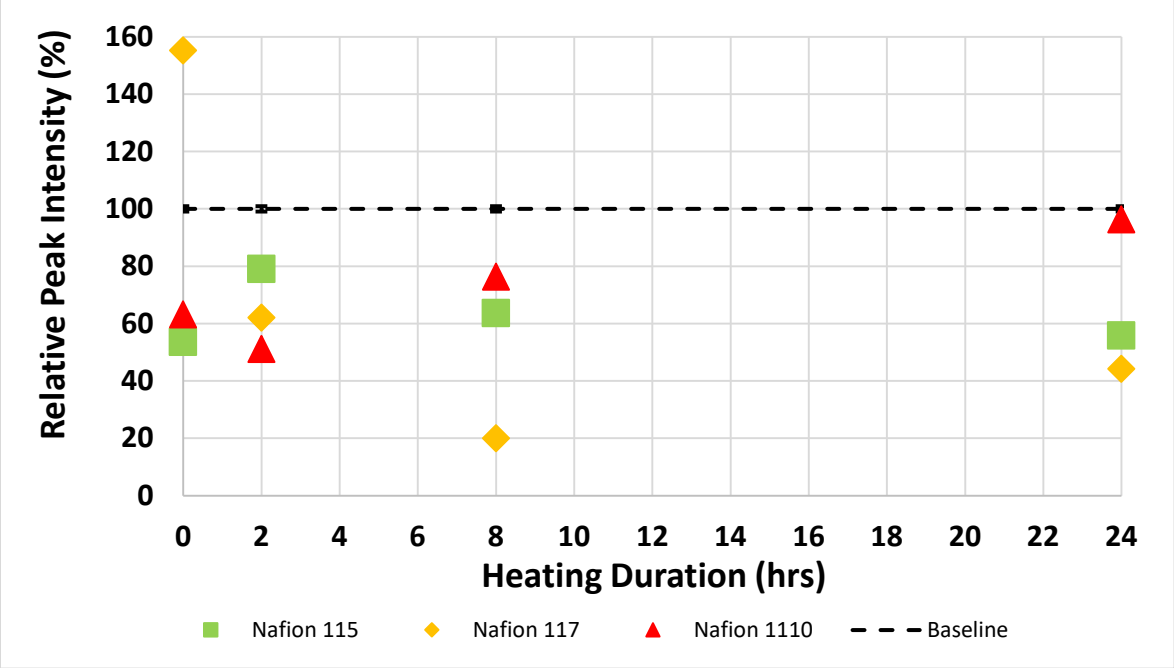

Figure 46: In-Situ Calculated 115, 117 and 1110 Relative Peak II Intensity after Heated to 120°C for 10 min, 2hr, 8hr and 24hr. Results are Compared to Baseline Measurements.

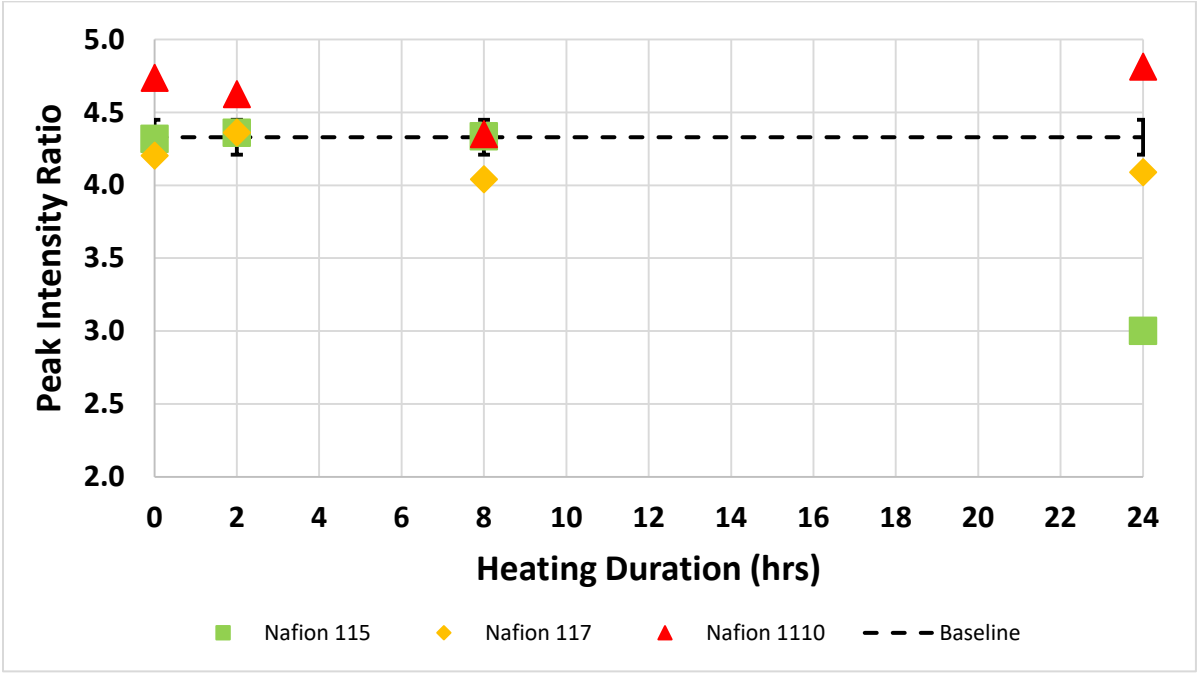

Figure 47: In-Situ Calculated 115, 117 and 1110 Peak Ratio Intensities after Heated to 120°C for 10 min, 2hr, 8hr and 24hr. Results are Compared to Baseline Measurements.

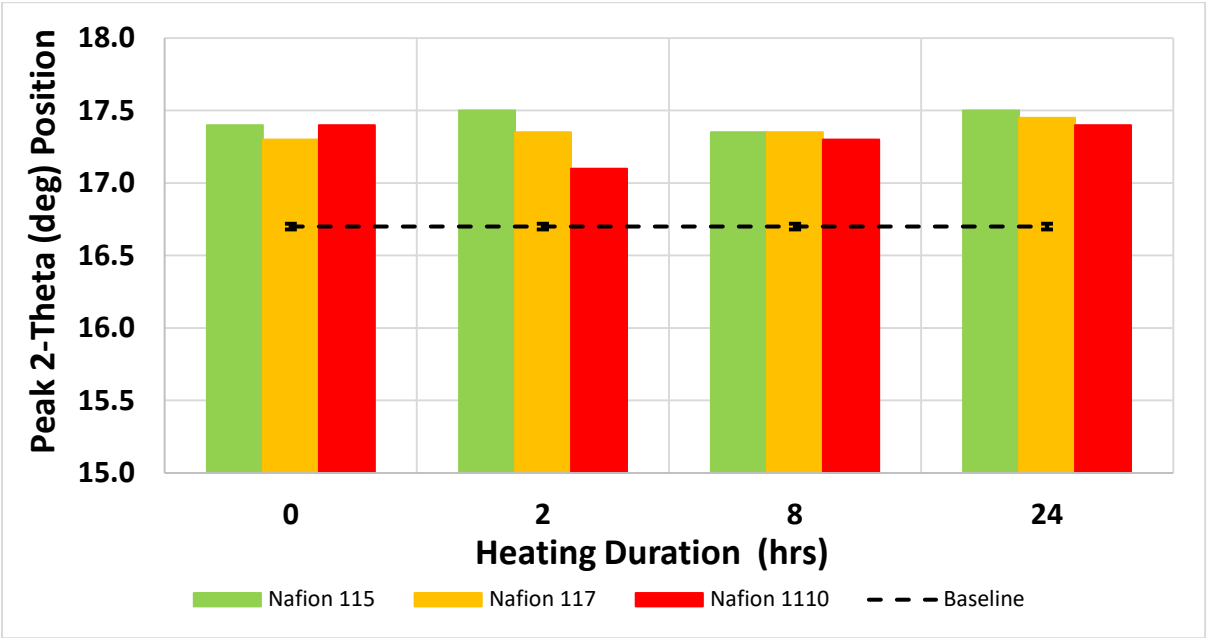

Figure 48: Post-Heating Calculated 115, 117 and 1110 2-Theta Peak I Position Taken at 25°C after Heated to 120°C for 10 min, 2hr, 8hr and 24hr. Results Compared to Peak I Baseline Measurements.

Figure 49 showed the 120°C post-heating relative Peak I intensity, for 115, 117 and 1110 after being heated for 10 minutes and 2, 8 and 24 hours, as a percentage of its original baseline intensity. At this operating temperature none of the samples matched the baseline for any heating duration. Samples showed both increased and decreased peak intensities at the different heating durations. The 115 maintained an elevated Peak I intensity over the baseline with its average intensity ~119% greater than the baseline. The 117 also stayed mostly above the baseline with an average intensity ~70% greater. Finally, the 1110 was closer to the baseline but still averaged ~36% higher. Despite the increased offset from the baseline the 1110 material was the closest on average to the baseline, which has been a trend throughout this study.

Figure 50 showed the 120°C post-heating relative Peak II intensity, for 115, 117 and 1110 after being heated for 10 minutes and 2, 8 and 24 hours, as a percentage of its original baseline intensity. The Peak II results showed a similar level of instability as the Peak I results did for all three membrane thicknesses. On average the 115 was ~60.3% higher than its baseline, the 117 was ~26.3% higher and the 1110 was ~19% lower. When the Peak I and II are looked at together their trends suggest changes in intensity were the result of a combination between crystallization, depolymerization and preferred cluster orientation, since the changes in Peak I and II are not identical. If the changes in intensity occurred in a similar direction then crystallization or depolymerization alone would be hypothesized. The inability of both Peak I and II to stay consistent with time, let alone being able to return to their original baseline would potentially make it very difficult to generate a stable power profile from a fuel cell stack after operating at this temperature. Future evaluations would be required to determine actual material property changes.

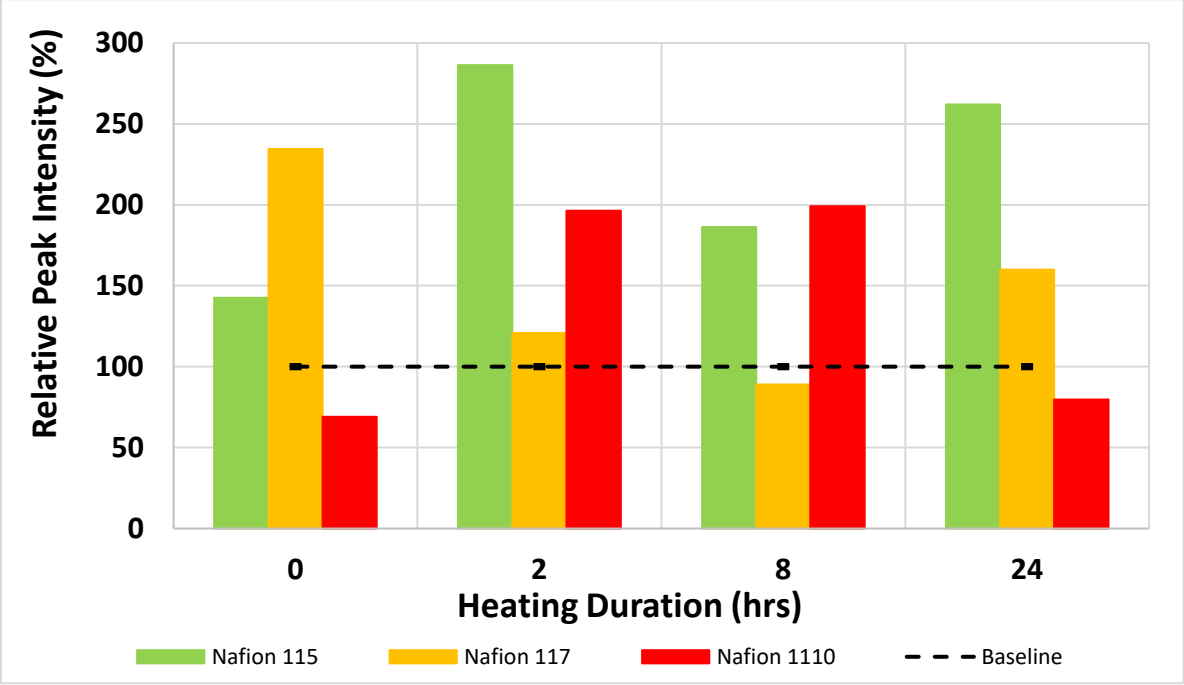

Figure 49: Post-Heating Calculated 115, 117 and 1110 Relative Peak I Intensity after Heated to 120°C for 10 min, 2hr, 8hr and 24hr. Results are Compared to Baseline Measurements.

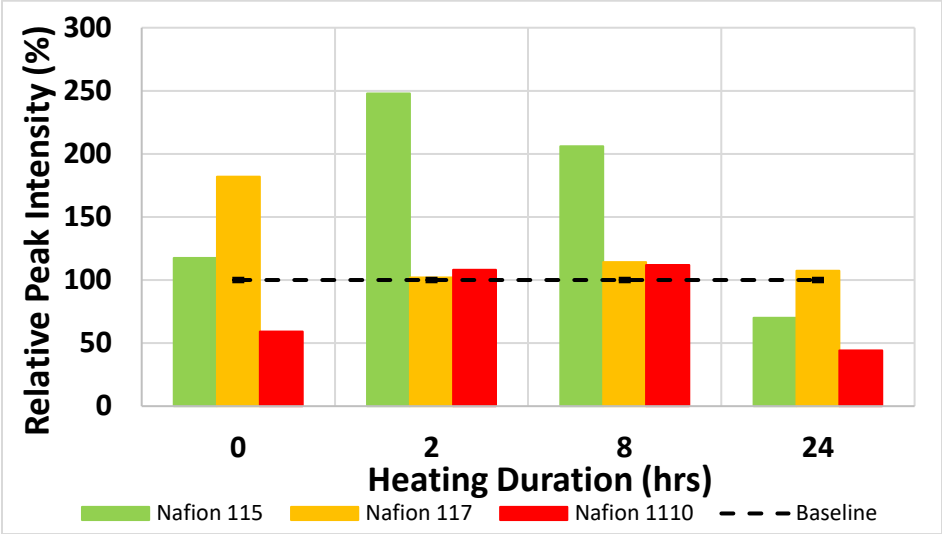

Figure 50: Post-Heating Calculated 115, 117 and 1110 Relative Peak II Intensity after Heated to 120°C for 10 min, 2hr, 8hr and 24hr. Results are Compared to Baseline Measurements.

Figure 51 showed the 120°C post-heating ratio between Peak I and Peak II for 115, 117 and 1110 taken at 25°C after being heated for 10 minutes and 2, 8 and 24 hours. Peak ratios were calculated by dividing the Peak I intensity by the Peak II intensity. Despite the large variations in Peak I and II intensities, compared to the baseline, the calculated ratio is much closer to the baseline than anticipated. All three thicknesses are relatively close for the 10 minute and 2 hour experiments, but even then they are 9.5-18% higher than the baseline. After 2 hours the 115 and 117 started to deviate from the baseline. The 1110 required 24 hours before it statistically deviated too. On average the 115 was ~64.5% higher than the baseline, the 117 was ~27.6% higher and the 1110 was ~24.3% higher.

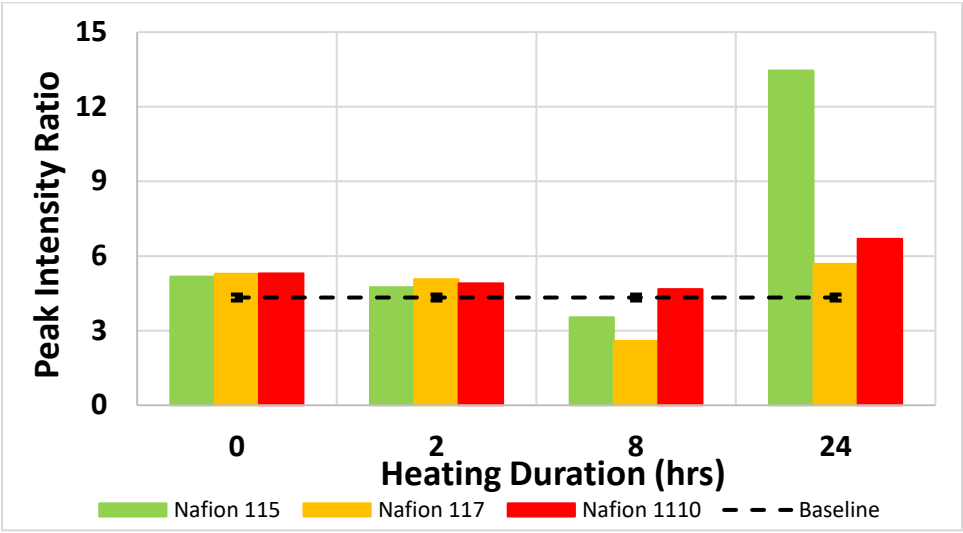

Figure 51: Post-Heating Calculated 115, 117 and 1110 Peak Ratio Intensities after Heated to 120°C for 10 min, 2hr, 8hr and 24hr. Results are Compared to Baseline Measurements.

7.3.3. In-Depth In-Situ and Post-Heating Analysis at 140°C Operating Temperature

Figure 52 showed the 140°C In-Situ Peak I 2-Theta positions for 115, 117 and 1110 after being heated for 10 minutes and 2, 8 and 24 hours. These results showed none of the polymers, despite having fairly consistent Peak I values over time, were nowhere near their baseline. Despite the parameters determined for samples heated to 120°C being significantly different from the baseline, there were a few instances where the In-Situ datasets showed similarities to the baseline. The following In-Situ results for samples heated to 140°C showed none of the polymer samples were close to their original baseline scans for any heating duration or material thickness.

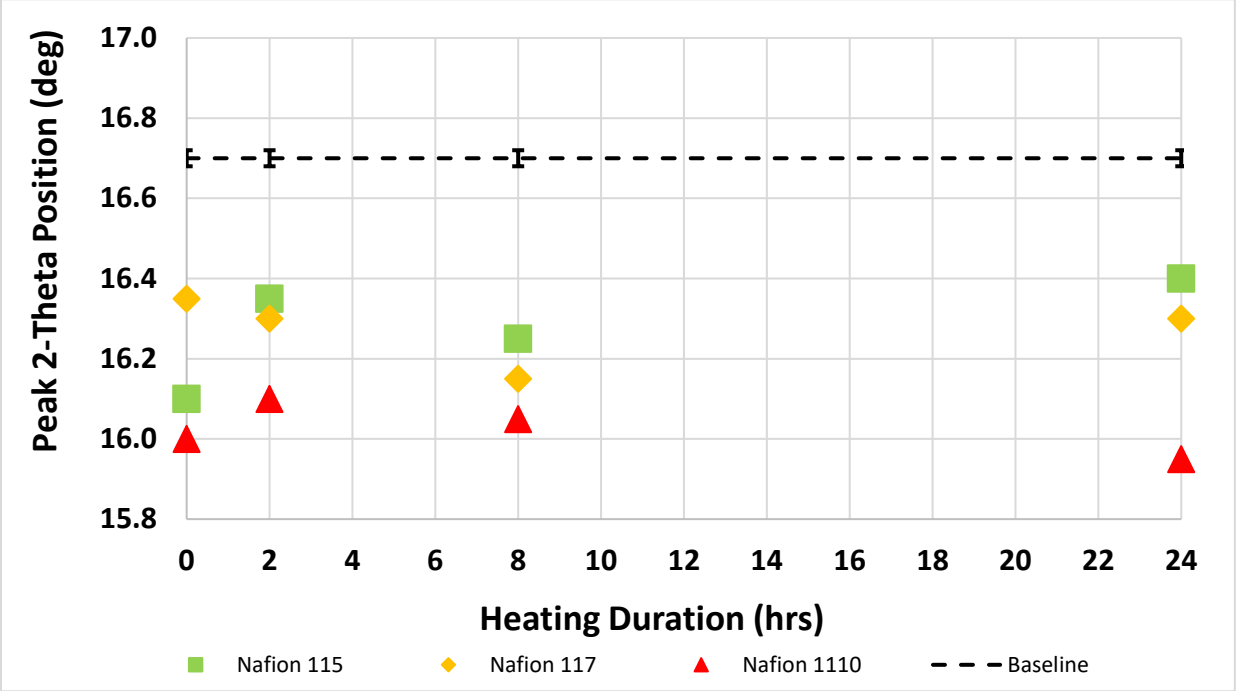

Figure 52: In-Situ Calculated 115, 117 and 1110 2-Theta Peak I Position after Heated to 140°C for 10 min, 2hr, 8hr and 24hr. Results Compared to Peak I Baseline Measurements.

Figure 53 showed the 140°C In-Situ relative Peak I intensity, for 115, 117 and 1110 after being heated for 10 minutes and 2, 8 and 24 hours, as a percentage of its original baseline intensity. All three membrane thicknesses were not consistently the same as the baseline. Both the 115 and 117 materials appeared to maintain reduced Peak I intensities for all heating duration. The 115 was on average ~73.4% below the baseline and 117 was ~51.6% below. The 1110 initially increased its intensity to a maximum after 8 hours of 25% above, then reduced it intensity after being heated for 24 hours. The 1110 still averaged ~11.9% below the baseline as well.

Figure 54 showed the 140°C In-Situ relative Peak II intensity, for 115, 117 and 1110 after being heated for 10 minutes and 2, 8 and 24 hours, as a percentage of its original baseline intensity. The Peak II relative intensity results follow a very similar trend to the Peak I relative intensity results shown above and

demonstrated the structural properties of both peaks within the polymer samples can be changed by the operating temperature.

Figure 55 showed the 140°C In-Situ ratio between Peak I and Peak II for 115, 117 and 1110 after being heated for 10 minutes and 2, 8 and 24 hours. Peak ratios were calculated by dividing the Peak I intensity by the Peak II intensity. As mentioned at the beginning of this section (Section 7.3.3) the 120°C In-Situ results did have a few points of relative consistency with the baseline and the 117 and 1110 material thicknesses peak ratio results (heated to 120°C) were at least close to the baseline. Here, when heated to 140°C, all the tested samples were completely different from the baseline.

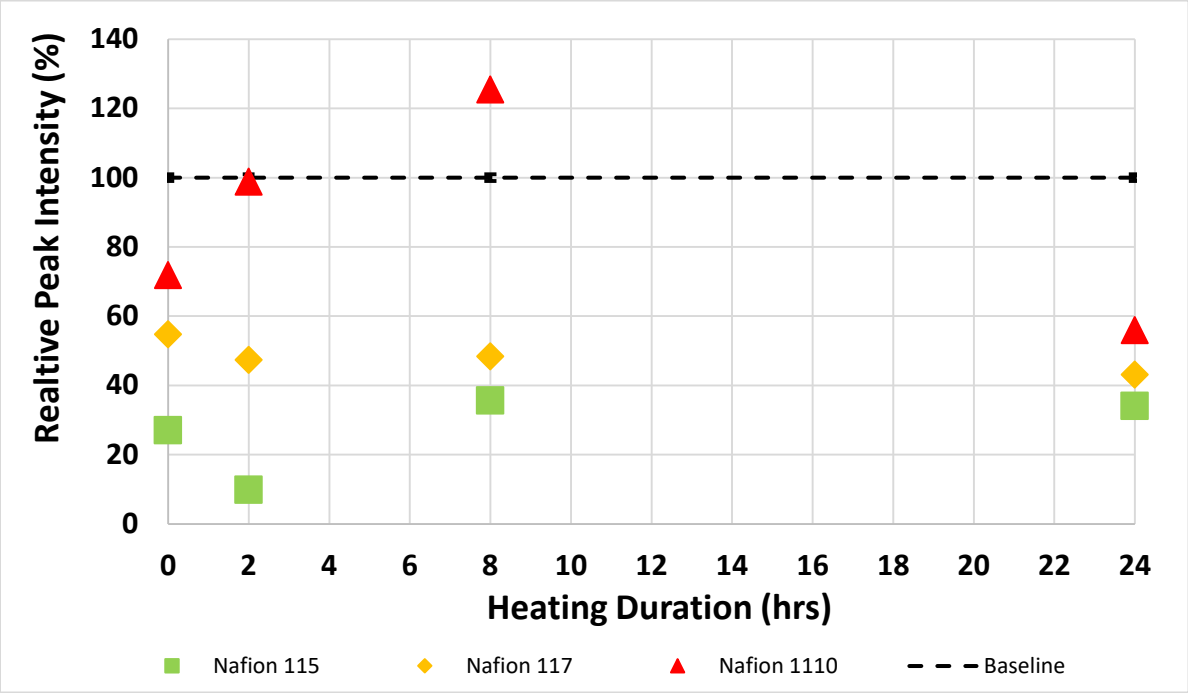

Figure 53: In-Situ Calculated 115, 117 and 1110 Relative Peak I Intensity after Heated to 140°C for 10 min, 2hr, 8hr and 24hr. Results Compared to Peak II Baseline Measurements.

Figure 56 showed the 140°C post-heated Peak I 2-Theta positions for 115, 117 and 1110 taken at 25°C after being heated for 10 minutes and 2, 8 and 24 hours. While the previous 120°C post-heating results have shown all three sample thicknesses were unable to return to their baseline even at that temperature the following post-heating results taken from the different samples heated to 140°C are consistently worse. The 120°C Peak I position deviated between 2.4% and 4.8%, but these results deviate 4.2% to 8.1%, which is close to double.

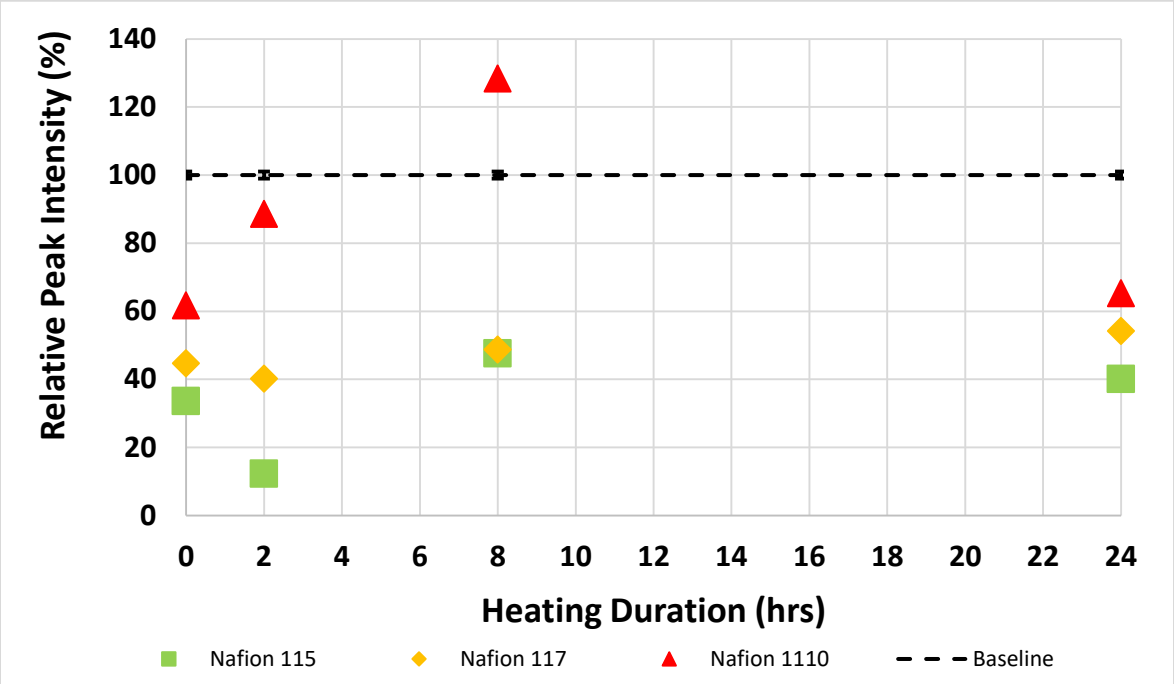

Figure 54: In-Situ Calculated 115, 117 and 1110 Relative Peak II Intensity after Heated to 140°C for 10 min, 2hr, 8hr and 24hr. Results Compared to Peak II Baseline Measurements.

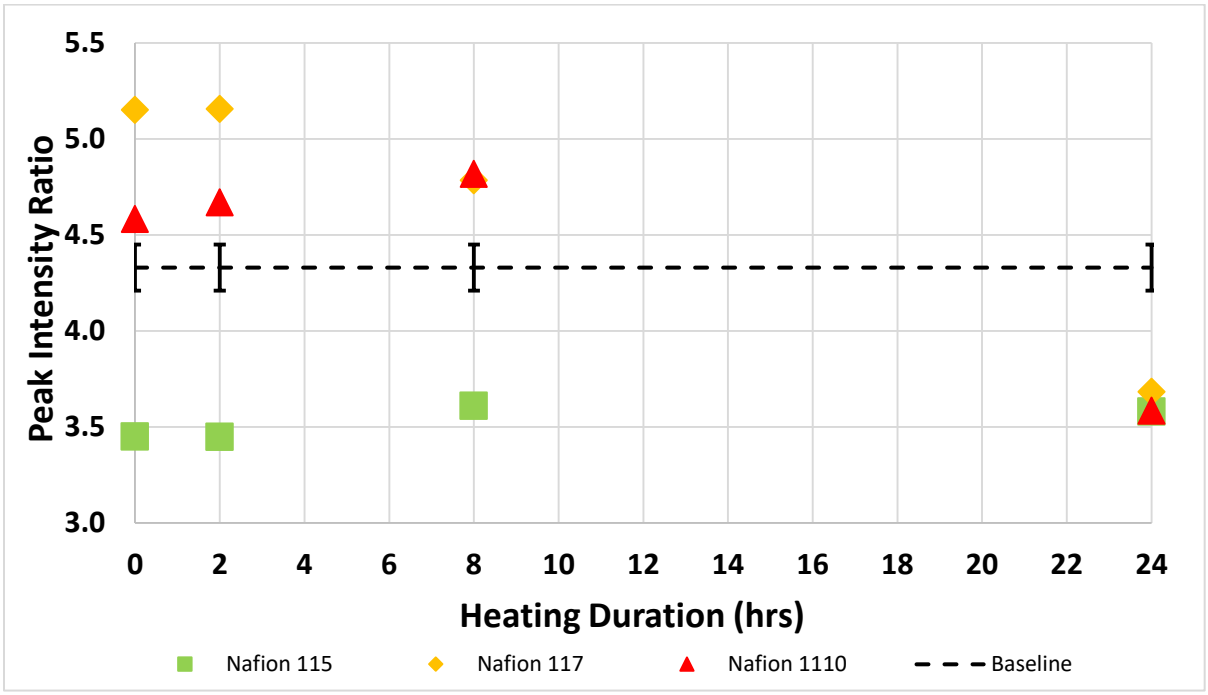

Figure 55: In-Situ Calculated 115, 117 and 1110 Peak Ratio Intensities after Heated to 140°C for 10 min, 2hr, 8hr and 24hr. Results are Compared to Baseline Measurements.

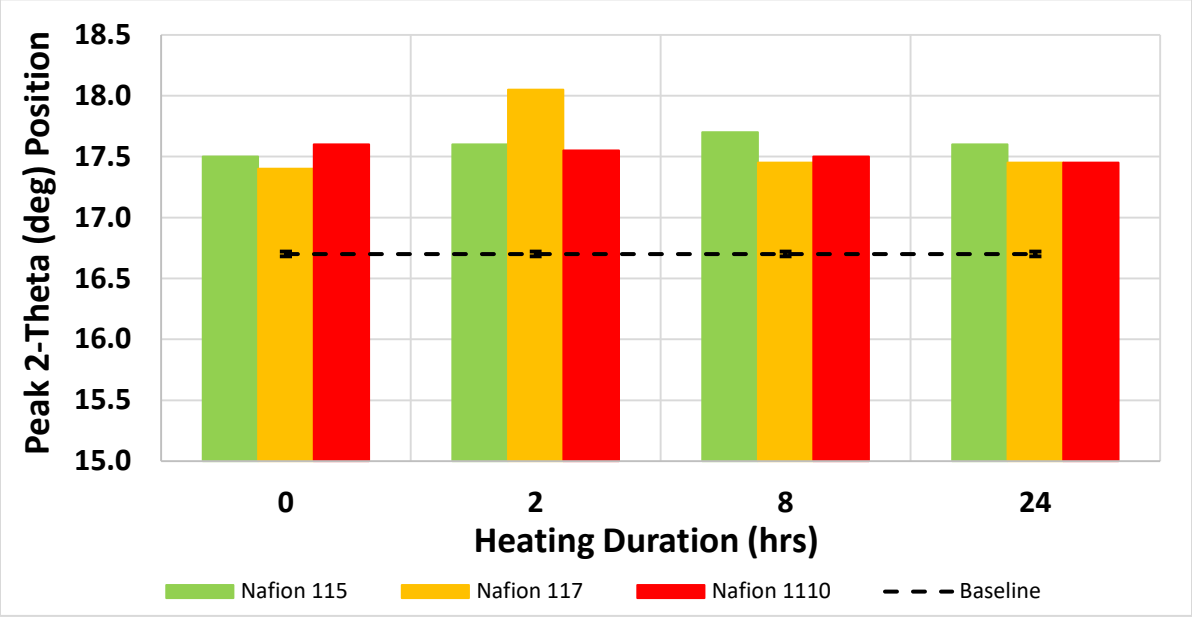

Figure 56: Post-Heating Calculated 115, 117 and 1110 2-Theta Peak I Position Taken at 25°C after Heated to 140°C for 10 min, 2hr, 8hr and 24hr. Results Compared to Peak I Baseline Measurements.

Figure 57 showed the 140°C post-heating relative Peak I intensity, for 115, 117 and 1110 after being heated for 10 minutes and 2, 8 and 24 hours, as a percentage of its original baseline intensity. Peak I intensity values were, at the most, nearly 300% different from the baseline. The 120°C post-heating Peak I intensity were only 186% different at most, which is still a very large difference, but still not as large as the results seen here at 140°C.

Figure 58 showed the 140°C post-heating relative Peak II intensity, for 115, 117 and 1110 after being heated for 10 minutes and 2, 8 and 24 hours, as a percentage of its original baseline intensity. The Peak II relative intensities for samples heated to 140°C deviated even more than the Peak I intensities, with intensities increased by nearly 384% over the baseline, compared to the 120°C post-heating results which only increased at most by 150%.

Figure 59 showed the 140°C post-heating ratio between Peak I and Peak II for 115, 117 and 1110 taken at 25°C after being heated for 10 minutes and 2, 8 and 24 hours. Peak ratios were calculated by dividing the Peak I intensity by the Peak II intensity. The peak ratio was the only metric that did not deviate more than the 120°C post-heating results, but was still nearly identical to those previous results. The average peak ratio for 140°C was 36% different from the baseline while the 120°C results were on average 38% different.

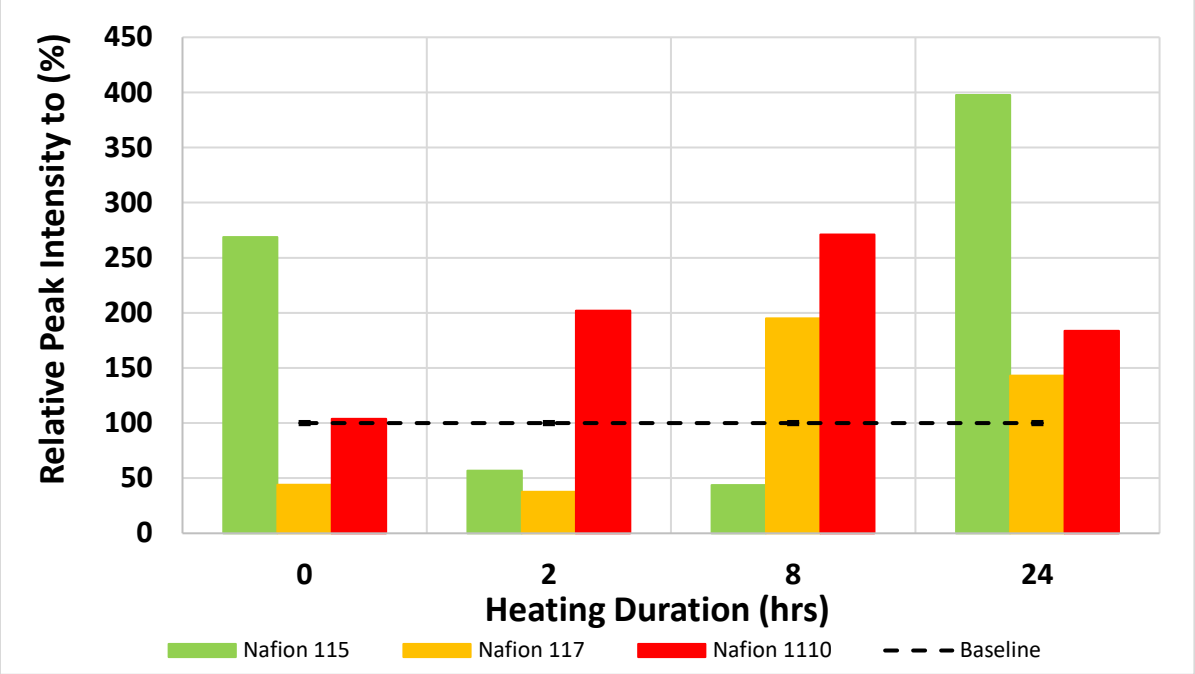

Figure 57: Post-Heating Calculated 115, 117 and 1110 Relative Peak I Intensity after Heated to 140°C for 10 min, 2hr, 8hr and 24hr. Results are Compared to Baseline Measurements.

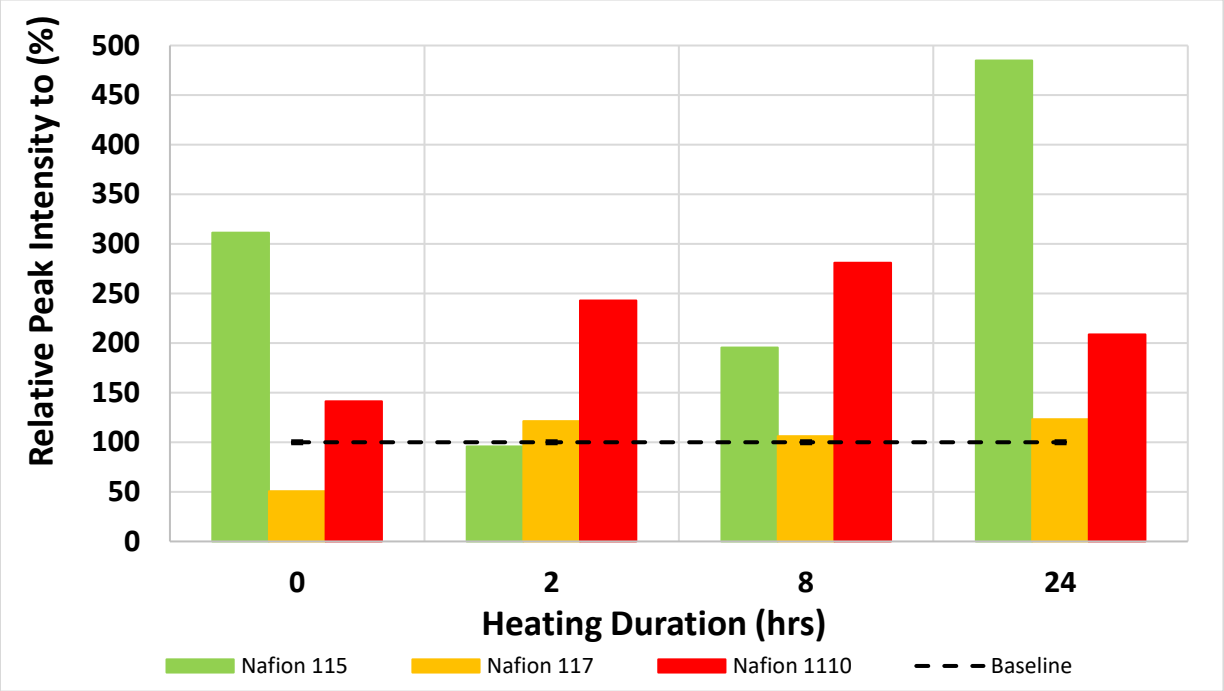

Figure 58: Post-Heating Calculated 115, 117 and 1110 Relative Peak II Intensity after Heated to 140°C for 10 min, 2hr, 8hr and 24hr. Results are Compared to Baseline Measurements.

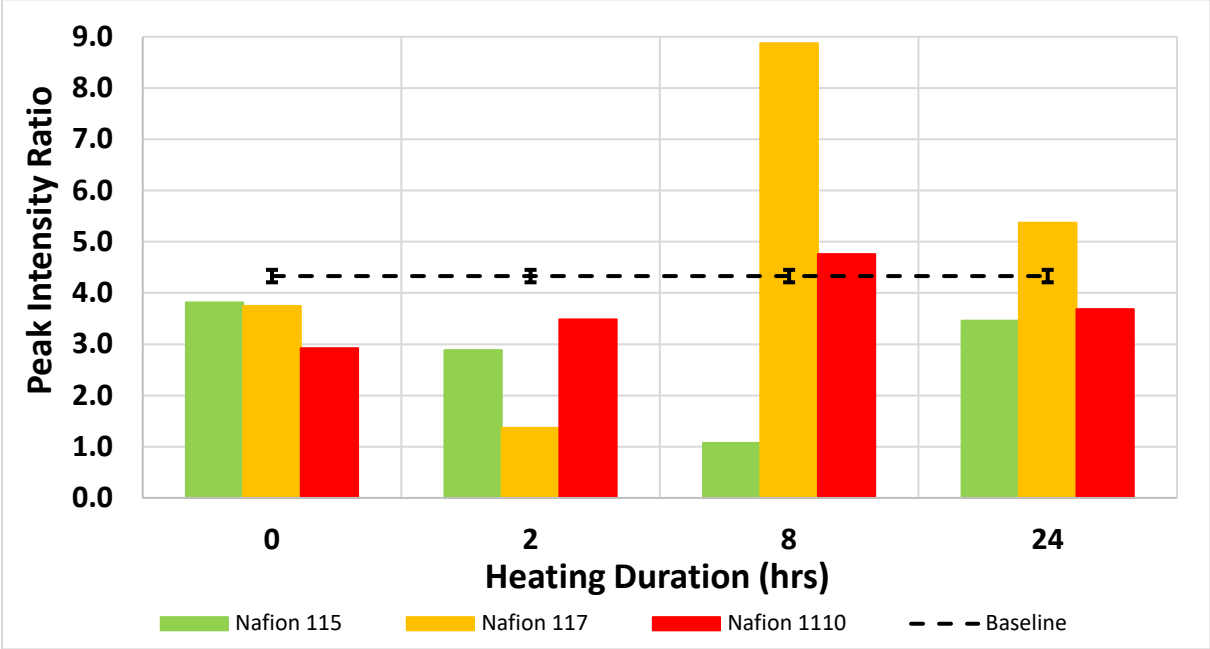

Figure 59: Post-Heating Calculated 115, 117 and 1110 Peak Ratio Intensities after Heated to 140°C for 10 min, 2hr, 8hr and 24hr. Results are Compared to Baseline Measurements.

7.4. Long-Term In-Situ Nafion© 115, 117 and 1110 XRD In-Situ and Post-Heating Measurements Summary

In summary, the following In-Situ and post-heating trends were observed for the 115, 117 and 1110 materials after being heated to 60°C, 120°C and 140°C operating temperatures.

In-Situ Data Trends:

1. Typically, data trends were more stable with heating duration at lower operating temperature and started to deviate from the baseline more as time increased with increased operating temperatures.
2. Peak I 2-Theta positions were typically lower than the baseline, if they deviated.
3. Increasing the operating temperature from 60°C to 140°C gradually increased the amount all three membrane thicknesses deviated from their baselines.
4. The thinnest membrane, 115, was by far the most unstable. The 115 was never able to match it baseline values, even when heated to 60°C.
5. The thickest membrane, 1110, was the most stable overall. It was able to maintain exactly the same or close to the baseline when heated to 60°C. It was also able to maintain fairly consistent baseline values, at 60°C, when heated for 24 hours. The 1110 membrane was, however, not able to maintain baseline values effectively once heated to 120°C or above.

Post-Heating Data Trends:

1. The 115 membrane was unable to return to the same peak position, peak intensities or peak ratio as it baseline at the 60°C operating temperature. The 117 was able to return to some of its

baseline values, such as Peak I position and its peak ratio, however it progressive increased its deviation from the baseline as heating duration increased. The 1110 was the most stable when heated to 60°C and was exactly the same or close to its baseline values for all metrics.

2. Peak I 2-Theta positions were typically greater than the baseline if they deviated. This was caused by the formation of a side peak at higher 2-Theta values.
3. All membrane thicknesses were unable to return to their baseline metrics once heated to 120°C or above.

8. Nafion© 1110 Material Structure Characterization for Combined Heating and Cooling Cycles

8.1. Introduction

Characterizing the effects of heating duration on polymer degradation, performed in Section 7, was only the first step to fully understanding polymer degradation at elevated temperatures. Testing each polymer up to 24 hours provided useful information on thermal degradation but that did not take into account the impact of thermal cycling on the crack propagation and membrane structural decomposition within each sample. Cycling membranes through a number of heating and cooling cycles would provide insight into how cycling impacts degradation. This also simulates a stack being operated during the day and then stored at ambient temperature during the night, which is something real stacks would experience.

The experimental conditions performed in this section will be slightly different from Section 7. First, each heating cycle will last for 24 hours as that was the maximum amount of time used in Section 7 and will simulate an entire day of operation. Second, only the 1110 membrane thickness will be used. Both the 115 and 117 materials structurally deviated from their baseline to such an extent after 24 hours of heating that additional testing, such as cyclical testing, will not be performed at this time. The impact of cyclical testing on the structural integrity of 115 and 117 may be re-evaluated once a correlation between internal structural change and material properties has been performed. If the material properties are found to not change significantly despite these severe internal changes then cyclical testing will be completed for 115 and 117. Even though the 1110 material was severely degraded at both the 120°C and 140°C operating temperatures it still showed internal structural stability after being heated to 60°C. Third, the same three operating temperatures will be used despite the 1110 membrane being severely damaged at 120°C and 140°C after only being heated for 24 hours. Those elevated temperatures were included for reference and to extend these results to the farthest extent possible within the scope of this study. In addition all samples had their baseline scans normalized as previously described in Section 4

Each experiment will take one sample and complete the following heating/cooling process for each operating temperature (a total of three samples will be used). First, each sample will be characterized at 25°C to obtain a baseline. Second, the sample was heated to the desired operating temperature using a ramp rate of 10°C/min and held at that temperature for 24 hours (simulates a day of use). Third, the sample was characterized at the set operating temperature. Fourth, the sample was cooled back down to 25°C at a ramp rate of 10°C/min and held at that temperature for 8 hours (simulates a night in storage). Fifth, the sample was characterized again at 25°C. Finally, steps 2 through 5 were repeated two additional times for a total of three heating/cooling characterization cycles.

8.2. Combined Heating/Cooling In-Situ and Post-Heating Nafion© 1110 Raw XRD Scan Comparison

In-Situ and post-heating cyclic raw XRD scans, taken at 60°C, 120°C and 140°C, are displayed below. All the raw data is being presented together, without discussion between each plot, since Section 7 previously discussed each discussed in great detail each temperature In-Situ and post-heating plot which does not require repeating. One additional point to mention is there were small differences between the 24 hour results in Section 7 and the following Cycle 1 raw data despite both these datasets using the same experimental conditions. Small variations in the raw data were expected due to variability in the sample composition and equipment operating conditions, but these differences were not viewed as significant enough to warrant repeat discussion of each plot in this section too.

8.2.1. Raw XRD Scan Comparison In-Situ and Post-Heating at 60°C Operating Temperature

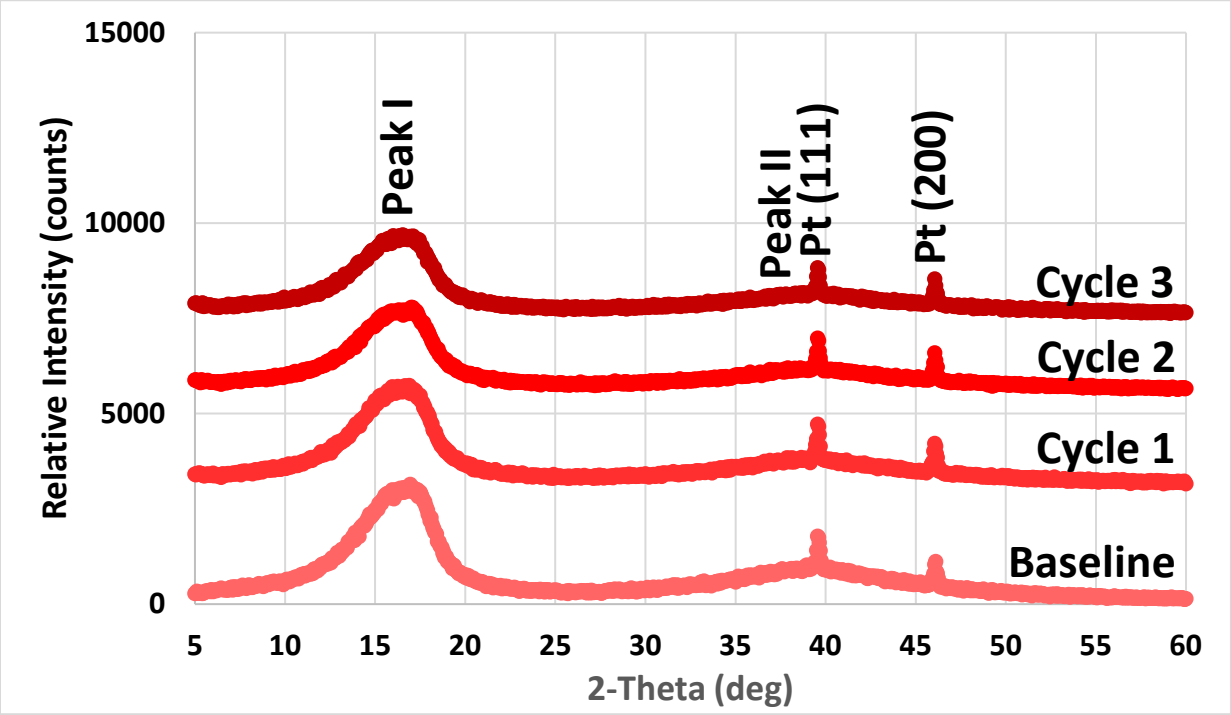

Figure 60: In-Situ Raw XRD Scans for 1110 Taken after 3 Heating Cycles to 60°C for 24hrs. Baseline Raw XRD Data Provided for Comparison.

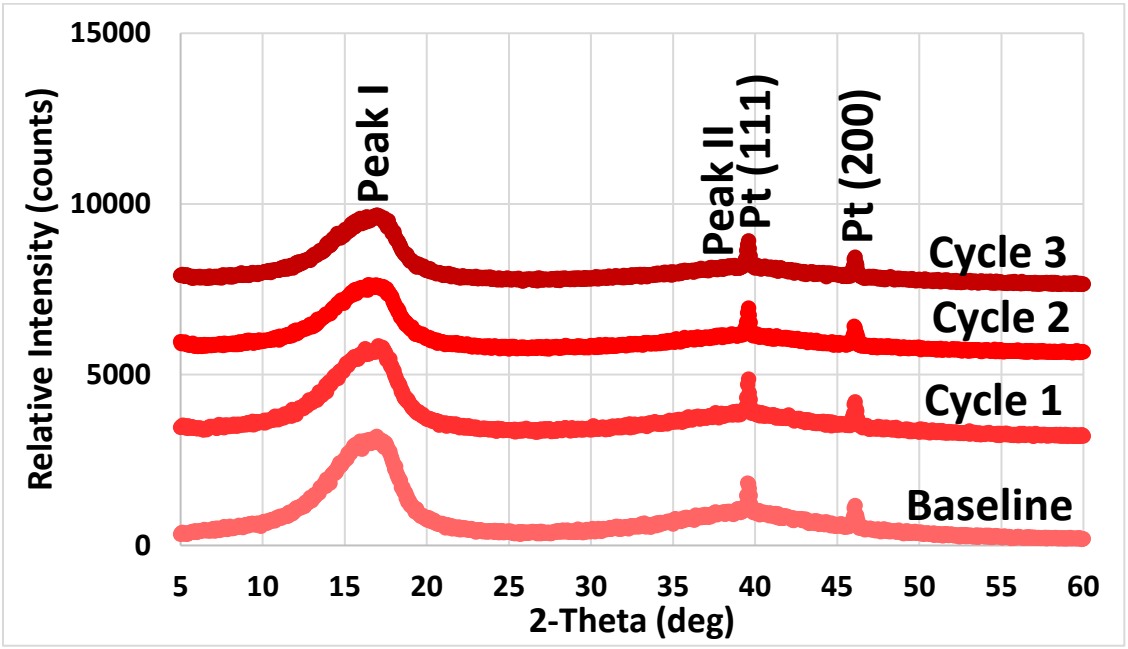

Figure 61: Post-Heating Raw XRD Scans for 1110 Taken after 3 Cooling Cycles to 60°C for 24hrs. Baseline Raw XRD Data Provided for Comparison.

8.2.2. Raw XRD Scan Comparison In-Situ and Post-Heating at 120°C Operating Temperature

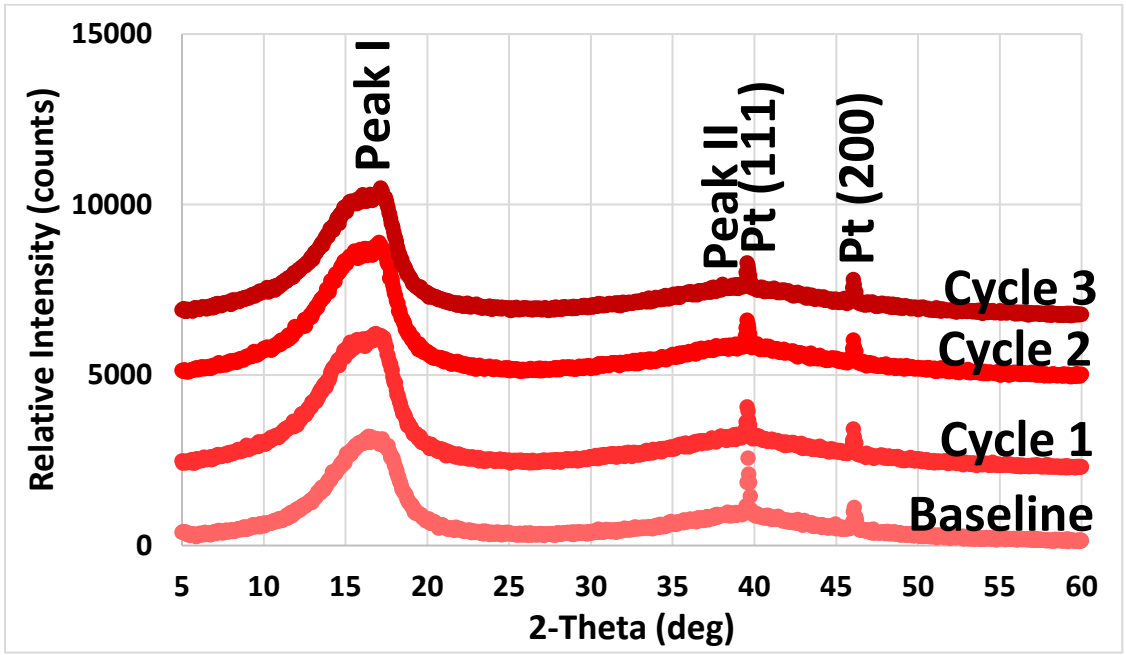

Figure 62: In-Situ Raw XRD Scans for 1110 Taken after 3 Heating Cycles to 120°C for 24hrs. Baseline Raw XRD Data Provided for Comparison.

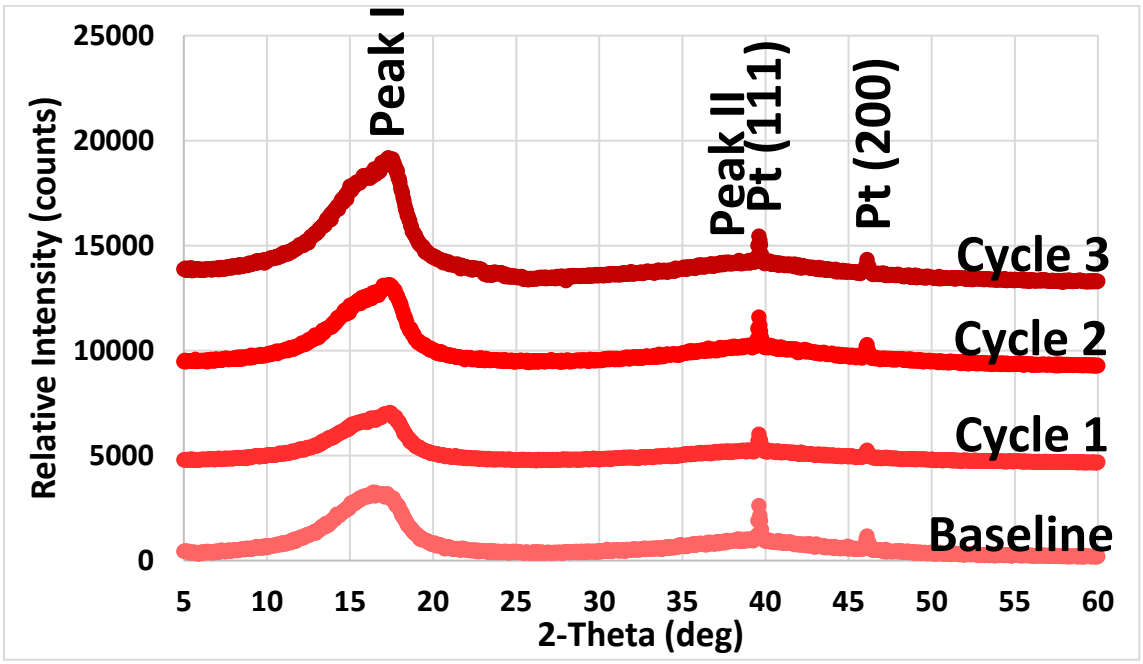

Figure 63: Post-Heating Raw XRD Scans for 1110 Taken after 3 Cooling Cycles to 120°C for 24hrs. Baseline Raw XRD Data Provided for Comparison.

8.2.3. Raw XRD Scan Comparison In-Situ and Post-Heating at 140°C Operating Temperature

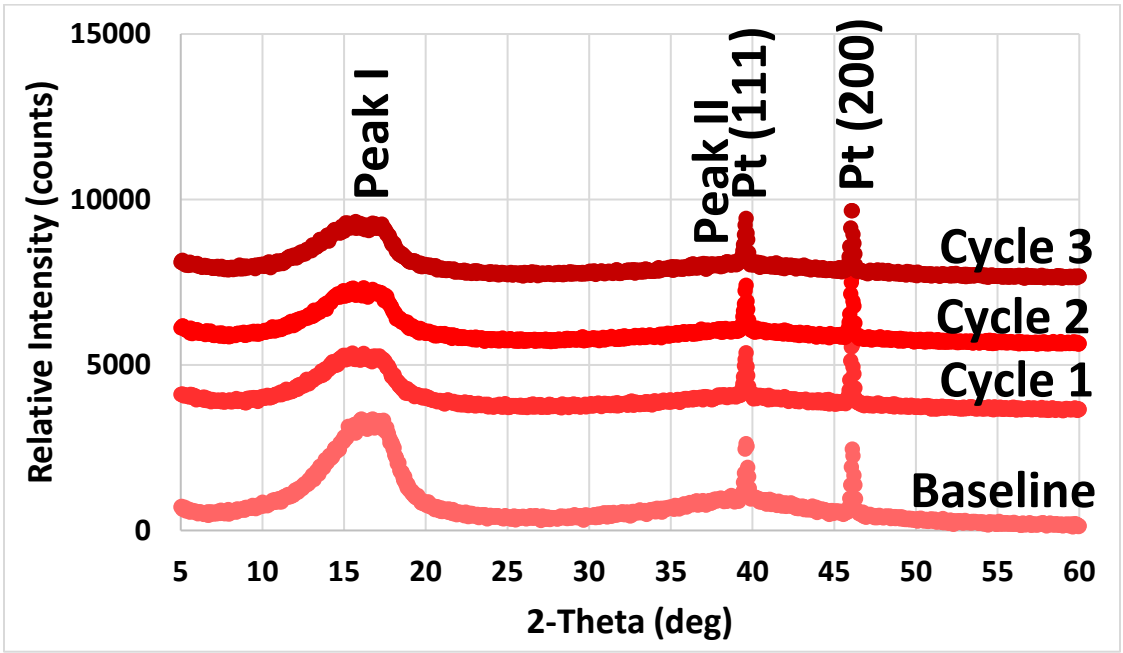

Figure 64: In-Situ Raw XRD Scans for 1110 Taken after 3 Heating Cycles to 140°C for 24hrs. Baseline Raw XRD Data Provided for Comparison.

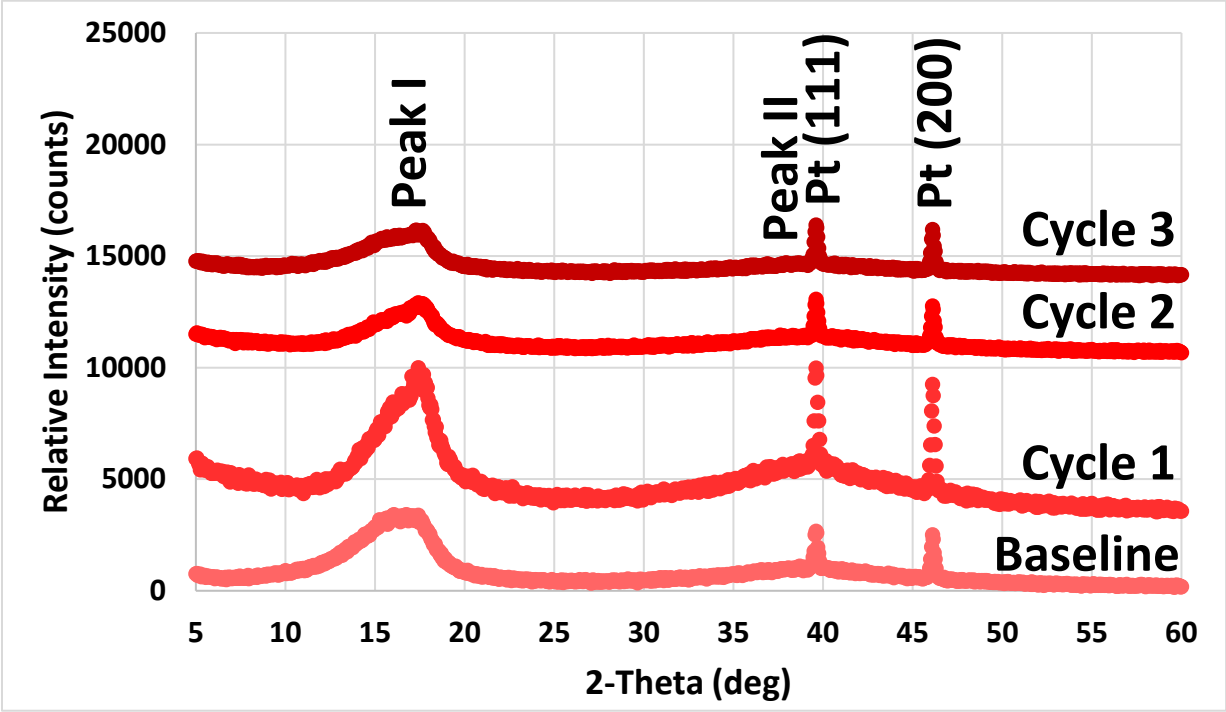

Figure 65: Post-Heating Raw XRD Scans for 1110 Taken after 3 Cooling Cycles to 140°C for 24hrs. Baseline Raw XRD Data Provided for Comparison.

Figure 60, Figure 62 and Figure 64 showed the In-Situ raw XRD scans taken after heating to 60°C, 120°C and 140°C for 24 hours, respectively. Each plot showed the baseline scan and scans taken after 1, 2 and 3 cycles were performed. Unsurprisingly, the raw scans for the 1110 membrane taken at 120°C and 140°C deviate from their respective baselines and progressively deviated more with an increasing number of heating/cooling cycles. The In-Situ raw scans taken after heating at 60°C appeared to remain relatively close to the baseline from just a visual inspection, which is promising a start for the 1110 material.

Figure 61, Figure 63 and Figure 65 showed the post-heating raw XRD scans taken at 25°C after heating at 60°C, 120°C and 140°C for 24 hours, respectively. Each plot showed the baseline scan and scans taken after 1, 2 and 3 cycles were performed. Very similar post-heating results were seen compared to the In-Situ results, which is also promising since the 60°C results still appear to show minimal peak degradation.

Next, and in-depth analysis of the raw XRD data will be completed and discussed below. Structural metric parameters were calculated to analyze the impact of cyclical heating/cooling cycles on the internal structure.

8.3. Combined Heating/Cooling In-Situ and Post-Heating In-Depth Analysis of Nafion© 1110 Raw XRD Scans at 60°C, 120°C and 140°C Operating Temperatures

8.3.1. In-Depth In-Situ and Post-Heating Analysis at 60°C Operating Temperature

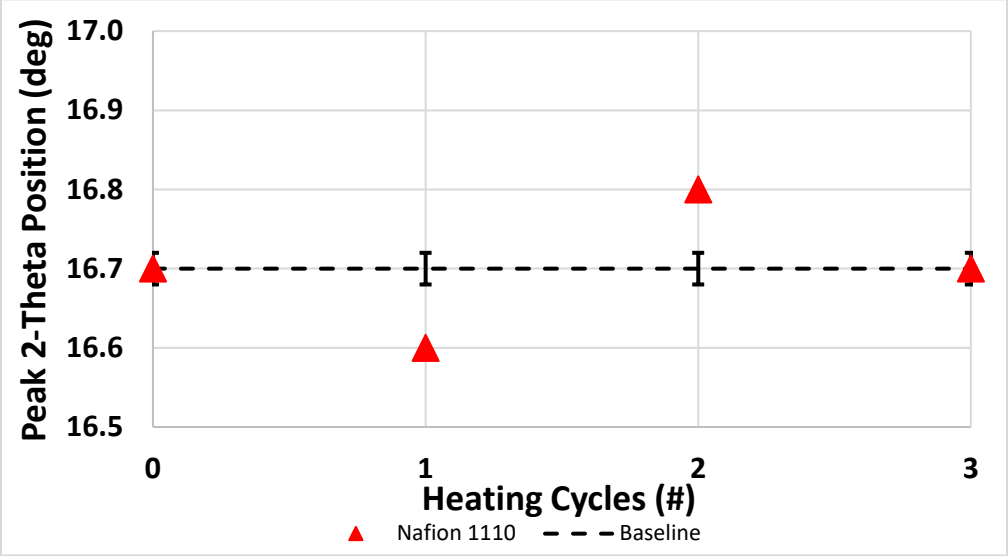

Figure 66: In-Situ Calculated 1110 2-Theta Peak I Position after 3 Heating Cycles to 60°C for 24hr. Baseline Raw XRD Data Provided for Comparison.

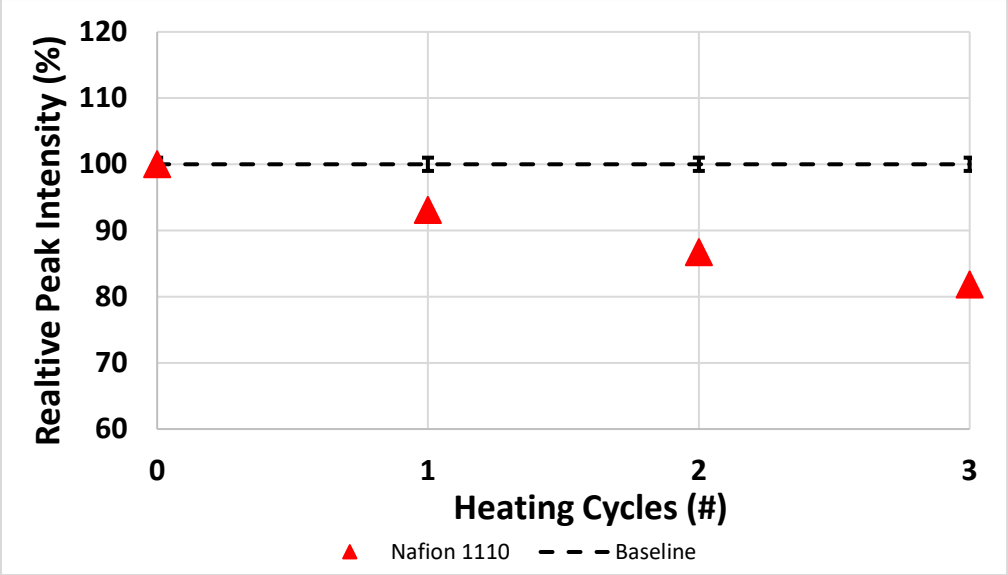

Figure 67: In-Situ Calculated 1110 Relative Peak I Intensity after 3 Heating Cycles to 60°C for 24hr. Baseline Raw XRD Data Provided for Comparison.

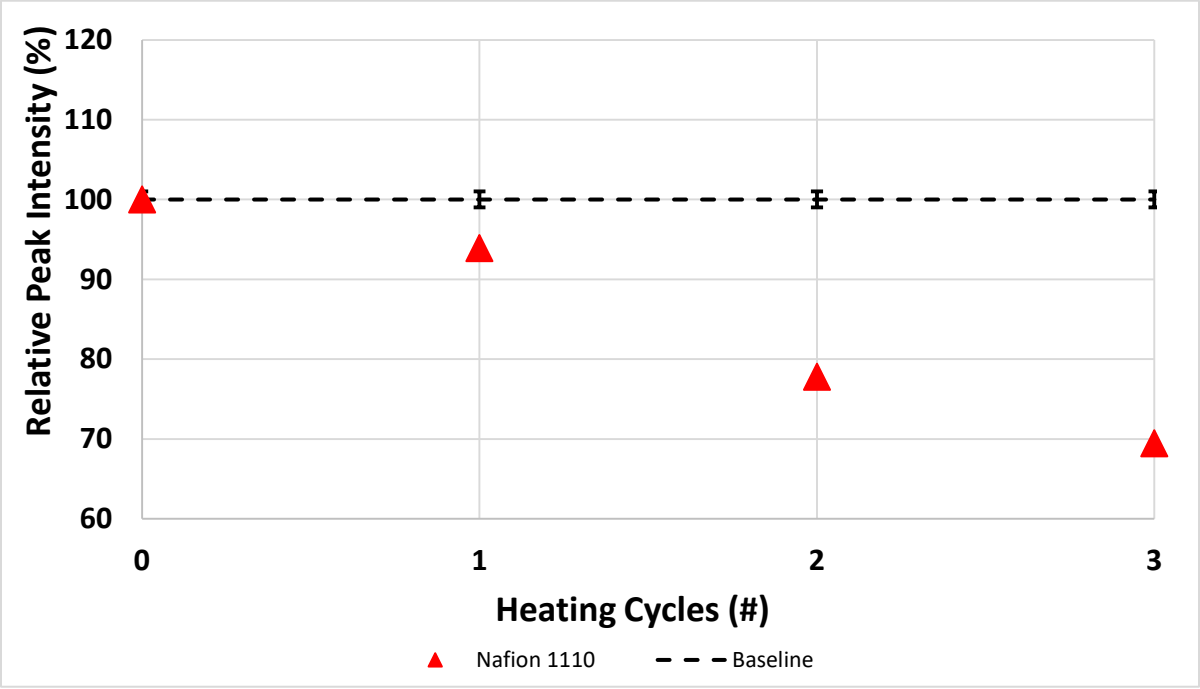

Figure 68: In-Situ Calculated 1110 Relative Peak II Intensity after 3 Heating Cycles to 60°C for 24hr. Results Compared to Peak II Baseline Measurements.

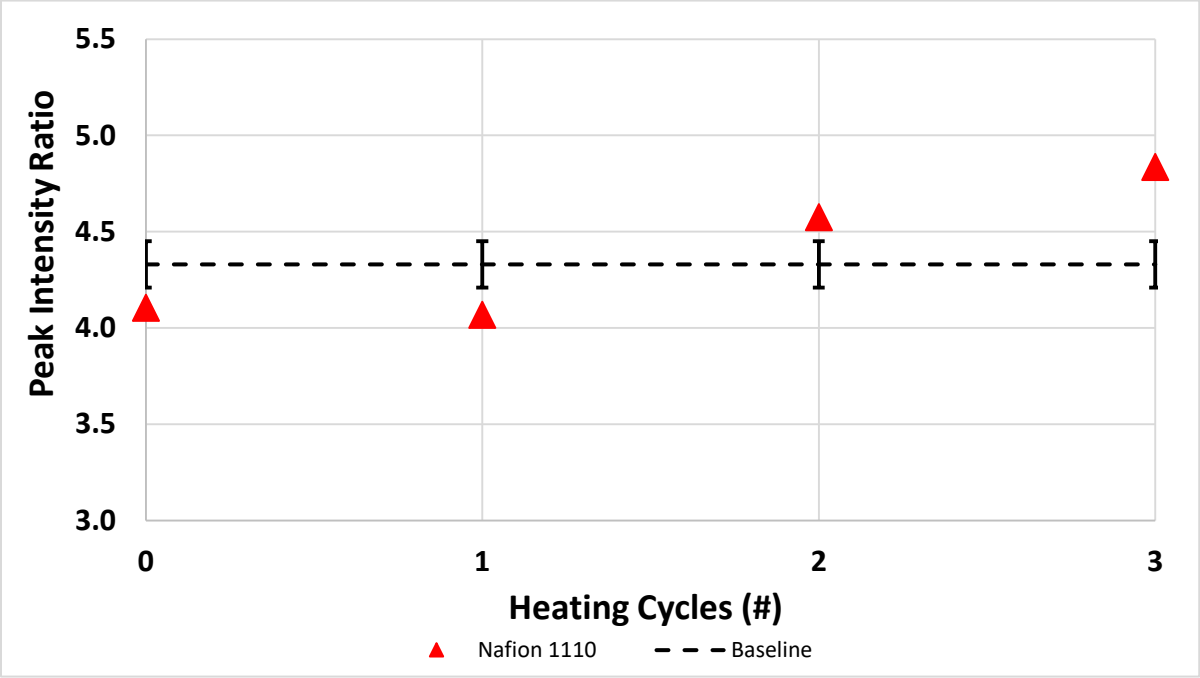

Figure 69: In-Situ Calculated 1110 Peak Ratio Intensities after 3 Heating Cycles to 60°C for 24hr. Results are Compared to Baseline Measurement.

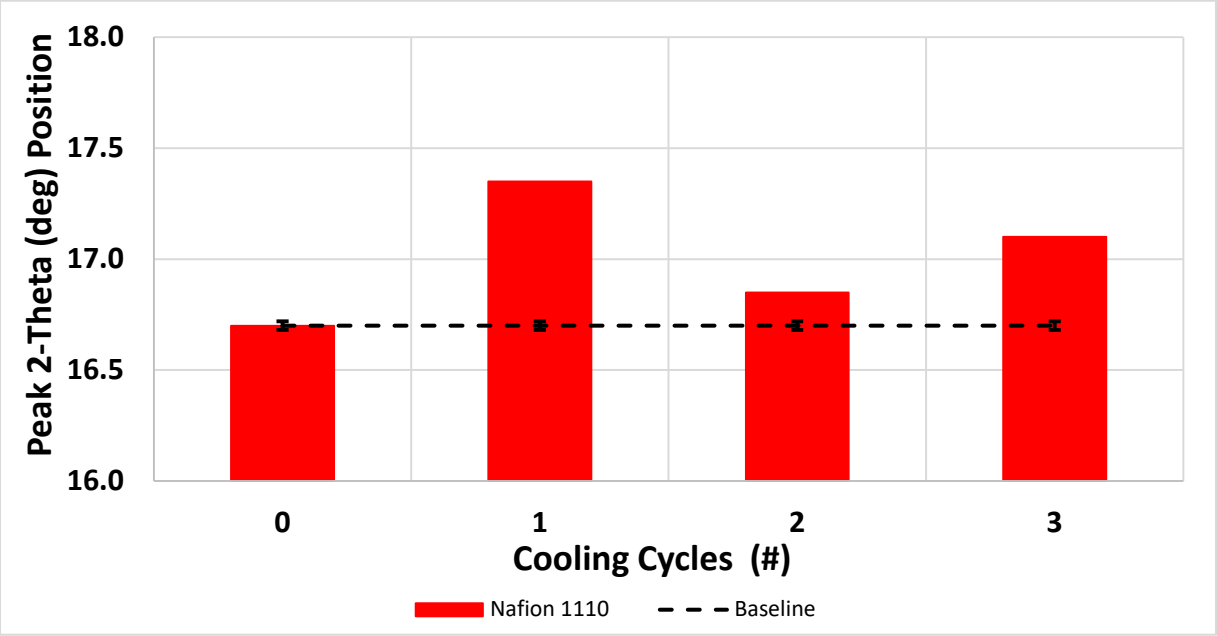

Figure 70: Post-Heated Calculated 1110 2-Theta Peak I Position after 3 Cooling Cycles to 60°C for 24hr. Baseline Raw XRD Data Provided for Comparison.

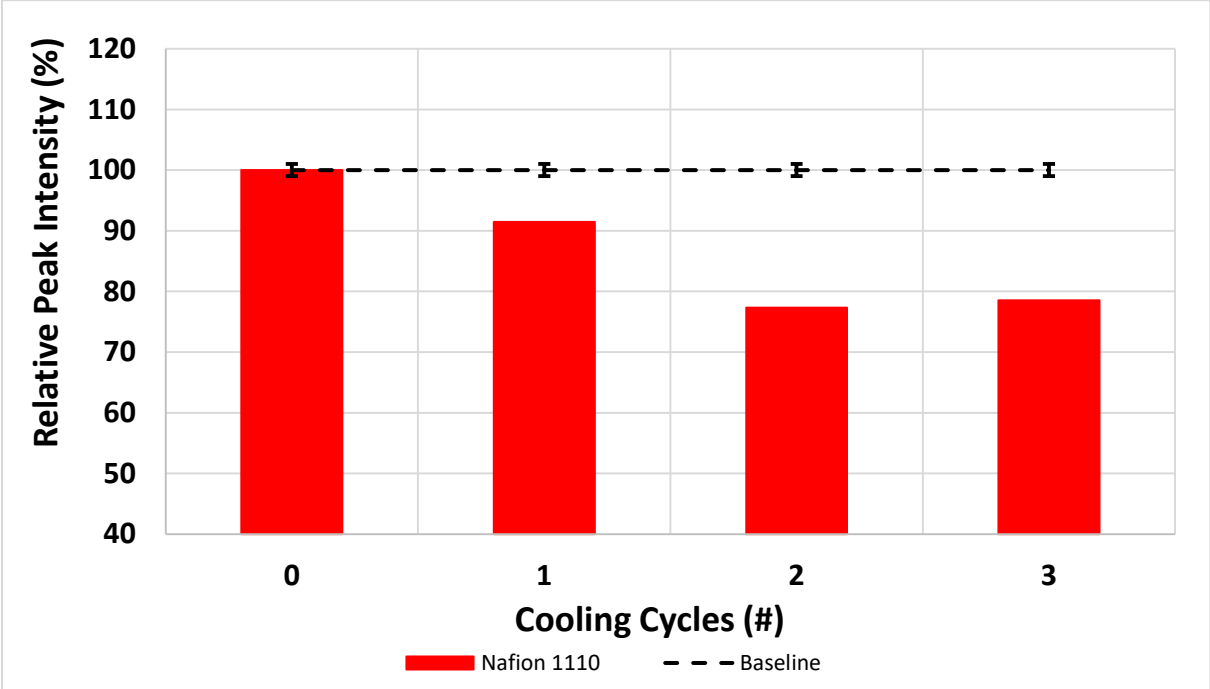

Figure 71: Post-Cooling Calculated 1110 Relative Peak I Intensity after 3 Cooling Cycles to 60°C for 24hr. Baseline Raw XRD Data Provided for Comparison.

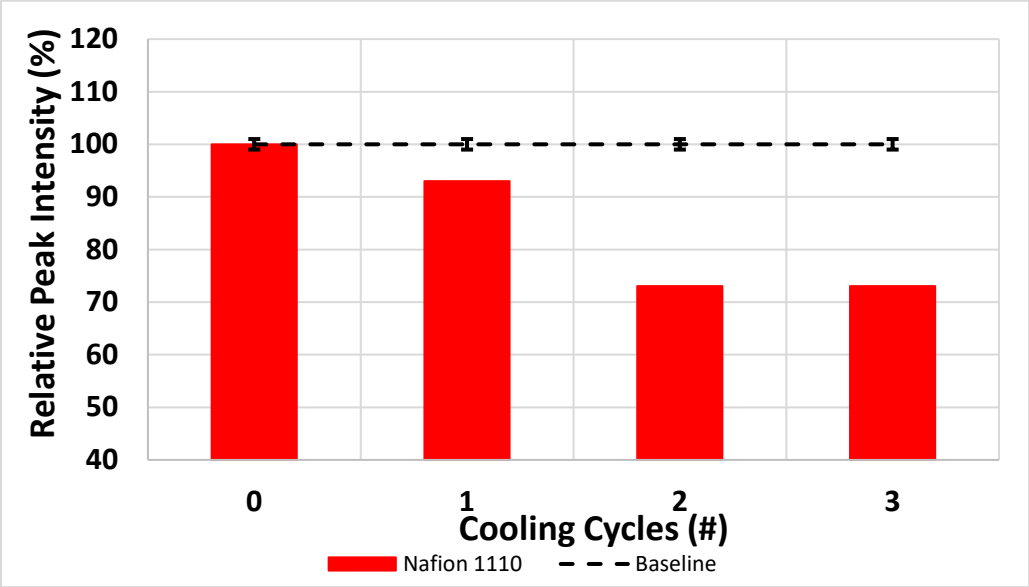

Figure 72: Post-Heating Calculated 1110 Relative Peak II Intensity after 3 Cooling Cycles to 60°C for 24hr. Results Compared to Peak II Baseline Measurements.

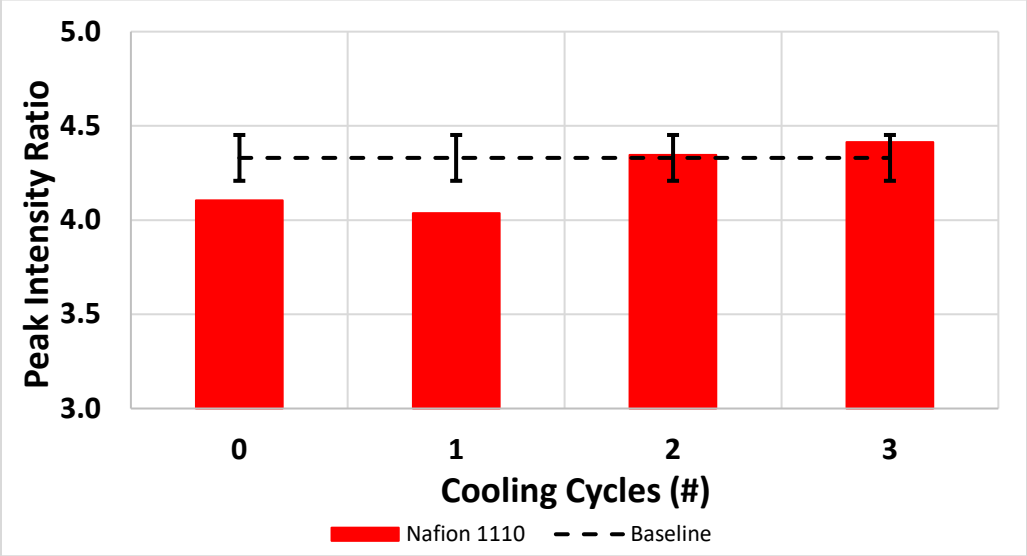

Figure 73: Post-Heating Calculated 1110 Peak Ratio Intensities after 3 Cooling Cycles to 60°C for 24hr. Results are Compared to Baseline Measurement.

Figure 66 through Figure 69 showed the In-Situ parameters for the 1110 material after being heated to 60°C for 3 cycles. The overall results were mixed, at best, with the Peak I 2-Theta positions remaining relatively constant, while the Peak I intensities continuously decreased after each cycle and the reduction in intensity did not appear to have plateaued. The peak ratio between Peak I and II intensities also continuous increased and was not plateauing either, which indicates the internal structure of the material was becoming continuously unstable.

Figure 70 through Figure 73 showed the post-heating parameters for the 1110 material once it had been cooled down to 25°C after being heated to 60°C for 3 cycles. Despite the raw data visually appearing as if minimal changes occurred, a different picture was painted after analyzing the raw XRD data. The Peak I 2-Theta position statistically increased on average 1.79% over the baseline, while both Peak I and II also statistically decreased their intensities by 13.2% and 15.2% below the baseline, respectively. Both Peak I and II did were starting to plateau their peak intensity reductions and potentially becoming stable, however a 13-15% peak reduction is still a significant factor to consider. The only metric that was stable was the peak ratio which on average deviated by 2.4% and stayed within the error bars of the baseline.

These results showed that even when cycled only 3 times between 60°C and 25°C the 1110 material was not able to maintain a constant internal structure. Typically, in Section 7, the calculated parameters deviated the most after the sample was returned to near room temperature. The opposite appear to be true when the samples were cycled as the internal structural parameters changed the most while being heated. This difference when structural instability occurred (post-heating vs. In-Situ) may be dependent upon other factors introduced during the cycling process, such as residual stress introduced into the sample after being cooled which destabilized the internal structure additionally during heating. As stated previously the impact these changes to the structure had on actual material properties needs to be evaluated further. Since Nafion© is a common membrane material used for many years in PEM fuel cells these structural changes may not result in unacceptable membrane performance, but this would still need to be investigated.

8.3.2. In-Depth In-Situ and Post-Heating Analysis at 120°C Operating Temperature

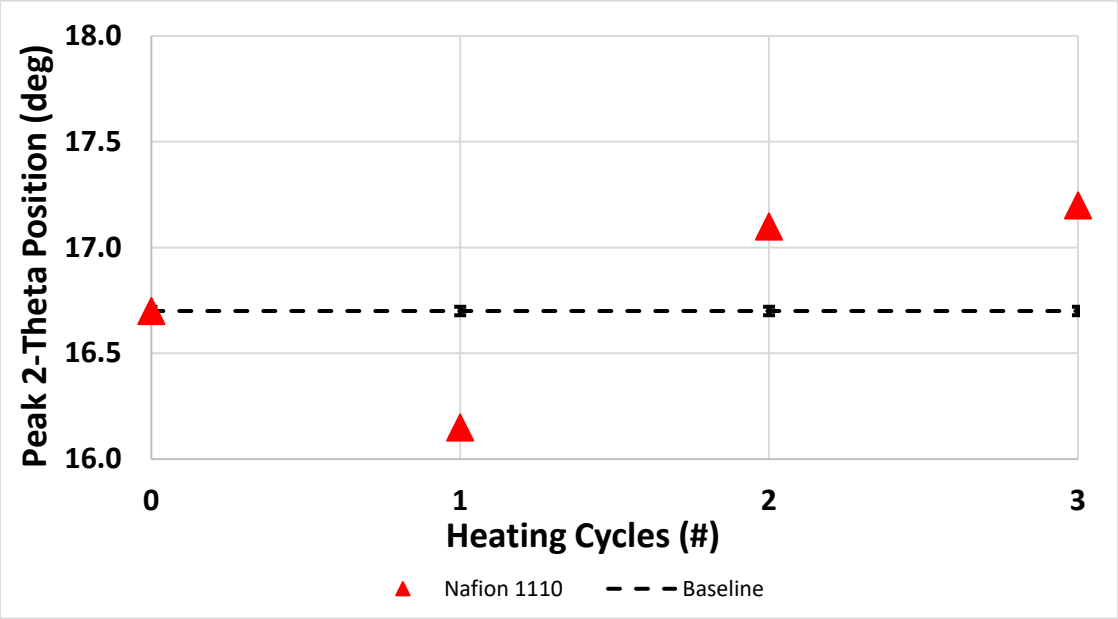

Figure 74: In-Situ Calculated 1110 2-Theta Peak I Position after 3 Heating Cycles to 120°C for 24hr. Baseline Raw XRD Data Provided for Comparison.

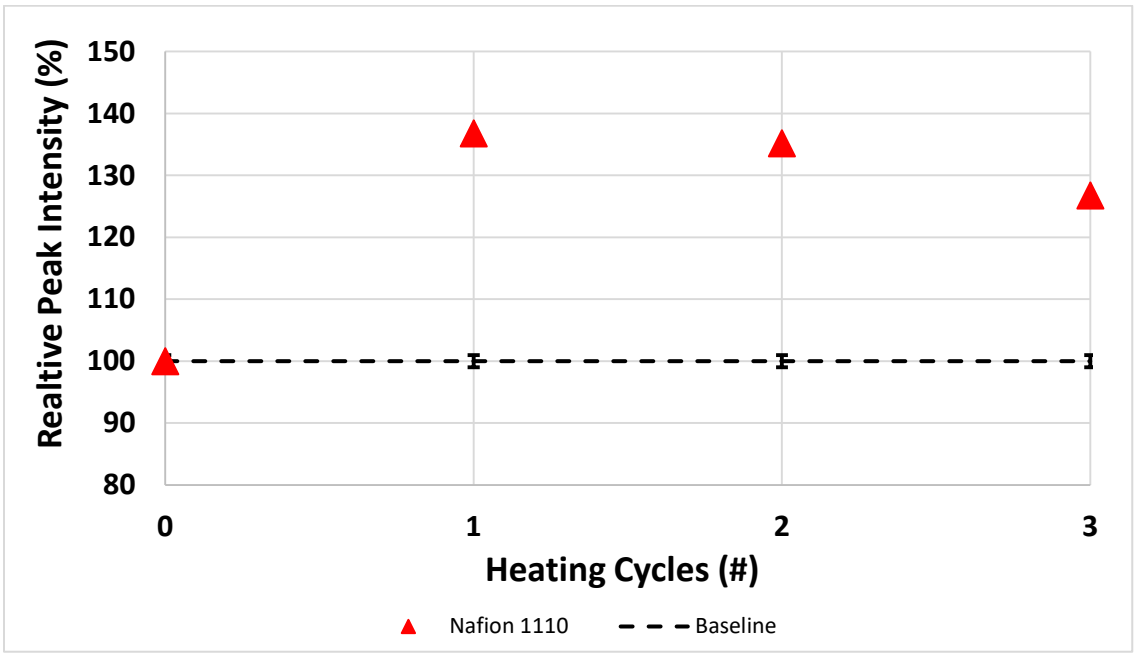

Figure 75: In-Situ Calculated 1110 Relative Peak I Intensity after 3 Heating Cycles to 120°C for 24hr. Baseline Raw XRD Data Provided for Comparison.

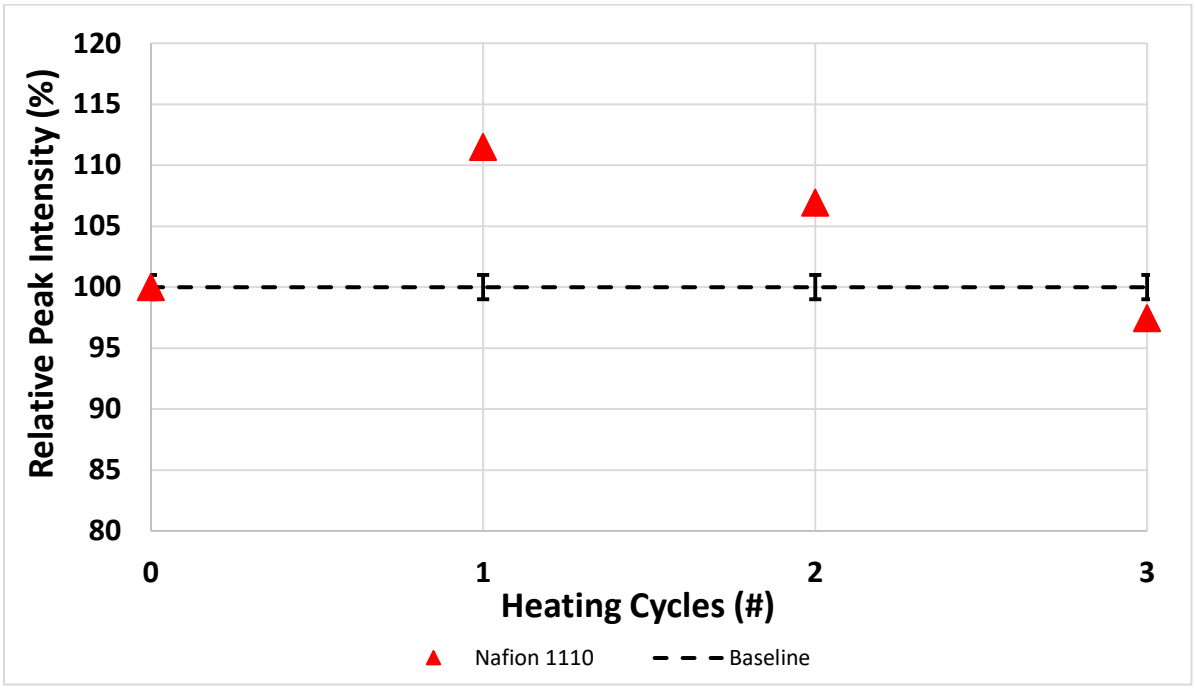

Figure 76: In-Situ Calculated 1110 Relative Peak II Intensity after 3 Heating Cycles to 120°C for 24hr. Results Compared to Peak II Baseline Measurements.

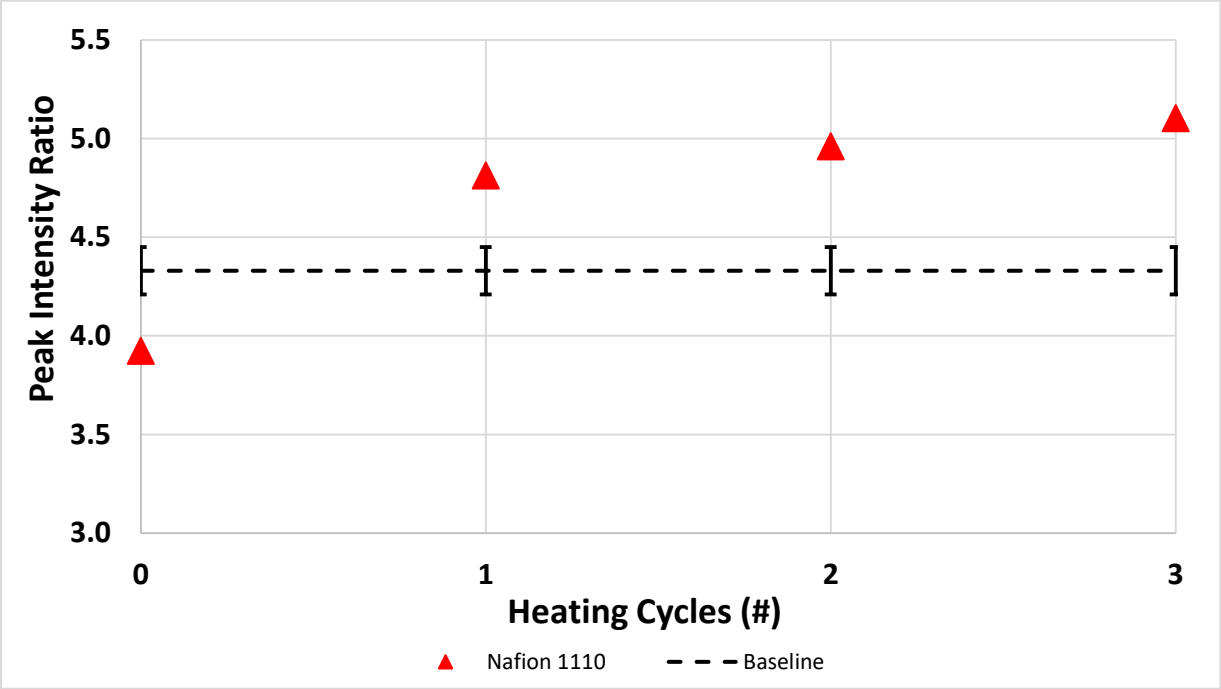

Figure 77: In-Situ Calculated 1110 Peak Ratio Intensities after 3 Heating Cycles to 120°C for 24hr. Results are Compared to Baseline Measurement.

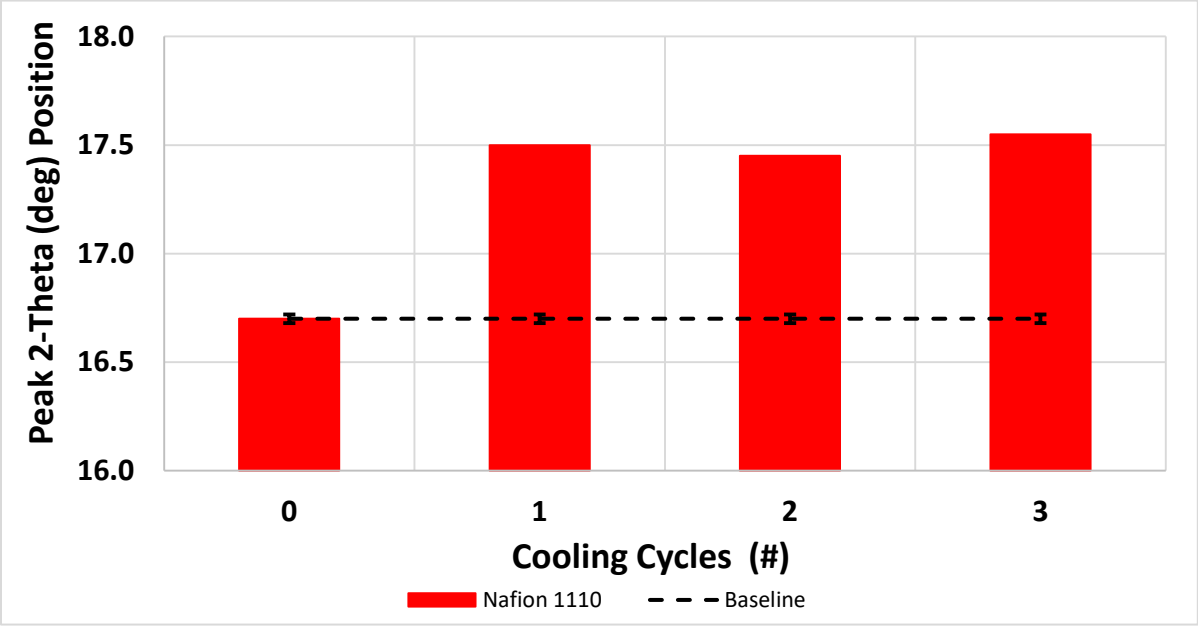

Figure 78: Post-Heated Calculated 1110 2-Theta Peak I Position after 3 Cooling Cycles to 120°C for 24hr. Baseline Raw XRD Data Provided for Comparison.

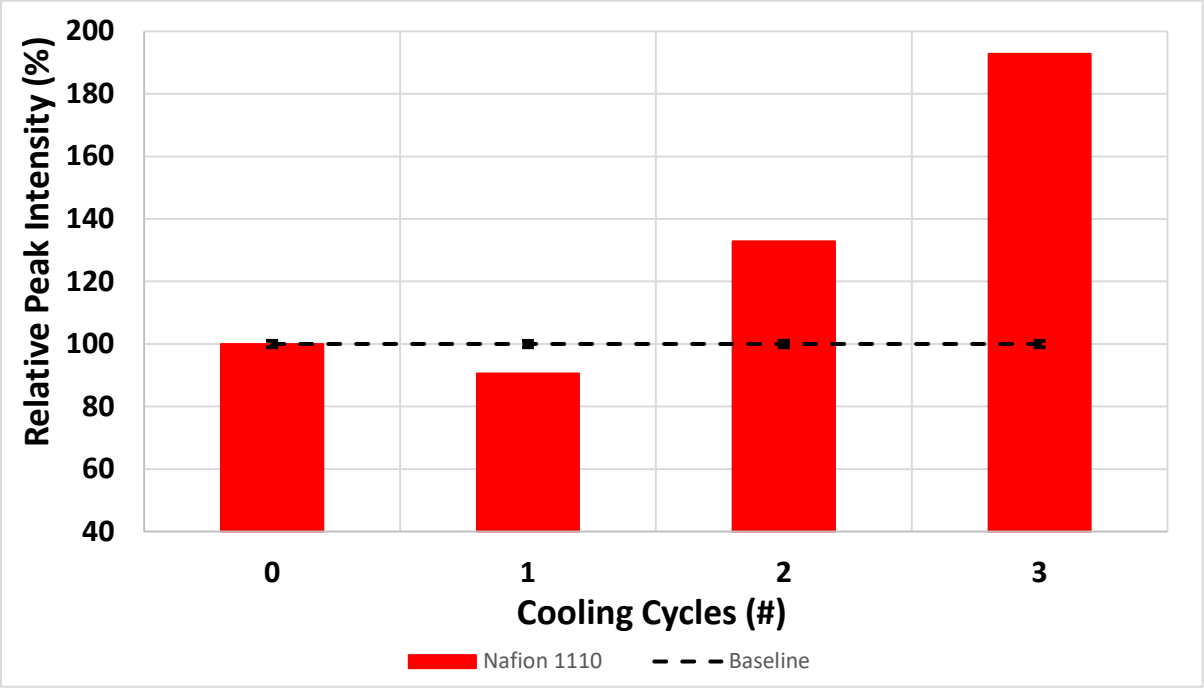

Figure 79: Post-Cooling Calculated 1110 Relative Peak I Intensity after 3 Cooling Cycles to 120°C for 24hr. Baseline Raw XRD Data Provided for Comparison.

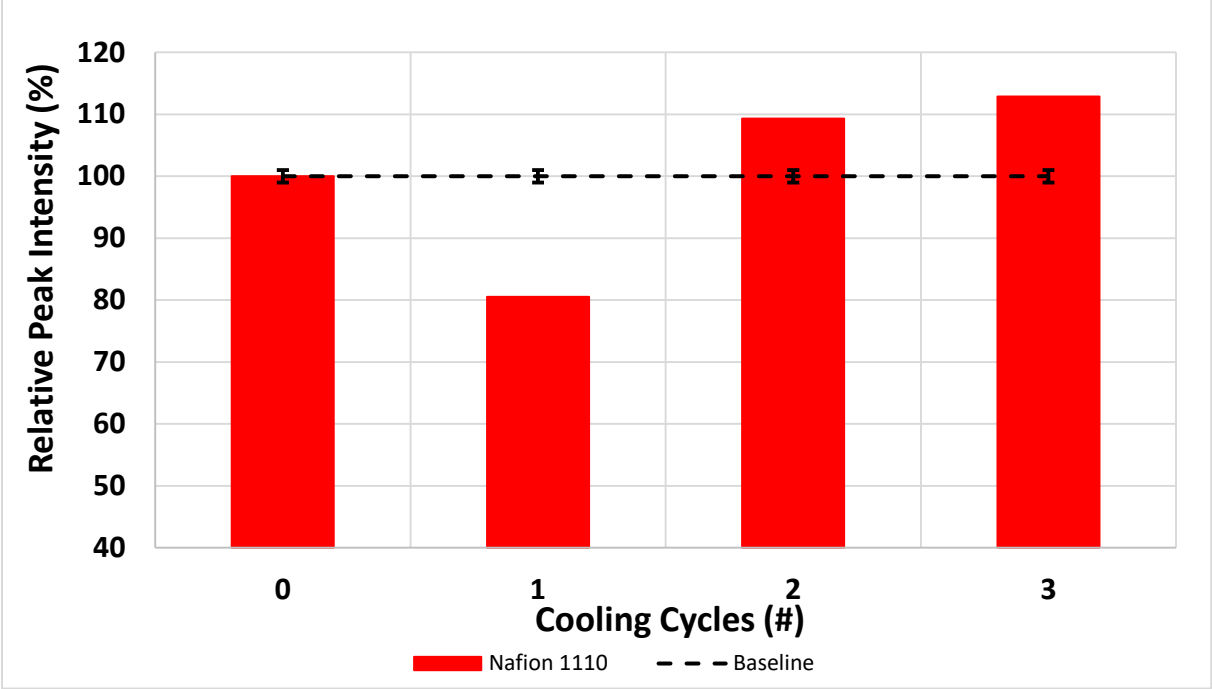

Figure 80: Post-Heating Calculated 1110 Relative Peak II Intensity after 3 Cooling Cycles to 120°C for 24hr. Results Compared to Peak II Baseline Measurements.

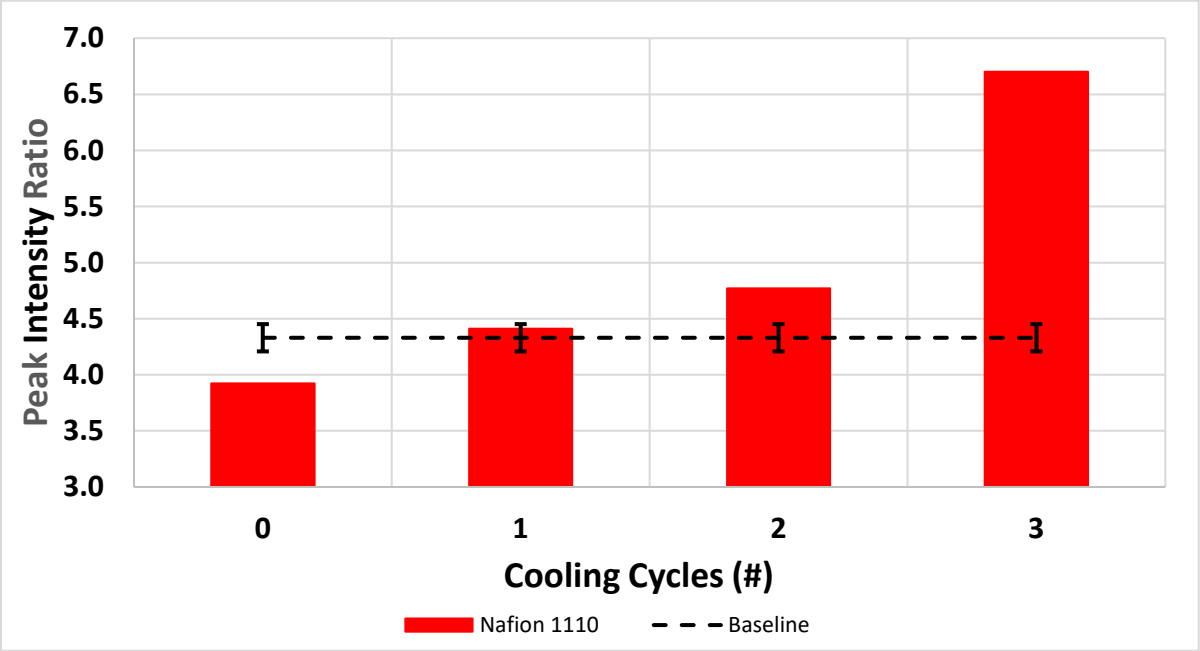

Figure 81: Post-Heating Calculated 1110 Peak Ratio Intensities after 3 Cooling Cycles to 120°C for 24hr. Results are Compared to Baseline Measurement.

Figure 74 through Figure 77 showed the In-Situ parameters for the 1110 material after being heated to 120°C for 3 cycles. Overall the 1110 material gradually showed an increase in the Peak I position, intensity and the peak intensity ratio. The Peak II intensity initially increased but then dramatically decreased following the first cycle. One interesting point to make is the In-Situ Peak I 2-Theta positions generally were lower than the baseline in previous sections of this study, but the Peak I 2-Theta position increased above the baseline when sample were heating/cooling cycles were performed. As mentioned earlier in this section, cycling the samples may have placed additional residual stress within the membrane which, when heated, caused increased peak intensities. Finally, the peak ratio, over time continued to gradually increase to 17.8% above the baseline by the end of the third cycle.

Figure 78 through Figure 81 showed the post-heating parameters for the 1110 material once it had been cooled down to 25°C after being heated to 120°C for 3 cycles. As was seen in Section 7 almost all the calculated parameters shifted away from the baseline starting at the first cycle. The amount each parameter shifted from the baseline, for the most part, became greater as the number of cycles increased.

The results shown here from three 120°C cycles should not be surprising since the 1110 material previously in Section 7 demonstrated its internal structural parameters varied as a function of time. These additional experimental results further demonstrated that the added complications of cycling the membrane, similar to what a PEM fuel cell would experience, produced internal instability as well.

8.3.3. *In-Depth In-Situ and Post-Heating Analysis at 140°C Operating Temperature*

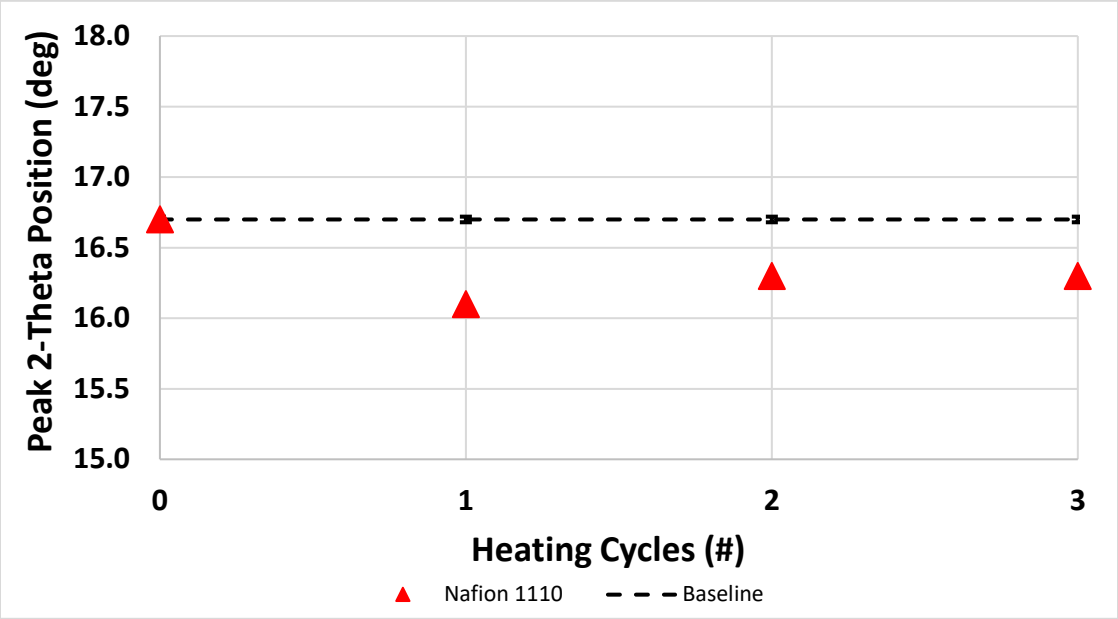

Figure 82: In-Situ Calculated 1110 2-Theta Peak I Position after 3 Heating Cycles to 140°C for 24hr. Baseline Raw XRD Data Provided for Comparison.

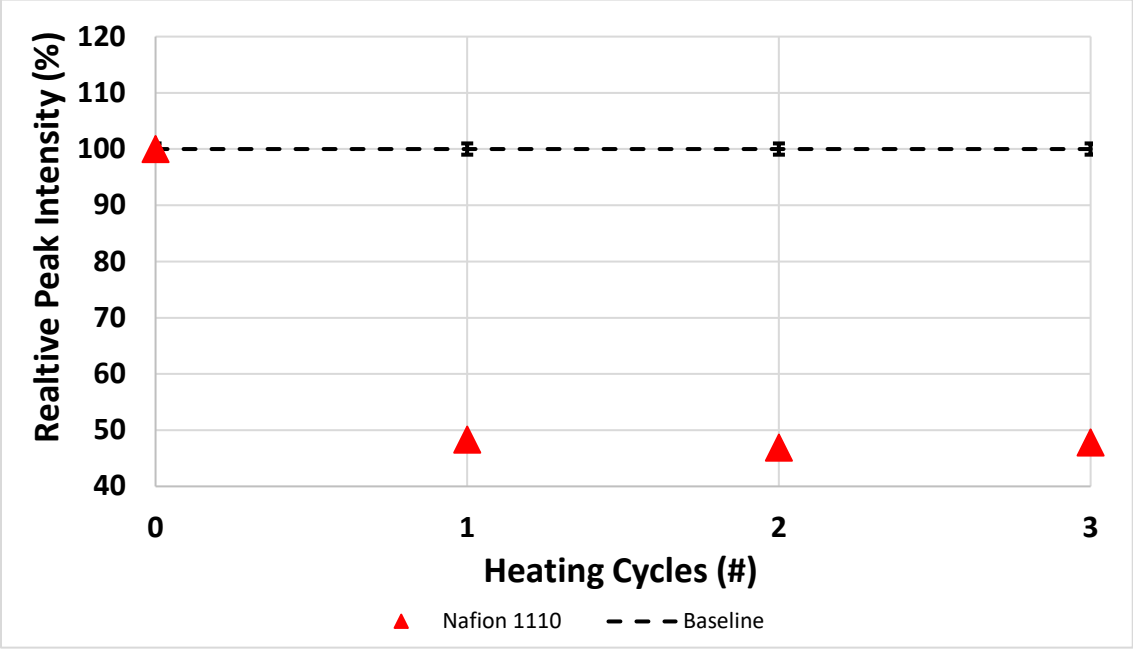

Figure 83: In-Situ Calculated 1110 Relative Peak I Intensity after 3 Heating Cycles to 140°C for 24hr. Baseline Raw XRD Data Provided for Comparison.

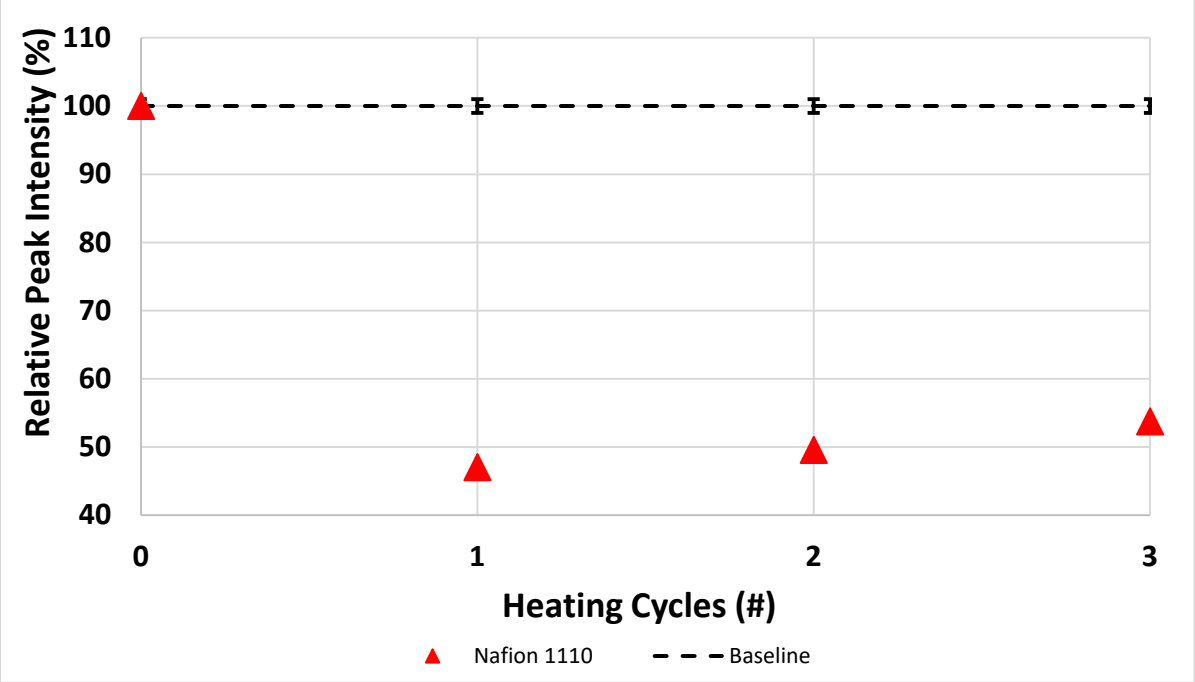

Figure 84: In-Situ Calculated 1110 Relative Peak II Intensity after 3 Heating Cycles to 140°C for 24hr. Results Compared to Peak II Baseline Measurements.

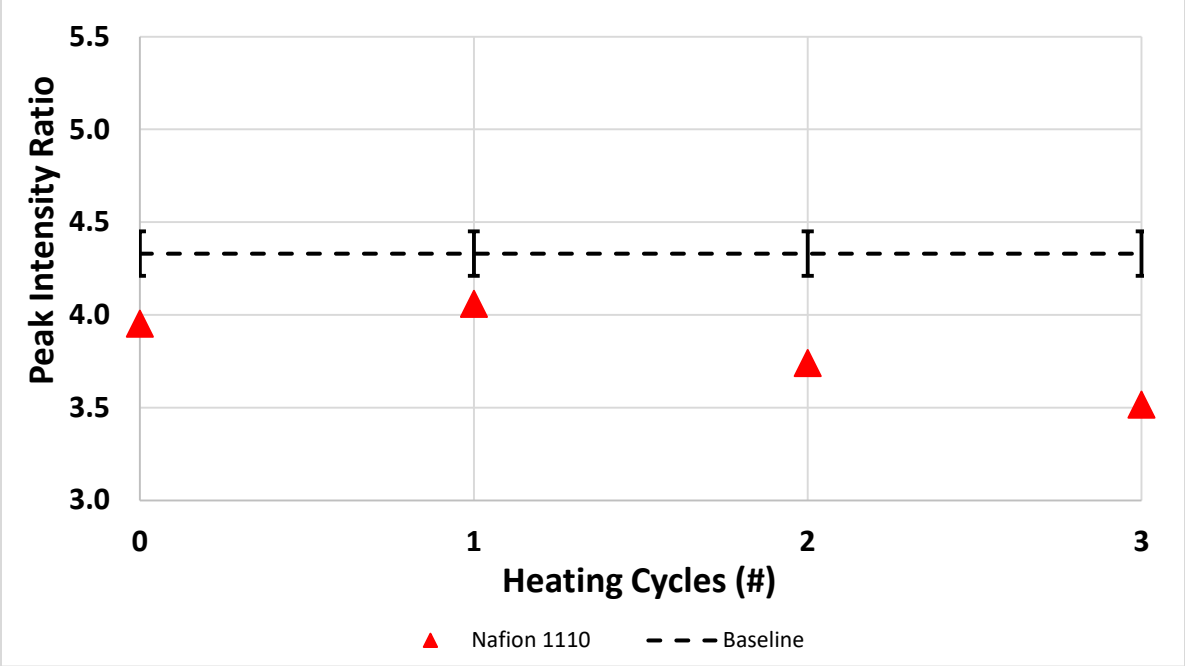

Figure 85: In-Situ Calculated 1110 Peak Ratio Intensities after 3 Heating Cycles to 140°C for 24hr. Results are Compared to Baseline Measurement.

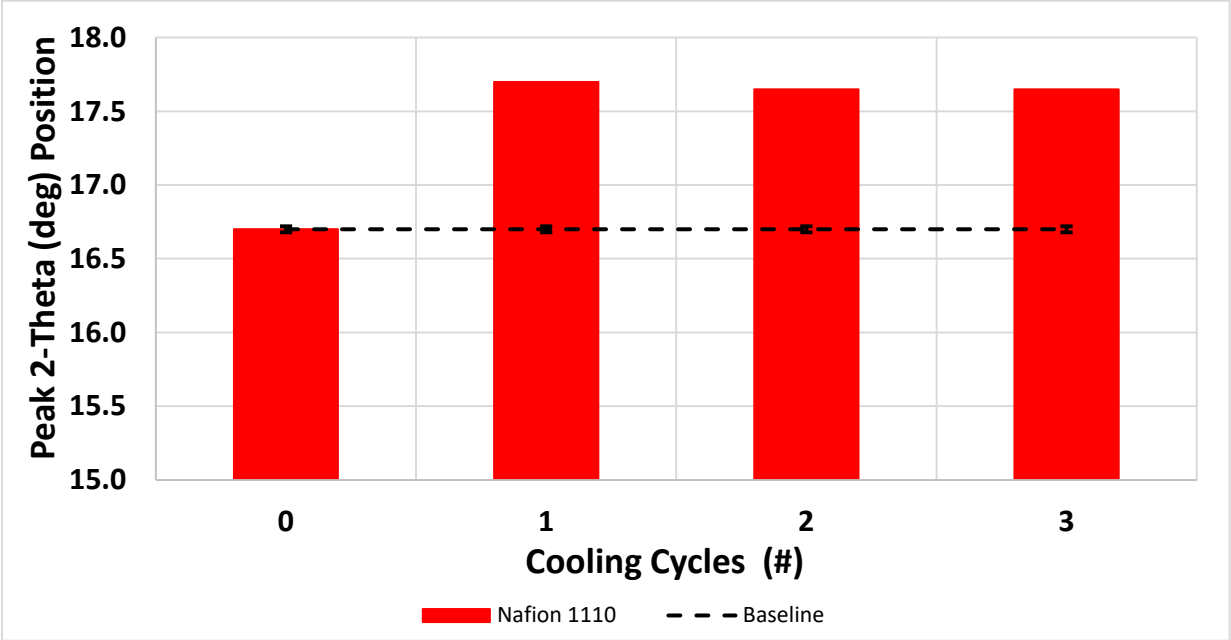

Figure 86: Post-Heated Calculated 1110 2-Theta Peak I Position after 3 Cooling Cycles to 140°C for 24hr. Baseline Raw XRD Data Provided for Comparison.

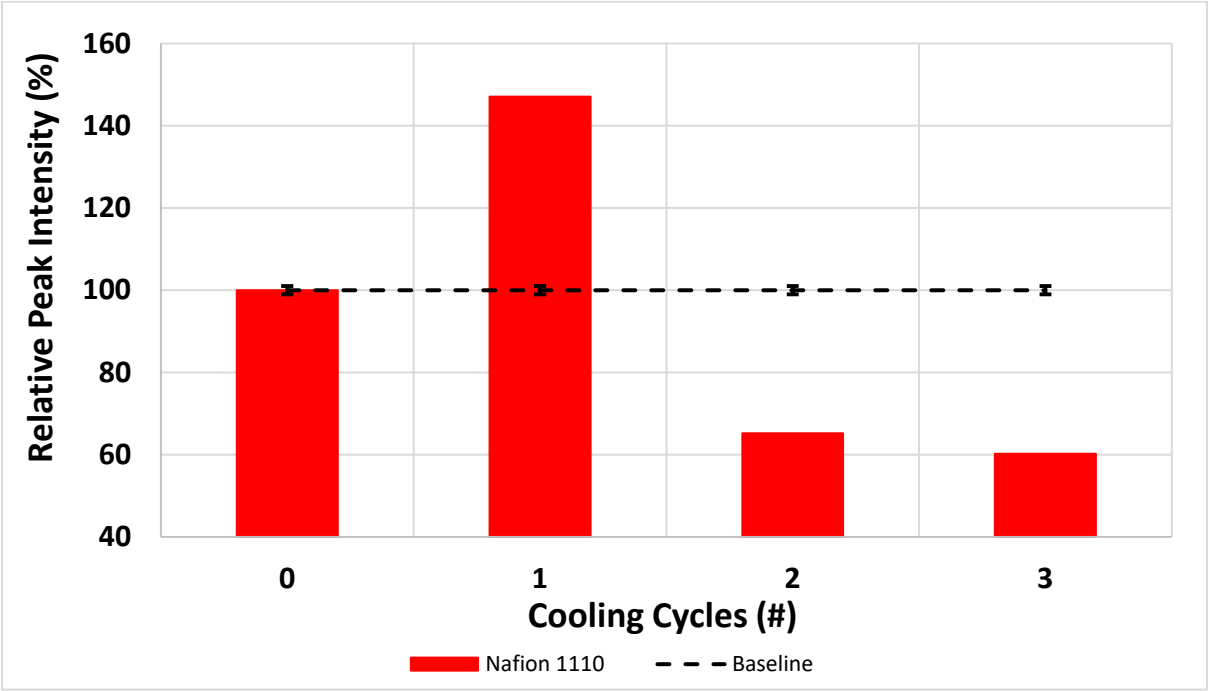

Figure 87: Post-Cooling Calculated 1110 Relative Peak I Intensity after 3 Cooling Cycles to 140°C for 24hr. Baseline Raw XRD Data Provided for Comparison.

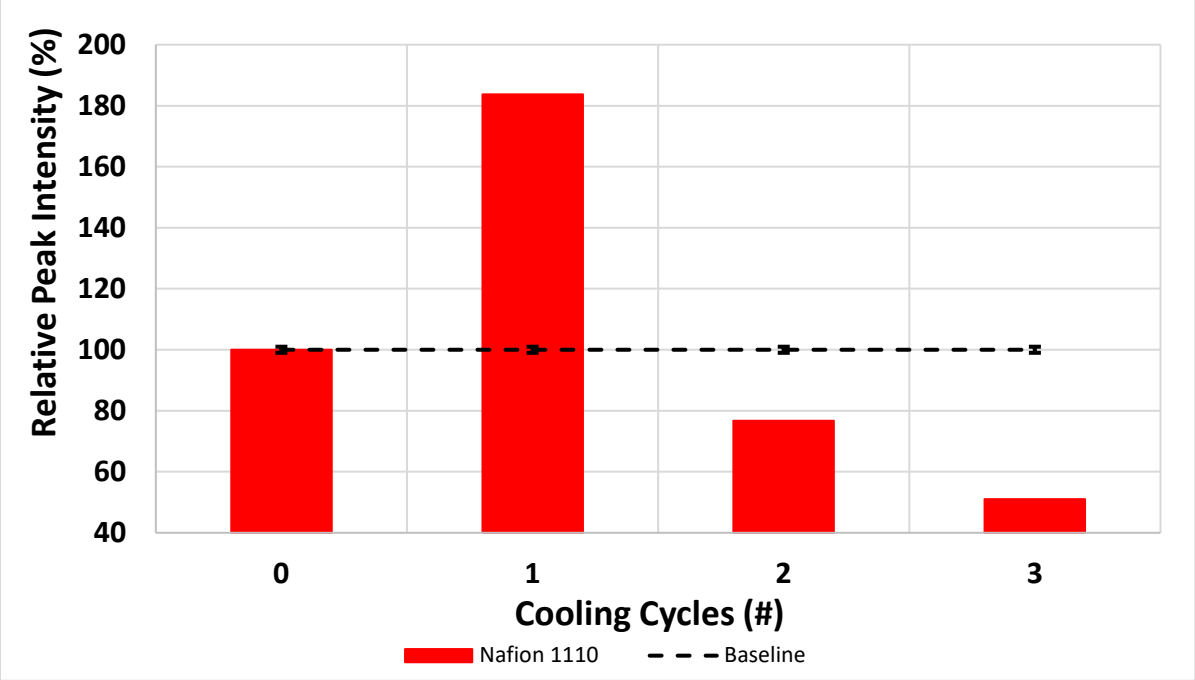

Figure 88: Post-Heating Calculated 1110 Relative Peak II Intensity after 3 Cooling Cycles to 140°C for 24hr. Results Compared to Peak II Baseline Measurements.

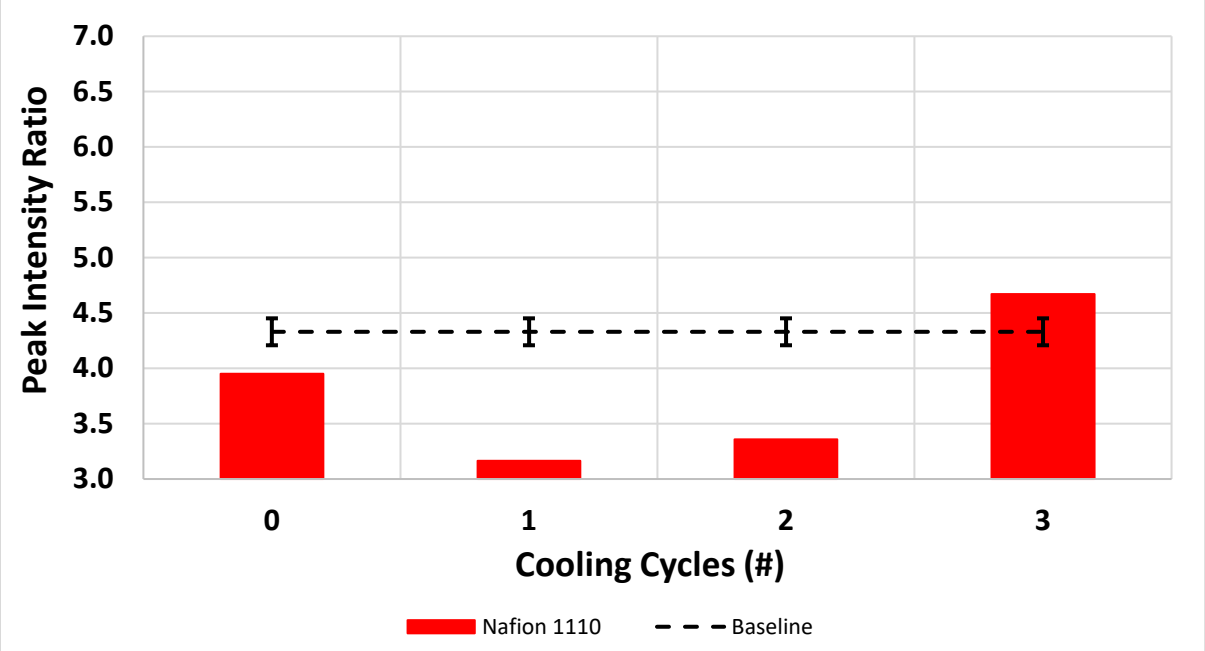

Figure 89: Post-Heating Calculated 1110 Peak Ratio Intensities after 3 Cooling Cycles to 140°C for 24hr. Results are Compared to Baseline Measurement.

Figure 82 through Figure 85 showed the In-Situ parameters for the 1110 material after being heated to 140°C for 3 cycles. The overall structural changes to the 1110 material when heated to 140°C were more severe, as would be expected, compared to the 120°C results. In addition to being more severe, the following In-Situ results displayed a different set of trends (compared to the 120°C results) which should be analyzed as well. First, the calculated 120°C Peak I 2-Theta position was shown to increase by 3% by the third cycle, but heating the polymer sample at 140°C resulted in the 2-Theta position decreasing 2.4%. Overall the magnitude in change for the Peak I position was similar but just a different direction. The increased operating temperature being used is hypothesized to influence the direction of the Phase I 2-Theta location, but additional analysis would be required. Both the Peak I and II intensities decreased by an average of ~52% and ~50%, respectively. These peak intensity results also occurred in the opposite direction compared to 120°C In-Situ peak intensity analysis, which increased by ~33% and ~5% respectively. Finally, the peak ratio values at 120°C increases systematically above the baseline, but here the values systematically decrease below the baseline.

Figure 86 through Figure 89 showed the post-heating parameters for the 1110 material after being cooled back down to 25°C after being heated to 140°C for 3 cycles. Many of these post-heating results also display the opposite response observed with the 120°C parameters as was observed with the In-Situ analysis. The only parameter that followed a similar trend to the 120°C post-heating results was the Peak I 2-Theta position which increased on average ~5.8, which was still a 1% larger shift in position than the 120°C results. By the end of the third cycle both the Peak I and II intensities decreased on average ~9%. Finally, the peak ratio first decreased to maximum of ~27% below the baseline, then increased ~7.8% above the baseline by the third cycle. The peak ratio still decreased by ~12.5% on average.

Just as was observed for samples heated at 120°C these results also should not be surprising considering the conclusions made in Section 7 for the 1110 material. Additional correlation between these internal structural degradation results and material properties after heating at 140°C does appear to be necessary since these results indicate continued internal structural degradation.

8.4. Combined Heating/Cooling In-Situ Nafion© 1110 XRD In-Situ and Post-Heating Measurements Summary

In summary, the following In-Situ and post-heating trends were observed for the 1110 material after being heated to 60°C, 120°C and 140°C operating temperatures for 3 cycles.

In-Situ Data Trends:

1. All three operating temperatures show moderate to severe degradation by the third cycle for the 1110 membrane. The 120°C and 140°C operating temperatures showed the severe degradation, but even 60°C, which showed fairly stable results in Section 6 and 7, showed moderate fluctuations compared to the baseline.
2. All the parameters, except the Peak II 2-Theta position, showed changes at all operating temperatures.
3. Overall, based on these In-Situ results, the 1110 membrane is not suitable for temperatures above 100°C. The 1110 membranes ability to be used at 60°C for multiple cycles is questionable also.

Post-Heating Data Trends:

1. The 1110 membrane had better success at returning to its baseline after being cooled to 25°C post-heating. The 60°C results showed a relatively stable Peak I 2-Theta position and peak ratio values. The Peak I and II intensities decreased by 20-25%, which were the most severe cases of degradation at that temperature.

2. The 1110 membrane was not successful at returning to its baseline values after being heated to 120°C or 140°C. Nearly all material properties calculated showed drastic changes in peak position, peak intensity and/or peak ratio.
3. Overall, based on these post-heating results, the 1110 membrane is not suitable for temperatures above 100°C. The 1110 membrane does appear to be more capable of returning to a stable baseline when cooled after being heated to 60°C, but still showed some instability.

9. Conclusions

Based on the results collected in this report the following overarching conclusions were made.

1. The internal structural stability of Nafion© does have some correlation to the thickness of the material. Generally the thicker the material the more resilient it was from deviating from the calculated baseline parameters determined from the raw XRD scans.
2. All calculated variables were found to be influenced by the operating temperature, except for the Peak II 2-Theta position, which always maintained the same value as the baseline, which was 39.3° 2-Theta. The magnitude of these parameter changes was found to be minimized by operating at lower temperatures and using increased membrane thicknesses.
3. All materials ultimately showed some form of internal structural change compared to the baseline for In-Situ or post-heating parameter calculations. The 1110 material, however, was nearly unchanged when heated at 60°C up to 24 hours. The 1110 material had ~90% of its calculated parameters (In-Situ and post-heating combined) statistically unchanged from the baseline. This same analysis for the 115 and 117 materials, at 60°C, showed a 20% and 50% statistical similarity with their baselines, respectively.
4. Three long-term heating/cooling cycles, performed at 60°C, destabilized the internal structure of the 1110 material. Heating and cooling cycles applied to a membrane material would be the next logical experiment to test the membrane internal structural durability in real world applications. The 1110 membranes internal structure appeared permanently altered after the final cycle was completed. This test did combine the effect of operating temperature and thermal cycling which may be why the membrane failed, but was still is a valid test.

10. References

[1] S. Cleghorn, X. Ren, T. Springer, C. Z. M.S. Wilson, T. Zawodzinski and S. Gottesfeld, "PEM Fuel Cells for Transportation and Stationary Power Generation Applications," *Int. J. Hydrog. Energy,* vol. 22, pp. 1137-1144, 1997.

[2] A. Kirubakaran, S. Jain and R. Nema, "A Review on Fuel Cell Technologies and Power Electronic Interface," *Renew. Sust. Energ. Rev.,* vol. 13, pp. 2430-2440, 2009.

[3] M. Gencoglu and Z. Ural, "Design of a PEM Fuel Cell System for Residential Application," *Int. J. Hydrog. Energy,* vol. 34, pp. 5242-5248, 2009.

[4] J. A. R. Mann, B. Peppley, P. Roberge and A. Rodrigues, "A Practical PEM Fuel Cell Model for Simulating Vehicle Power Sources," in *IEEE*, Long Beach, CA, 1995.

[5] J.-H. Wee, "Applications of Proton Exchange Membrane Fuel Cell Systems," *Renew. Sustain. Energy Rev,* vol. 11, pp. 1720-1738, 2007.

[6] J. Wind, R. Späh, W. Kaiser and G. Böhm, "Metallic Bipolar Plates for PEM Fuel Cells," *J. Power Sources,* vol. 105, pp. 256-260, 2002.

[7] J. Gilbert, N. Kariuki, X. Wang, A. Kropf, K. Yu, D. Groom, P. Ferreira, D. Morgan and D. Myers, "Pt Catalyst Degradation in Aqueous and Fuel Cell Environments Studied via In-Operando Anomalous Small-Angle X-Ray Scattering," *Electrochim. Acta.,* vol. 173, pp. 223-234, 2015.

[8] S. Lang, T. Kazdal and M. H. F. Kühl, "Experimental Investigation and Numerical Simulation of the Electrolyte Loss in a HT-PEM Fuel Cell," *Int. J. Hydrog, Energy,* vol. 40, pp. 1163-1172, 2015.

[9] F. Wang, D. Yang, B. Li, H. Zhang, C. Hao, F. Chang and J. Ma, "Investigation of the Recoverable Degradation of PEM Fuel Cell Operated under Drive Cycle and Different Humidities," *Int. J. Hydrog. Energy,* vol. 39, pp. 14441-14447, 2014.

[10] J. Kang and J. Kim, "Membrane Electrode Assembly Degradation by Dry/Wet Gas on a PEM Fuel Cell," *Int. J. Hydrog. Energy,* vol. 35, pp. 13125-13130, 2010.

[11] R. Kerr, H. García, M. Rastedt, P. Wagner, S. Alfaro, M. Romero, C. Terkelsen, T. Steenberg and H. Hjuler, "Lifetime and Degradation of High Temperature PEM Membrane Electrode Assemblies," *Int. J. Hydrog. Energy,* vol. 40, pp. 16860-16866, 2015.

[12] A. U. M.A. Rubio and S. Dormido, "Diagnosis of Performance Degradation Phenomena in PEM Fuel Cells," *Int. J. Hydrog. Energy,* vol. 35, pp. 2586-2590, 2010.

[13] K. Yu, D. Groom, X. Wang, Z. Yang, M. Gummalla, S. Ball, D. Myers and P. Ferreira, "Degradation Mechanisms of Platinum Nanoparticle Catalysts in Proton Exchange Membrane Fuel Cells: The Role of Particle Size," *Chem. Mater.,* vol. 26, pp. 5540-5548, 2014.

[14] T. Burye, "Effect of Proton Exchange Membrane Fuel Cell Exhaust Water Conductivity on Catalyst Degradation using Thermal Degradation Resistant Polymer Membranes," *Int. J. Hydrog. Energy,* vol. 45, pp. 11733-11748, 2020.

[15] A. Collier, H. Wang, X. Yuan, J. Zhang and D. Wilkinson, "Degradation of Polymer Electrolyte Membranes," *Int. J. Hydrog, Energy,* vol. 31, pp. 1838-1854, 2006.

[16] J. Zhang, Z. Xie, J. Zhang, Y. Tang, C. Song, T. Navessin, Z. Shi, D. Song, H. Wang, D. Wilkinson, Z.-S. Liu and S. Holdcroft, "High Temperature PEM Fuel Cells," *J. Power Sources,* vol. 160, pp. 872-891, 2006.

[17] X. G. F. Lu, X. Yan, H. Gao, L. Shi, H. Jia and L. Zheng, "Preparation and Characterization of Nonaqueous Proton-Conducting Membranes with Protic Ionic Liquids," *ACS. Appl. Mater. Interfaces,* vol. 5, pp. 7626-7632, 2013.

[18] A. Ozden, M. Ercelik, Y. Ozdemir, Y. Devrim and C. Colpan, "Enhancement of Direct Methanol Fuel Cell Performance through the Inclusion of Zirconium Phosphate," *Int. J. Hydrog. Energy,* vol. 42, pp. 21501-21517, 2017.

[19] P. Staiti, A. Aricò, V. Baglio, F. Lufrano, E. Passalacqua and V. Antonucci, "Hybrid Nafion-Silica Membranes Doped with Heteropolyacids for Application in Direct Methanol Fuel Cells," *Solid State Ionics,* vol. 145, pp. 101-107, 2001.

[20] S. Banerjee and D. Curtin, "Nafion Perfluorinated Membranes in Fuel Cells," *J. Fluor. Chem.,* vol. 125, pp. 1211-1216, 2004.

[21] P. Majsztrik, M. Satterfield, A. Bocarsly and J. Benziger, "Water Sorption, Desorption and Transport in Nafion Membranes," *J. Membrane Sci.,* vol. 301, pp. 93-106, 2007.

[22] Q. Duan, H. Wang and J. Benziger, "Transport of Liquid Water through Nafion Membranes," *J. Membrane Sci.,* Vols. 392-393, pp. 88-94, 2012.

[23] S. Goswami, S. Klaus and J. Benziger, "Wetting and Absorption of Water Drops on Nafion Films," *Langmuir,* vol. 24, pp. 8627-8633, 2008.

[24] H. Corti, F. Nores-Pondal and M. Buera, "Low Temperature Thermal Properties of Nafion 117 Membranes in Water and Methanol-Water Mixtures," *J. Power Sources,* vol. 161, pp. 799-805, 2006.

[25] R. Scipioni, D. Gazzoli, F. Teocoli, O. Palumbo, A. Paolone, N. Ibris, S. Brutti and M. Navarra, "Preparation and Characterization of Nanocomposite Polymer Membranes Containing Functionalized SnO2 Additives," *Membranes,* vol. 4, pp. 123-142, 2014.

[26] S. d. Almeida and Y. Kawano, "Thermal Behavior of Nafion Membranes," *J. Therm. Anal. Cal. ,* vol. 58, pp. 569-577, 1999.

[27] S.-J. Shin, A. Balabanovich, H. Kim and J. Jeong, "Deterioration of Nafion 115 Membrane in Direct Methanol Fuel Cells," *J. Power Sources,* vol. 191, pp. 312-319, 2009.

[28] S. Tan and D. Belanger, "Characterization and Transport Properties of Nafion/Polyaniline Composite Membranes," *J. Phys. Chem. B,* vol. 109, pp. 23480-23490, 2005.

[29] G. Corbel, M. Topic, A. Gibaud and C. Lang, "Selective Dry Oxidation of the Ordered Pt-11.1 at.% V Alloy Surface Evidenced by In-Situ Temperature-Controlled X-Ray Diffraction," *J. Alloys Compd.,* pp. 6532-6538, 2011.

[30] V. Darakchieva, J. Birch, M. Schubert, T. Paskova, S. Tungasmita, G. Wagner, A. Kasic and B. Monemar, "Strain-Related Structural and Vibrational Properties of Thin Epitaxial AlN Layers," *Phys. Rev. B,* vol. 70, p. 045411, 2004.

[31] A. Korchef, Y. Champion and N. Njah, "X-Ray Diffraction Analysis of Aluminum Containing Al8Fe2Si Processed by Equal Channel Angular Pressing," *J. Alloys Compd.,* vol. 427, pp. 176-182, 2007.

[32] J. Shakya, S. Kumar, D. Kanjilal and T. Mohanty, "Work Function Modulation of Molybdenum Disulfide Nanosheets by Introducing Systematic Lattic Strain," *Sci. Rep.,* vol. 7, p. 9576, 2017.

[33] B. Gržeta, E. Tkalčec, C. Goebbert, M. Takeda, M. Takahashi, K. Nomura and M. Jakšić, "Structural Studies of Nanocrystalline SnO2 Doped with Antimony: XRD and Mössbauer Spectroscopy," *J. Phys. Chem. Solids,* vol. 63, pp. 765-772, 2002.

[34] A. Srivastav and A. Panindre, "XRD Characterization of Microstructural Evolution During Mechanical Alloying of W-20 wt% Mo," *Trans. Indian Inst. Met.,* vol. 66, pp. 409-414, 2013.

[35] X. Yang, J. Lu, H. Zhang, Y. Chen, B. Kan, J. Zhang, J. Huang, B. Lu, Y. Zhang and Z. Ye, "Preparation and XRD Analyses of Na-Doped ZnO Nanorod Arrays Based on Experiment and Theory," *Chem. Phys. Lett.,* vol. 528, pp. 16-20, 2012.

[36] X. Zheng, C. Wu, S. Jha, Z. Li, K. Zhu and Z. Priya, "Improved Phase Stability of Formamidinium Lead Triiodide Perovskite by Strain Relaxation," *ACS Energy Lett.,* vol. 1, pp. 1014-1020, 2016.

[37] Y. Takeda, K. Kanno, T. Takada, O. Yamamoto, M. Takano, N. Nakayama and Y. Bando, "Phase Relation in the Oxygen Nonstoichiometry System, SrFeOx (2.5<x<3.0)," *J. Solid State Chem.,* vol. 63, pp. 237-249, 1986.

[38] M. Kuhn, S. Bishop, J. Rupp and H. Tuller, "Structural Characterization and Oxygen Nonstoichiometry of Ceria-Ziconia (Ce1-xZrxO2-d) Solid Solutions," *Acta Materialia,* vol. 61, pp. 4277-4288, 2013.

[39] R. v. d. Krol, A. Goossens and E. Meulenkamp, "In Situ X-Ray Diffraction of Lithium Intercalation in Nanostructured and Thin Film Anatase TiO2," *J. Electrochem. Soc.,* vol. 146, pp. 3151-3154, 1999.

[40] D. Hay, H. Jaeger and G. West, "Examination of the Monoclinic/Orthorhombic Transition in Silicalite using XRD and Silicon NMR," *J. Phys. Chem.,* vol. 89, pp. 1070-1072, 1985.

[41] R. Sharma, D. Bisen, U. Shukla and B. Sharma, "X-Ray Diffraction: A Powerful Method of Characterizing Nanomaterials," *Recent Res. Sci. Technol.,* vol. 4, no. 8, pp. 77-79, 2012.

[42] T. Benedict, S. Banumathi, A. Veluchamy, R. Gangadharan, A. Ahamad and S. Rajendran, "Characterization of Plasticized Solid Polymer Electrolyte by XRD and AC Impedance Methods," *J. Power Sources,* vol. 75, pp. 171-174, 1998.

[43] N. Murthy, S. Correale and H. Minor, "Structure of the Amorphous Phase in Crystallizable Polymers: Poly(ethylene terephthalate)," *Macromolecules,* vol. 24, pp. 1185-1189, 1991.

[44] S. Toki, T. Fujimaki and M. Okuyama, "Strain-Induced Crystallization of Natural Rubber as Detected Real-Time by Wide-Angle X-Ray Diffraction Technique," *Polymer,* vol. 41, no. 14, pp. 5423-5429, 2000.

[45] V. Mote, Y. Purushotham and B. Dole, "Williamson-Hall Analysis in Estimation of Lattice Strain in Nanometer-Sized ZnO Particles," *J. Theor. Appl. Phys.,* vol. 6, pp. 1-8, 2012.

[46] A. Patterson, "The Scherrer Formula for X-Ray Particle Size Determination," *Phys. Rev.,* vol. 56, p. 978, 1939.

[47] L. Rubatat, G. Gebel and O. Diat, "Fibrillar Structure of Nafion: Matching Fourier and Real Space Studies of Corresponding Films and Solutions," *Macromolecules,* vol. 37, pp. 7772-7783, 2004.

[48] M. Chomakova-Haefke, R. Nyffenegger and E. Schmidt, "Structure Reorganization in Polymer Films of Nafion due to Swelling Studied by Scanning Force Microscopy," *Appl. Phys. A,* vol. 59, pp. 151-153, 1994.

[49] N. Murthy, "Recent Developments in Polymer Characterization using X-Ray Diffraction," *The Rigaku Journal,* vol. 21, pp. 15-24, 2004.

[50] H. Virk, P. Chandi and A. Srivastava, "Physical and Chemical Changes Induced by 70 MeV Carbon Ions in Polyvinylidene Difluoride (PVDF) Polymer," *Nucl. Instr. amd Meth. in Phys. Res. B,* vol. 183, pp. 329-336, 2001.

[51] R. Kumar, S. Ali, P. Singh, U. De, H. Virk and R. Prasad, "Physical and Chemical Response of 145 MeV Ne6+ Ion Irradiated Polymethylmethacrylate (PMMA) Polymer," *Nucl. Instr. and Meth. in Phys. Res. B,* vol. 269, pp. 1755-1759, 2011.

[52] Y. E. Ryabov, H. Nuriel, G. Marom and Y. Feldman, "Relaxation Peak Broadening and Polymer Chain Dynamics in Aramid-Fiber-Reinforced Nylon-66 Microcomposites," *J. Polym. Sci. Pol. Phys.,* vol. 41, pp. 217-223, 2003.

[53] B. Christ and J. Cohen, "Fourier Analysis of Polymer X-Ray Diffraction Patterns," *J. Polym. Sci.,* vol. 17, pp. 1001-1010, 1979.

[54] R. Narducci, P. Knauth, J.-F. Chailan and M. D. Vona, "How to Improve Nafion with Tailor Made Annealing," *RSC Adv.,* vol. 8, pp. 27268-27274, 2018.

[55] Y. Yan, X. Ge, Z. Liu, J. Wang, J.-M. Lee and X. Wang, "Facile Synthesis of Low Crystalline MoS2 Nanosheet-Coated CNTs for Enhanced Hydrogen Evolution Reaction," *Nanoscale,* vol. 5, pp. 7768-7771, 2013.

[56] L. Ottaviano, L. Lozzi, A. Phani, A. Ciattoni, S. Santucci and S. Nardo, "Thermally Induced Phase Transition in Crystalline Lead Phthalocyanine Films Investigated by XRD and Atomic Force Microscopy," *Appl. Surf. Sci.,* vol. 136, pp. 81-86, 1998.

[57] J. Greene, J.-E. Sundgren, L. Hultman, I. Petrov and D. Bergstrom, "Development of Preferred Orientation in Polycrystalline TiN Layers Grown by Ultrahigh Vaccum Reactive Magnetron Sputtering," *Appl. Phys. Lett.,* vol. 67, pp. 2928-2930, 1995.

[58] T. Goto, R. Banal and T. Kimura, "Morphology and Preferred Orientation of Y2O3 Film Preparred by High-Speed Laser CVD," *Surf. Coat. Tech.,* vol. 201, pp. 5776-5781, 2007.

[59] M. Ohyama, H. Kozuka and T. Yoko, "Sol-Gel Preparation of ZnO Films with Extremely Preferred Orientation along (002) Plane from Zinc Acetate Solution," *Thin Solid Films,* vol. 306, pp. 78-85, 1997.

[60] A. Jenkins, P. Kratchvil, R. Stepto and U. Suter, "Glossary of Basic Terms in Polymer Science," *Pure & Appl. Chem.,* vol. 68, pp. 2287-2311, 1996.

[61] C. Badini, E. Padovano, R. D. Camillis, V. Lambertini and M. Pietroluongo, "Preferred Orientation of Chopped Fibers in Polymer-Based Composites Processed by Selective Laser Sintering and Fused Depostion Modeling: Effects on Mechanical Properties," *J. Appl. Polym. Sci.,* 2020.

[62] D. Papkov, N. Delpouve, L. Delbreilh, S. Araujo, T. Stockdale, S. Mamedov, K. Maleckis, Y. Zou, M. Andalib, E. Dargent, V. Dravid, M. Holt, C. Pellerin and Y. Dzenis, "Quantifying Polymer Chain Orientation in Strong and Tough Nanofibers with Low Crystallinity: Toward Next Generation Nonstructured Superfibers," *ACS Nano,* vol. 13, pp. 4893-4927, 2019.

[63] C. Burger, B. Hsiao and B. Chu, "Preferred Orientation in Polymer Fiber Scattering," *Polym. Rev.,* vol. 1, pp. 91-111, 2010.

[64] A. Zhang, H. Jiang, Z. Wu, C. Wu and B. Qian, "Internal Stress, Lattice Deformation, and Modulus of Polymers," *Appl. Polym. Sci.,* vol. 42, pp. 1779-1791, 1991.

11. Supplemental Information

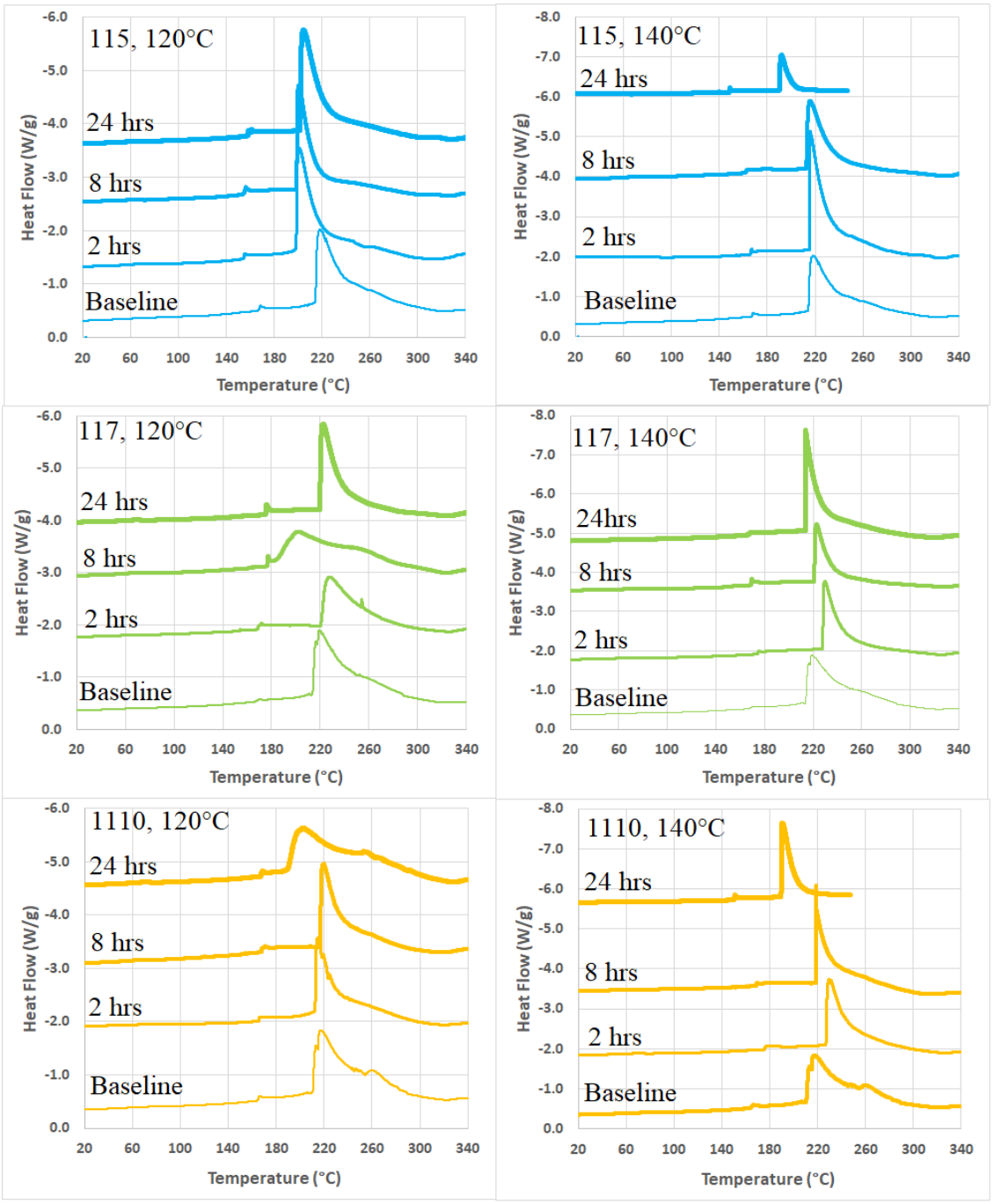

Figure 90: Raw DSC Data for Dry 115, 117 and 1110 Materials Heated to 120°C (Left Column) and 140°C (Right Column) for 2, 8 and 24 hrs Prior to DSC Characterization. DSC Characterization on Untested (Baseline) Samples are Shown for Comparison.

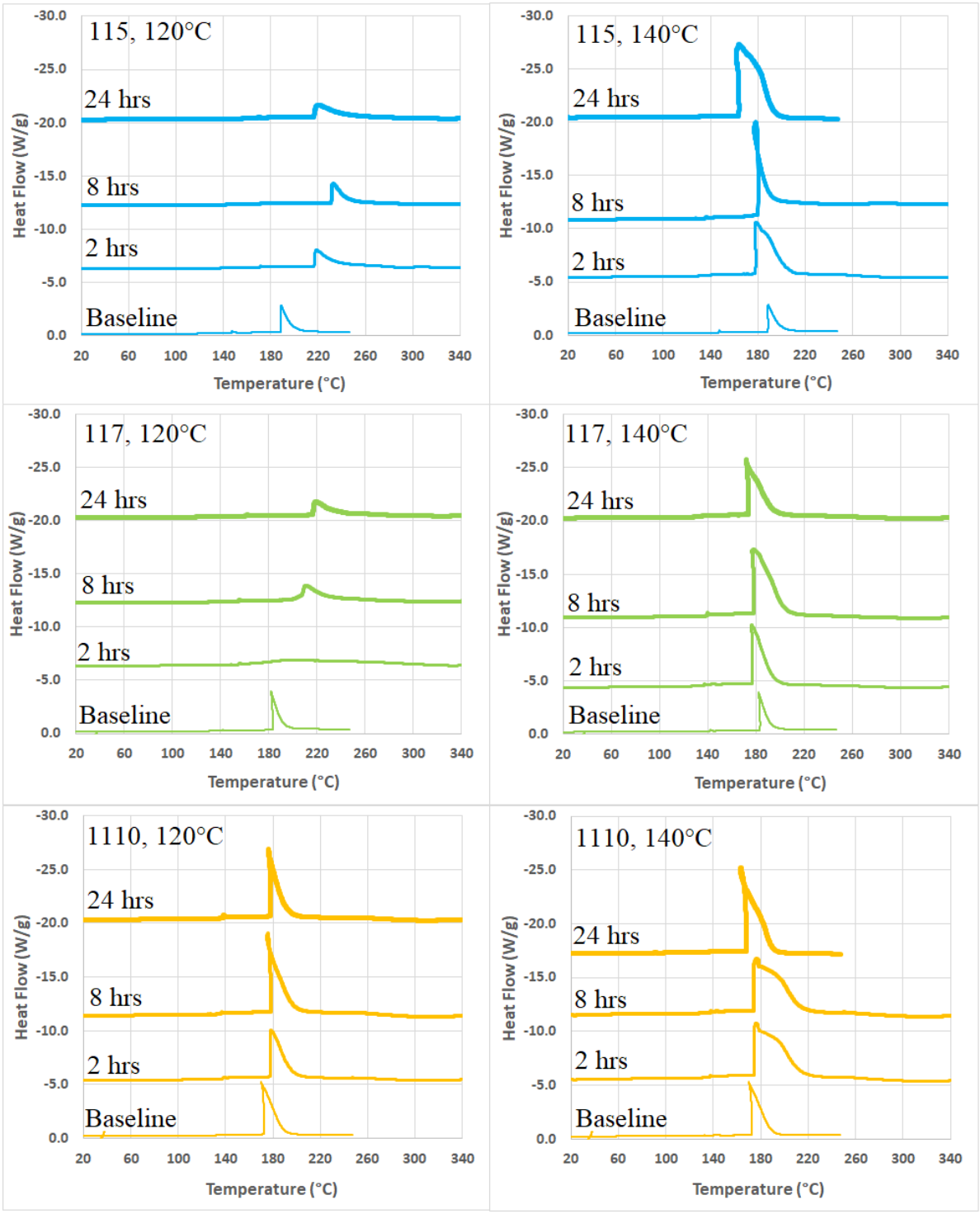

Figure 91: Raw DSC Data for Saturated 115, 117 and 1110 Materials Heated to 120°C (Left Column) and 140°C (Right Column) for 2, 8 and 24 hrs Prior to DSC Characterization. DSC Characterization on Untested (Baseline) Samples are Shown for Comparison.

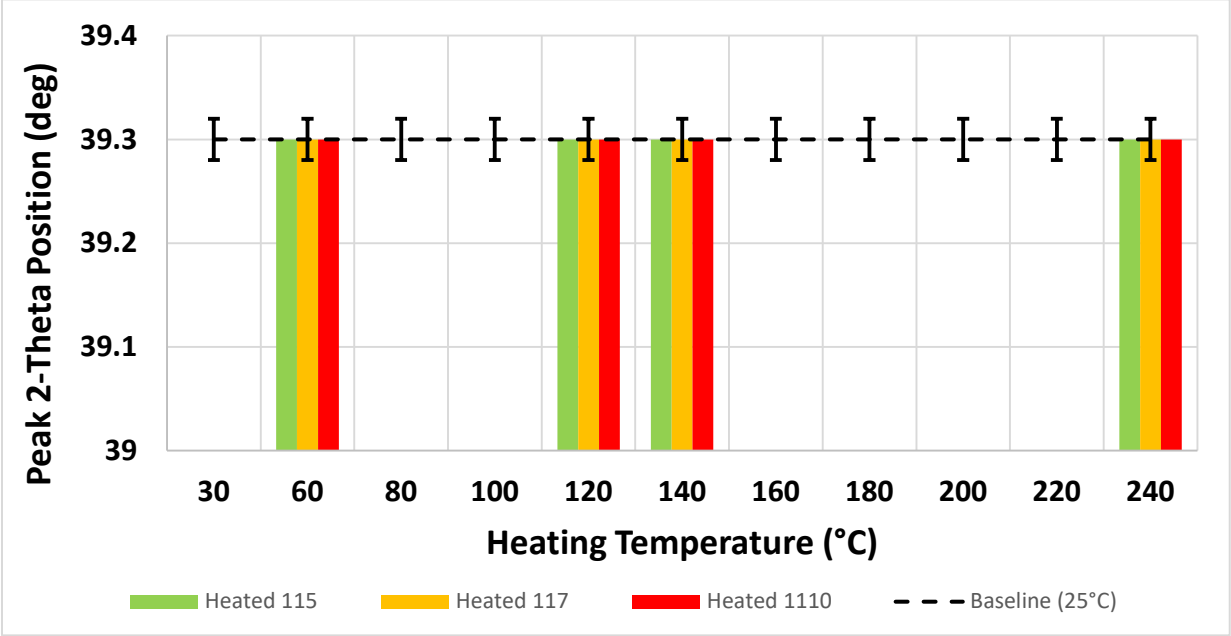

Figure 92: Calculated 115, 117 and 1110 2-Theta Peak Position for Peak II Compared to Baseline Measurements

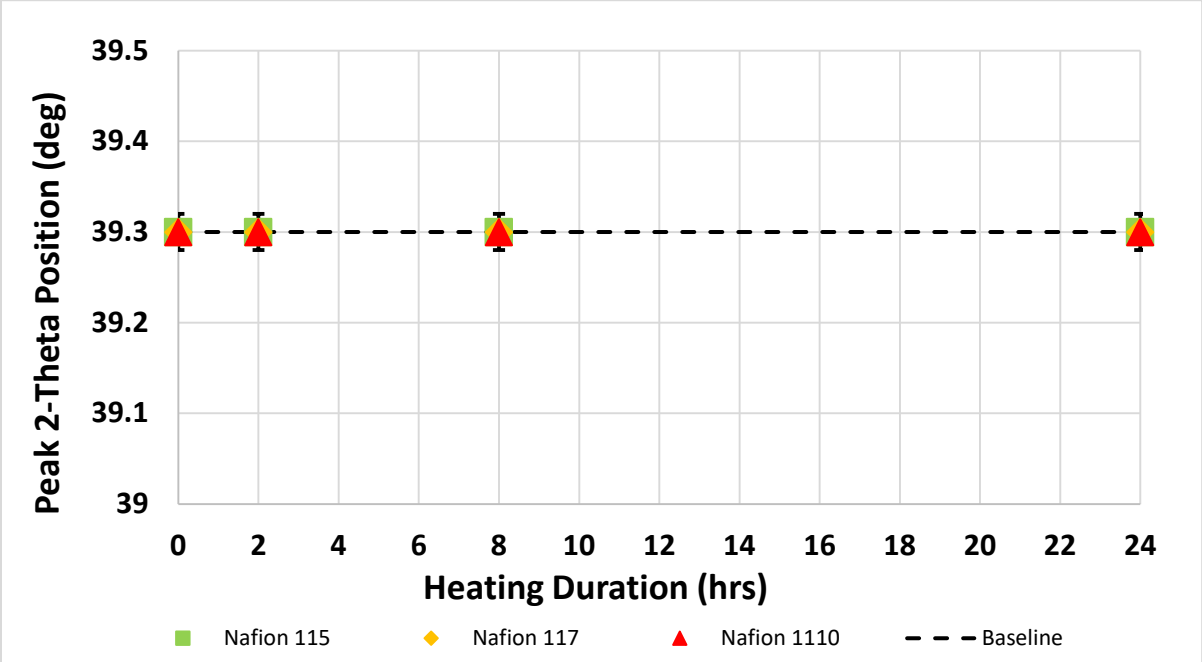

Figure 93: In-Situ Calculated 115, 117 and 1110 2-Theta Peak II Position after Heated to 60°C for 10 min, 2hr, 8hr and 24hr. Results Compared to Peak II Baseline Measurements.

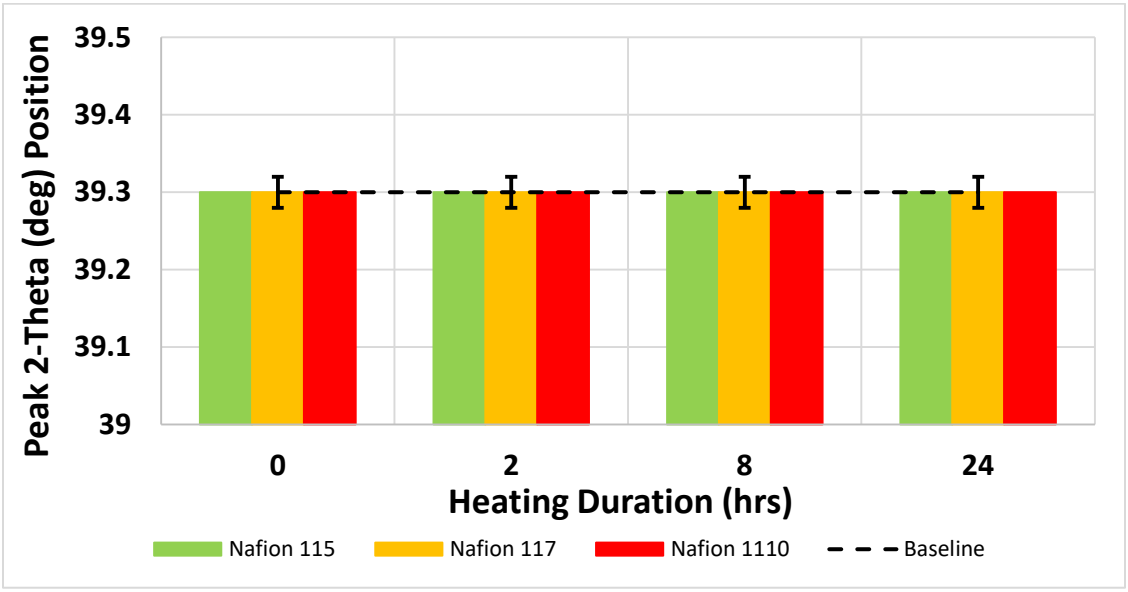

Figure 94: Post-Heating Calculated 115, 117 and 1110 2-Theta Peak II Position Taken at 25°C after Heated to 60°C for 10 min, 2hr, 8hr and 24hr. Results Compared to Peak I Baseline Measurements.

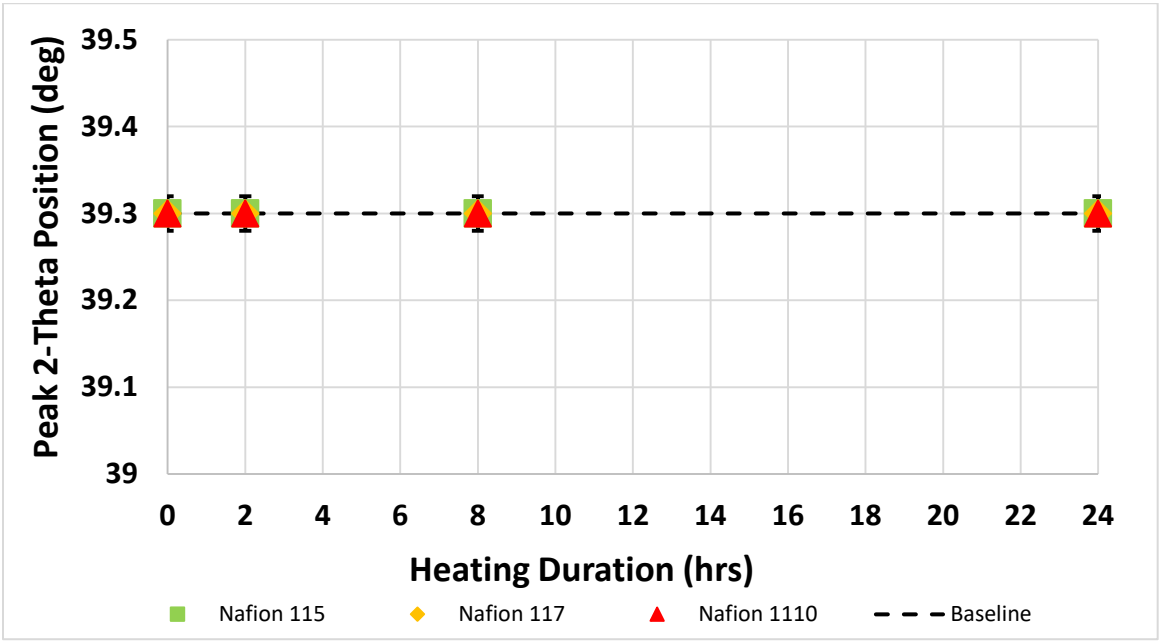

Figure 95: In-Situ Calculated 115, 117 and 1110 2-Theta Peak II Position after Heated to 120°C for 10 min, 2hr, 8hr and 24hr. Results Compared to Peak II Baseline Measurements.

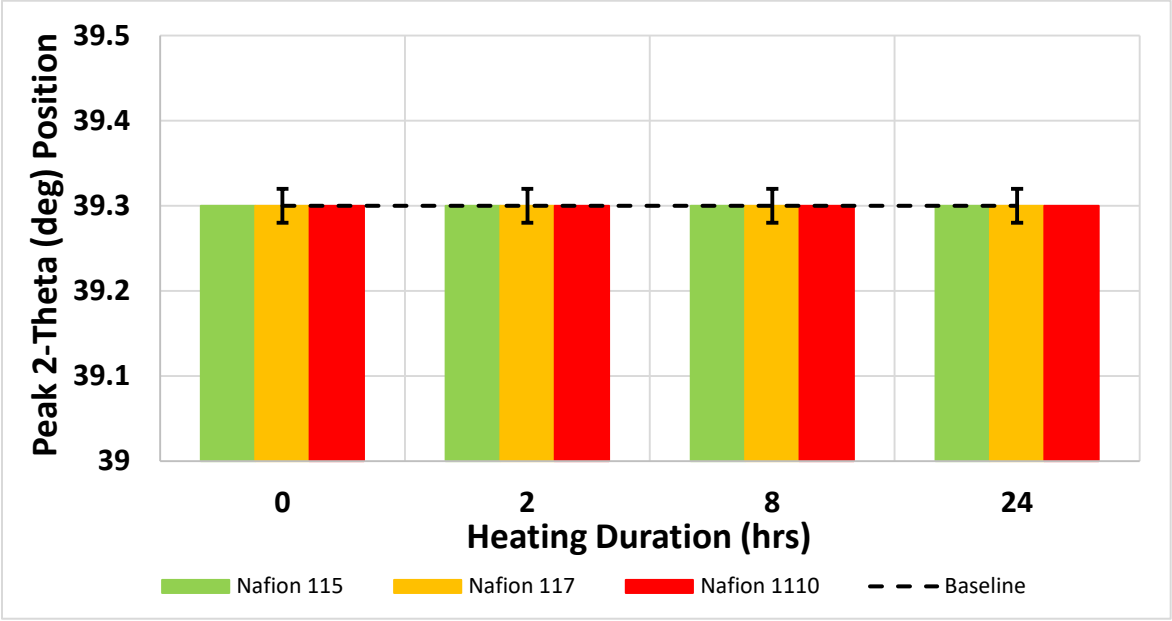

Figure 96: Post-Heating Calculated 115, 117 and 1110 2-Theta Peak II Position Taken at 25°C after Heated to 120°C for 10 min, 2hr, 8hr and 24hr. Results Compared to Peak I Baseline Measurements.

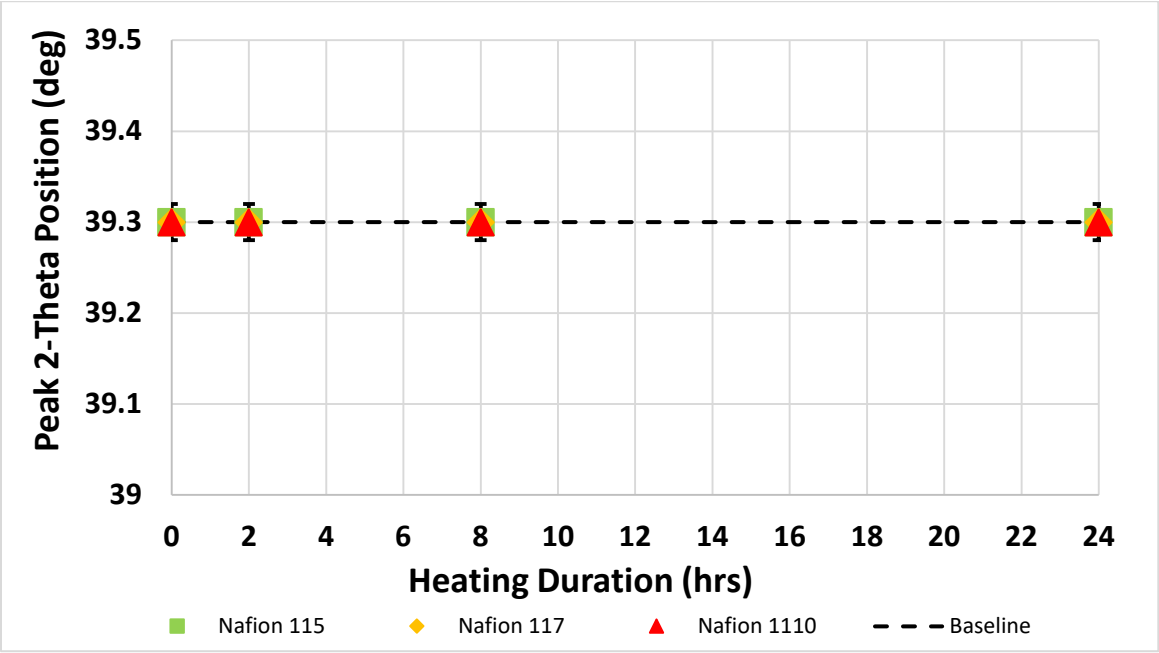

Figure 97: In-Situ Calculated 115, 117 and 1110 2-Theta Peak II Position after Heated to 140°C for 10 min, 2hr, 8hr and 24hr. Results Compared to Peak II Baseline Measurements.

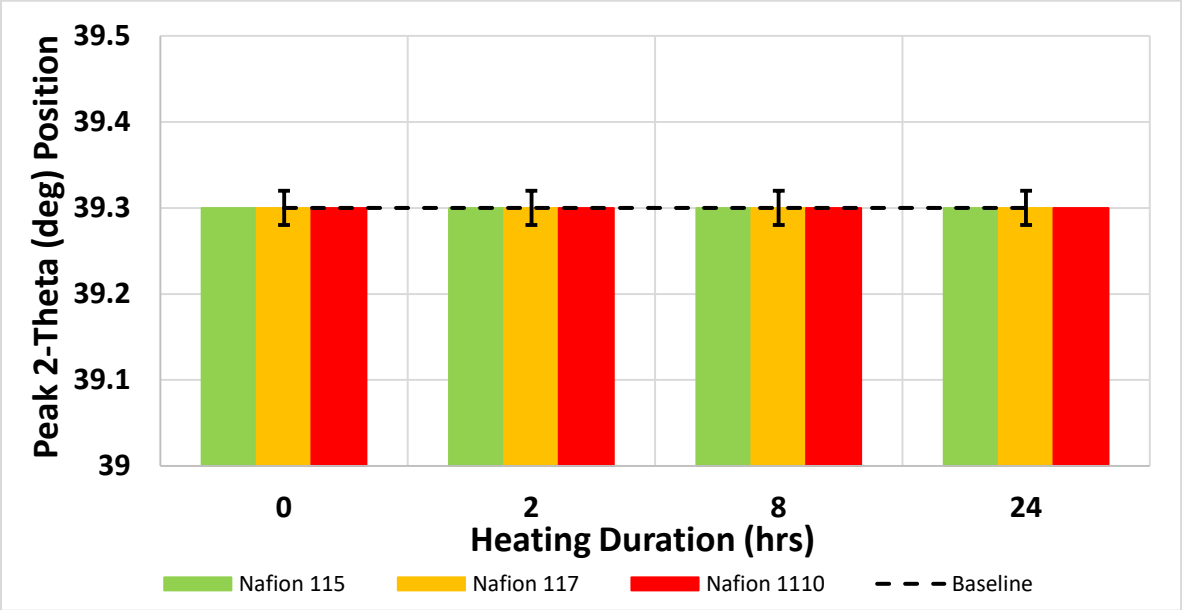

Figure 98: Post-Heating Calculated 115, 117 and 1110 2-Theta Peak II Position Taken at 25°C after Heated to 140°C for 10 min, 2hr, 8hr and 24hr. Results Compared to Peak I Baseline Measurements.

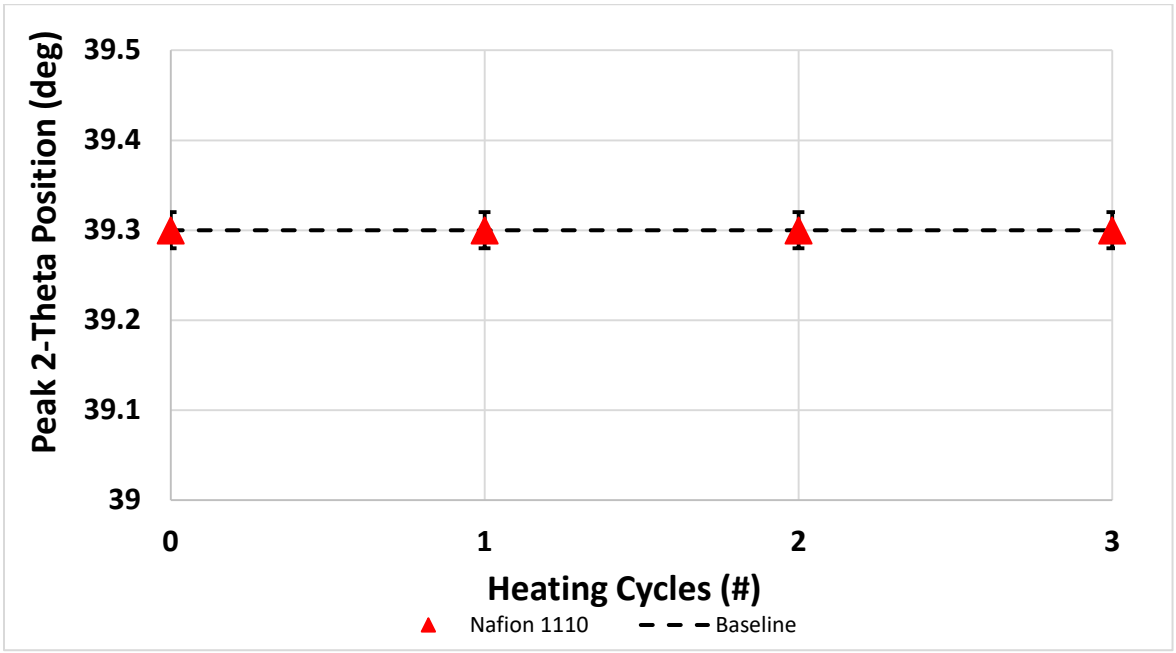

Figure 99: In-Situ Calculated 1110 2-Theta Peak II Position after 3 Heating Cycles to 60°C for 24hr. Baseline Raw XRD Data Provided for Comparison.

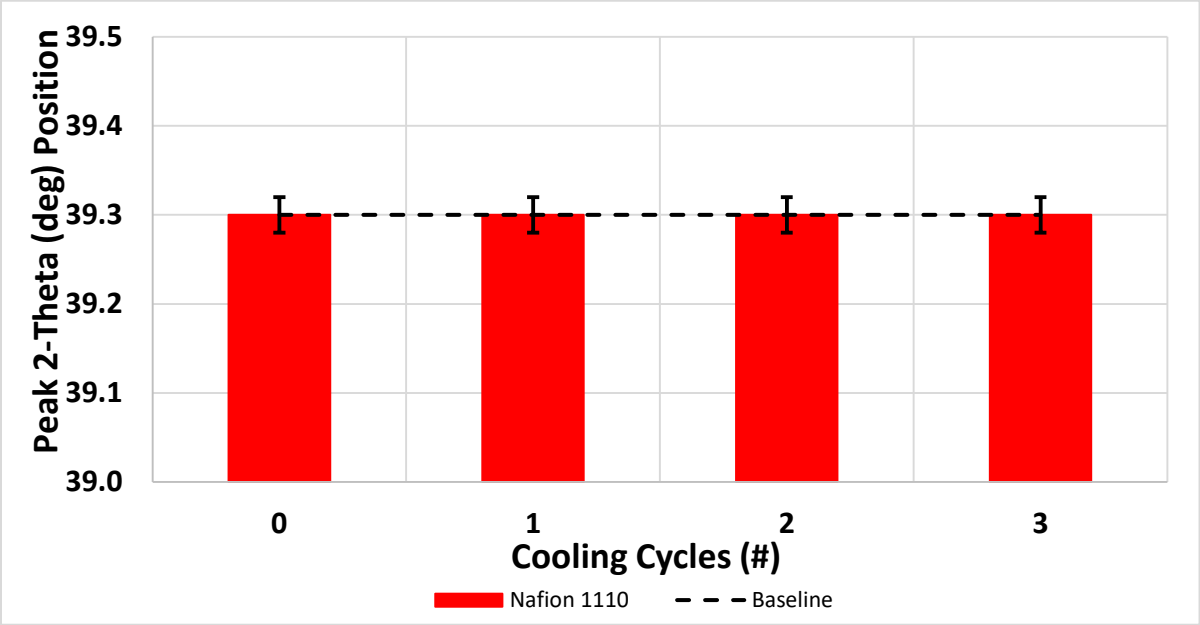

Figure 100: Post-Cooling Calculated 1110 2-Theta Peak II Position after 3 Cooling Cycles to 60°C for 24hr. Baseline Raw XRD Data Provided for Comparison.

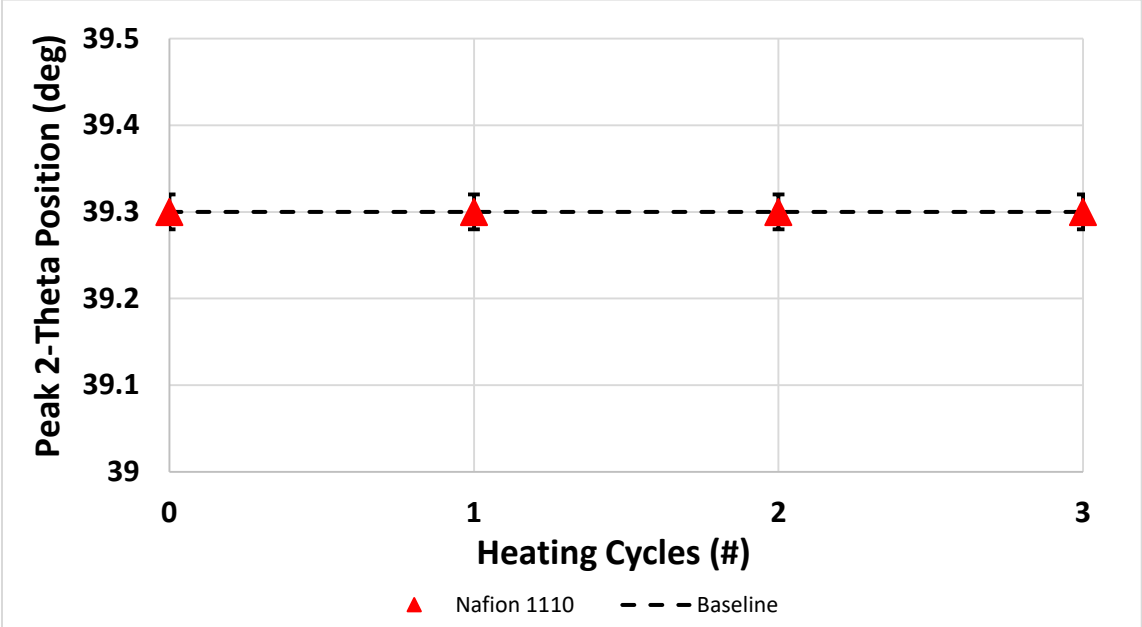

Figure 101: In-Situ Calculated 1110 2-Theta Peak II Position after 3 Heating Cycles to 120°C for 24hr. Baseline Raw XRD Data Provided for Comparison.

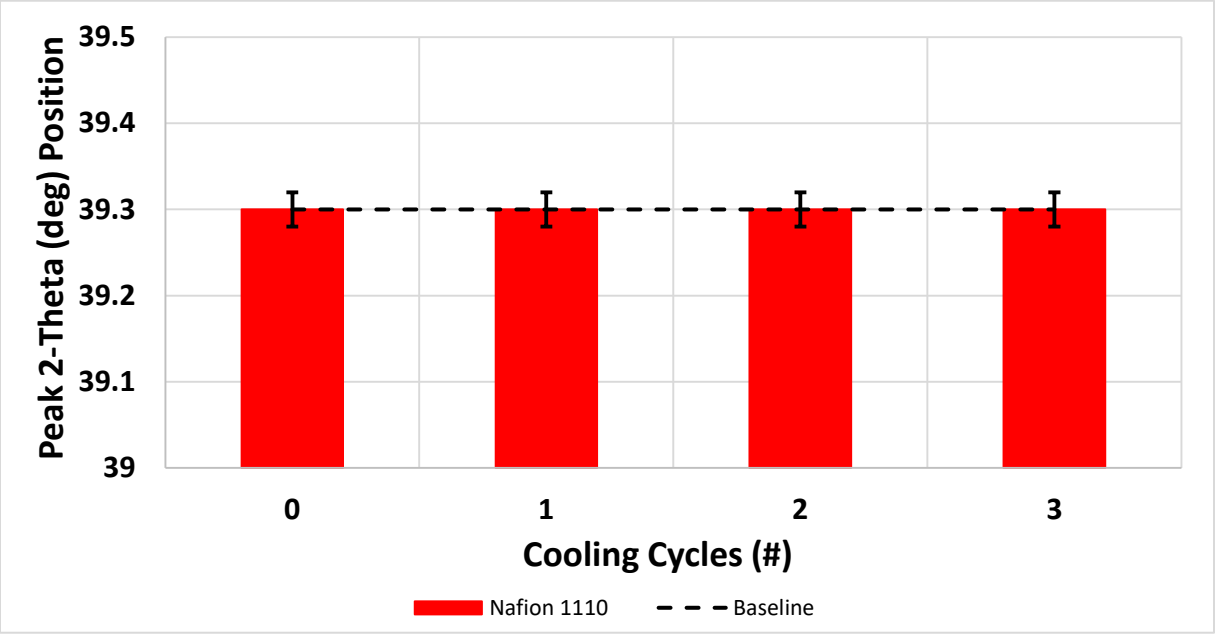

Figure 102: Post-Cooling Calculated 1110 2-Theta Peak II Position after 3 Cooling Cycles to 120°C for 24hr. Baseline Raw XRD Data Provided for Comparison.

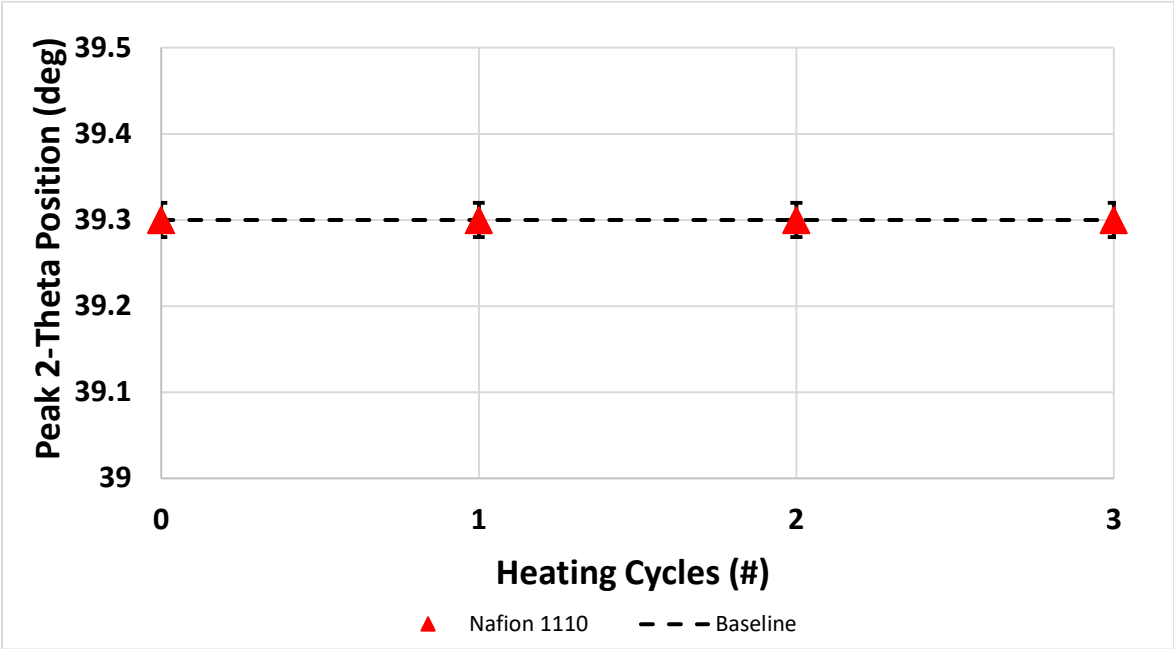

Figure 103: In-Situ Calculated 1110 2-Theta Peak II Position after 3 Heating Cycles to 140°C for 24hr. Baseline Raw XRD Data Provided for Comparison.

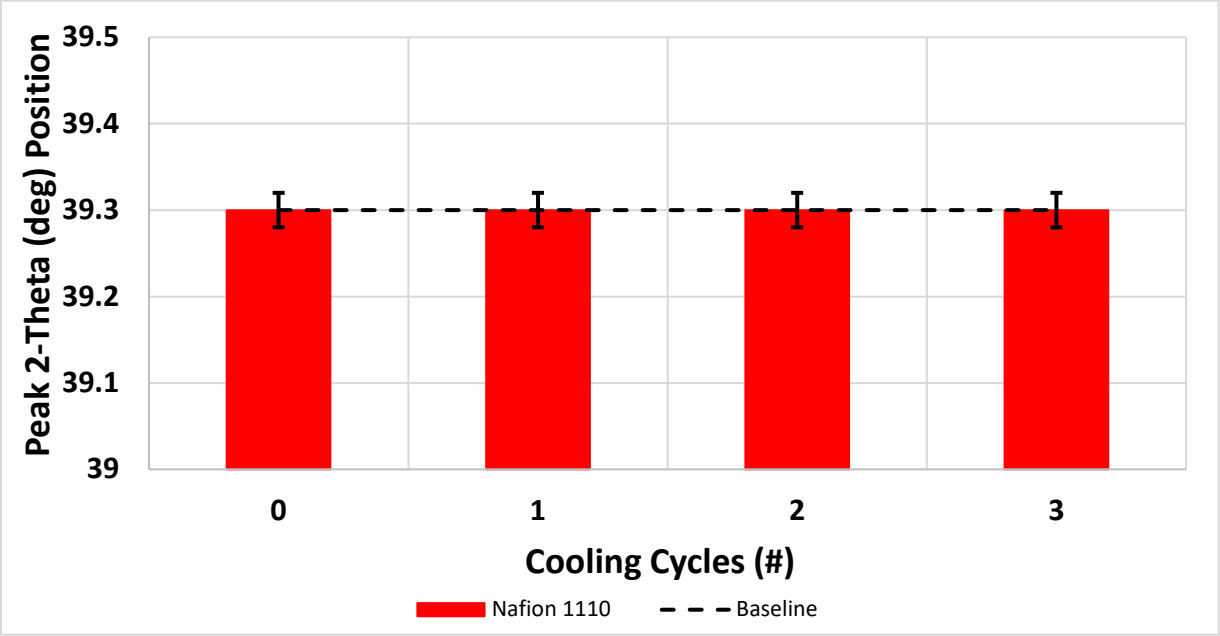

Figure 104: Post-Cooling Calculated 1110 2-Theta Peak II Position after 3 Cooling Cycles to 140°C for 24hr. Baseline Raw XRD Data Provided for Comparison.